



POLITECNICO DI TORINO
Repository ISTITUZIONALE

Smart Embedded Systems for Biomedical Applications

Original

Smart Embedded Systems for Biomedical Applications / Tuoheti, Abuduwalli. - (2019 Jun 11), pp. 1-165.

Availability:

This version is available at: 11583/2742529 since: 2019-07-17T09:24:43Z

Publisher:

Politecnico di Torino

Published

DOI:

Terms of use:

Altro tipo di accesso

This article is made available under terms and conditions as specified in the corresponding bibliographic description in the repository

Publisher copyright

(Article begins on next page)



ScuDo
Scuola di Dottorato ~ Doctoral School
WHAT YOU ARE, TAKES YOU FAR



Doctoral Dissertation
Doctoral Program in Electronic Engineering (31st cycle)

Smart Embedded Systems for Biomedical Applications

Abuduwaili Tuoheti

* * * * *

Supervisors

Prof. Danilo Demarchi, Supervisor
Prof. Sandro Carrara, Co-supervisor

Doctoral Examination Committee:

Prof. Maurizio Valle, Referee
Prof. Marco Crepaldi, Referee
Prof. Maurizio Martina, Referee
Prof. Guido Pagana, Referee
Dr. Stefano Sapienza, Referee

Politecnico di Torino
June 11, 2019

This thesis is licensed under a Creative Commons License, Attribution - Noncommercial-NoDerivative Works 4.0 International: see www.creativecommons.org. The text may be reproduced for non-commercial purposes, provided that credit is given to the original author.

I hereby declare that, the contents and organization of this dissertation constitute my own original work and does not compromise in any way the rights of third parties, including those relating to the security of personal data.

.....
Abuduwaili Tuoheti
Turin, June 11, 2019

Summary

Embedded systems are being widely used in health care related applications. They are used in imaging systems, regenerative medicine and tissue engineering, rehabilitation medicine, continuous monitoring and delivery of drugs, personalized medicine, detection of diseases and early stage diagnostics, and so on.

During the design of an embedded system for a specific application, there can be several constraints or requirements. The system might be required to carry out certain complex tasks; it might need to operate in real-time to meet timing deadlines; the system might need to consume very low power; the system might have restrictions on the dimension and weights. So, designing an embedded system can be very challenging and complicated depending on the actual applications and it is necessary to follow certain design procedures or design methodologies in order to guarantee that the designed system would meet all the functional or non-functional requirements of the application. The thesis focuses on designing embedded systems for five biomedical applications and each design follows a proper embedded system design methodology. The design of these embedded systems goes from ready-to-use to custom, then from custom to standard.

The first project is in Chapter Two and it is about designing an electrical and mechanical signal generation system for cell stimulation and monitoring application. The designed embedded system is based on a ready-to-use Raspberry Pi (RPi) board and only an external custom circuit board is designed for the project. So, the design of the system is very easy and not much extra effort is needed in terms of hardware design. However, the RPi contains many hardware resources that are not required for the project and they contribute to an excessive amount of power consumption. The board is also not flexible as its hardware design is fixed. So, in the following applications presented in Chapter Three, Four and Five, embedded systems are custom designed in order to achieve flexibility and optimization in hardware, reduction in area, optimization in performance, reduction in cost and also in power consumption.

In the Chapter Three, a custom designed wearable, wireless, low-power surface EMG system is presented. The main objective of the system is to acquire surface EMG signals from muscles of the patient for a long time of up to several days. The commercially available surface EMG devices could carry out maximum 12-hour

continuous EMG signal acquisition and are not suitable for long-term monitoring. So, a power efficient, wearable, wireless embedded system is designed for this purpose. The design of the system has followed the successive refinement model and three prototypes are designed. The measurement results show that the designed system could carry out continuous signal acquisition for 32 to 61 hours with a coin battery of 450 mAh capacity.

In the Chapter Four, a custom designed electrochemical biosensing platform for anesthesia monitoring and delivery is presented. The continuous monitoring and correct delivery of anesthesia is important as the anesthesia is a very powerful and dangerous drug that could result in serious safety problems if not monitored or delivered correctly to the patient. So, an embedded biosensing platform is presented in this chapter. The design of the system has strictly followed the hardware and software design methodology and relevant experiments are carried out on Paracetamol and Propofol using different electrochemical techniques.

In Chapter Five, a custom designed memristive biosensing platform for early stage cancer diagnostics is presented. Memristive biosensors are ideal candidates for the cancer detection due to their ultra-high sensitivity. However, commercially available electronic platforms for memristive biosensors are probe stations and parameter analyzers. These devices are very bulky and the test would take very long time. Therefore, a portable, easy-to-use embedded biosensing platform is required for the measurement and also for automatic data processing. So, by following hardware and software design methodology, an embedded system is designed and relevant tests are carried out for the Prostate Specific Antigen (PSA) detection. The test results confirm the functionality of the system and the correct design process.

After the design of the custom electrochemical and memristive biosensing platforms, the two hardware architectures are compared with each other and several similarities are found. For example, in both platforms, the voltage signals coming from the biosensor analog front end are processed by the Analog to Digital Conversion blocks, then analyzed by the data post processing blocks. Both platforms are controlled by similar Graphical User Interfaces (GUI). So, these hardware architectures can be standardized and in the final application in Chapter Six, the design target has switched from custom to standard and a general purpose embedded platform that supports various types of biosensors is presented. The system is validated with three types of electronic biosensors such as electrochemical, memristive and ion-sensitive biosensors and its generality, the design concept and the design approach are confirmed through experimental results.

Acknowledgements

First, my sincere gratitude goes to my supervisor Professor Danilo Demarchi for his continuous help and suggestions during my doctoral study. Throughout these years, Danilo has been a great supporter, an amazing mentor and a wonderful teacher to me not only in my carrier, but also in my life. Thanks to him, I had the possibility to be in world-famous top universities to carry-out research. Thanks to him, I learned how to face problems and handle them. Most importantly, thanks to him, I learned how to help others.

Then, I would like to thank my co-supervisor Sandro Carrara for his relentless help and guidance. Thanks to him, I had the opportunity to be part of the amazing research group and had so many fruitful research outcomes. I also would like to thank Professor Emilio Bizzi and Professor Paolo Bonato for hosting me in MIT and Harvard. It had been a wonderful experience for me and I appreciated a lot my stay and my work there.

Finally, I would like to thank my colleagues from MiNES group in our university and LSI group in EPFL. Thanks to their kind help and support, I have overcome many problems and I have come out with many nice results.

Of course, my beloved family have been life-time supporters to me for my study and I also send them my deepest appreciation and love.

*I would like to dedicate
this thesis to my
beloved family*

Contents

| | |
|---|-----------|
| List of Tables | XII |
| List of Figures | XIII |
| 1 Introduction and Thesis aims | 1 |
| 1.1 What is an Embedded System | 1 |
| 1.1.1 Definition | 1 |
| 1.1.2 Embedded System Types | 2 |
| 1.1.3 Advantages of Embedded Systems | 4 |
| 1.1.4 Challenges in Embedded Systems | 4 |
| 1.2 Embedded System Design Process | 5 |
| 1.2.1 Requirements | 6 |
| 1.2.2 Specification | 6 |
| 1.2.3 Architecture | 6 |
| 1.2.4 Hardware and Software Components Design | 7 |
| 1.2.5 System Integration | 7 |
| 1.3 Design Methodology | 7 |
| 1.3.1 Waterfall Model | 8 |
| 1.3.2 Spiral Model | 9 |
| 1.3.3 Successive Refinement Model | 10 |
| 1.3.4 Concurrent Model | 10 |
| 1.4 Embedded Systems in Biomedical Applications | 11 |
| 1.4.1 Embedded Systems in Regenerative Medicine | 12 |
| 1.4.2 Embedded Systems in Rehabilitation Therapy | 12 |
| 1.4.3 Embedded Systems in Therapeutic Drug Monitoring | 13 |
| 1.4.4 Embedded Systems in Cancer Diagnostics | 14 |
| 1.5 Research Challenges | 14 |
| 1.6 Thesis Outline | 15 |
| 2 Electromechanical Bioreactor System Design | 17 |
| 2.1 Introduction | 17 |
| 2.1.1 Regenerative Medicine | 17 |

| | | |
|----------|--|-----------|
| 2.1.2 | Stem Cell Differentiation | 17 |
| 2.1.3 | Research Objective | 18 |
| 2.2 | Project Analysis | 18 |
| 2.3 | Model Implementation | 19 |
| 2.3.1 | Requirements | 19 |
| 2.3.2 | Specification | 20 |
| 2.3.3 | Architecture | 20 |
| 2.3.4 | Components Design | 21 |
| 2.3.5 | System Integration | 28 |
| 2.3.6 | System Refinement | 29 |
| 2.4 | Validation of the System | 31 |
| 2.4.1 | Electrical Signal Generation | 31 |
| 2.4.2 | Mechanical Signal Generation | 33 |
| 2.4.3 | Real-time Monitoring | 34 |
| 2.5 | Experimental Results | 35 |
| 2.6 | Discussion and Conclusion | 36 |
| 3 | Wearable Wireless Surface EMG System Design for Muscle Synergies | 39 |
| 3.1 | Introduction | 39 |
| 3.1.1 | Muscular System | 39 |
| 3.1.2 | Surface Electromyography (sEMG) | 40 |
| 3.1.3 | Commercial EMG Devices | 42 |
| 3.1.4 | Research Objective | 42 |
| 3.1.5 | Project Analysis | 42 |
| 3.2 | Model Implementation | 43 |
| 3.2.1 | Requirements | 43 |
| 3.2.2 | Specification | 44 |
| 3.2.3 | Architecture | 45 |
| 3.2.4 | Components Design | 46 |
| 3.2.5 | System Integration | 53 |
| 3.2.6 | System Refinement | 53 |
| 3.3 | Experimental Results | 54 |
| 3.3.1 | Synchronization | 54 |
| 3.3.2 | Signal Acquisition | 55 |
| 3.3.3 | Wireless Data Transmission | 56 |
| 3.3.4 | Graphical User Interface (GUI) | 56 |
| 3.4 | Discussion and Conclusion | 57 |
| 4 | Electrochemical Sensing Platform for Continuous Monitoring of Anesthesia Delivery | 61 |
| 4.1 | Introduction | 61 |

| | | |
|----------|---|------------|
| 4.2 | Drug Monitoring with Electrochemical Sensors | 61 |
| 4.2.1 | Electrochemical Sensing Techniques | 62 |
| 4.2.2 | Sensor Calibration | 64 |
| 4.2.3 | Research Objective | 65 |
| 4.2.4 | Project Analysis | 65 |
| 4.3 | Model Implementation | 65 |
| 4.3.1 | Requirements | 66 |
| 4.3.2 | Specification | 67 |
| 4.3.3 | Architecture | 67 |
| 4.3.4 | Components Design | 68 |
| 4.3.5 | System Integration | 76 |
| 4.4 | Experimental Results | 76 |
| 4.4.1 | Test on Drug Monitoring | 77 |
| 4.4.2 | Test on Pump Injection | 84 |
| 4.5 | Discussion and Conclusion | 88 |
| 5 | Portable Memristive Biosensing System for Cancer Diagnostics | 91 |
| 5.1 | Introduction | 91 |
| 5.1.1 | Prostate Cancer | 91 |
| 5.1.2 | Therapeutic methods for Malignant Diseases | 92 |
| 5.1.3 | Nanotechnology in Diagnostics and Therapeutics | 93 |
| 5.1.4 | Memristive Phenomena | 93 |
| 5.1.5 | Memristive Biosensors for Cancer Detection | 95 |
| 5.1.6 | Research Objective | 96 |
| 5.1.7 | Project Analysis | 97 |
| 5.2 | Model Implementation | 97 |
| 5.2.1 | Requirements | 97 |
| 5.2.2 | Specification | 98 |
| 5.2.3 | Architecture Design | 99 |
| 5.2.4 | Components Design | 102 |
| 5.2.5 | System Integration | 108 |
| 5.3 | Experimental Results | 109 |
| 5.3.1 | Test on Silicon Nanowires | 109 |
| 5.3.2 | Test on Antibody-based Memristive Biosensors | 110 |
| 5.3.3 | Test on Prostate Specific Antigen (PSA) | 111 |
| 5.4 | Discussion and Conclusion | 112 |
| 6 | General Purpose Biosensing Platform Design | 115 |
| 6.1 | Introduction | 115 |
| 6.1.1 | Biosensors in Health Care | 115 |
| 6.1.2 | Definition and Characteristics of a Biosensor | 116 |
| 6.1.3 | Electronics for Biosensors | 117 |

| | | |
|----------|---|------------|
| 6.1.4 | Hewlett Packard Interface Bus (HP-IB) | 118 |
| 6.1.5 | Research Objective | 119 |
| 6.2 | Project Analysis | 120 |
| 6.3 | Model Implementation | 120 |
| 6.3.1 | Requirements | 120 |
| 6.3.2 | Specification | 121 |
| 6.3.3 | Architecture | 122 |
| 6.3.4 | Components Design | 125 |
| 6.3.5 | System Integration | 130 |
| 6.4 | Experimental Results | 131 |
| 6.4.1 | Electrochemical Sensor Experiment | 131 |
| 6.4.2 | Ion-Sensitive Biosensor Experiment | 131 |
| 6.4.3 | Memristive Biosensor Experiment | 131 |
| 6.5 | Conclusion | 133 |
| 7 | Conclusion and Future Work | 135 |
| | References | 143 |

List of Tables

| | | |
|-----|---|----|
| 3.1 | Current consumption test on different working modes | 59 |
| 5.1 | Cancer related mortality [53] | 91 |

List of Figures

| | | |
|------|--|----|
| 1.1 | Block representation of an embedded system. | 2 |
| 1.2 | Major steps involved in the embedded system design process [4] . . . | 5 |
| 1.3 | Waterfall model methodology in software development [4]. | 9 |
| 1.4 | Spiral model design methodology [4]. | 9 |
| 1.5 | Successive refinement model design methodology [4]. | 10 |
| 1.6 | Concurrent engineering model design methodology [4]. | 11 |
| 2.1 | Block representation of the hardware architecture of the system. . . | 21 |
| 2.2 | Block representation of the software architecture of the system. . . | 21 |
| 2.3 | The motor and scaffold connection [22] | 23 |
| 2.4 | The Raspberry Pi camera [22] | 24 |
| 2.5 | The Raspberry Pi camera based microscope [22]. | 24 |
| 2.6 | Software architecture of the bioreactor system [22]. | 25 |
| 2.7 | Graphical User Interface of the bioreactor system [22]. | 26 |
| 2.8 | Work flow of the electrical stimulation process on the client and server side [22]. | 27 |
| 2.9 | Work flow of the mechanical thread on the GUI project [22]. | 28 |
| 2.10 | Work flow of the mechanical project [22]. | 29 |
| 2.11 | Work flow of the decode project [22]. | 30 |
| 2.12 | Flow chart of the camera thread inside the GUI project [22]. | 31 |
| 2.13 | Flow chart of the camera control process on the server side [22]. . . | 32 |
| 2.14 | First Prototype Electrical-Mechanical Stimulation and Monitoring System [22]. | 32 |
| 2.15 | Encoder output at the mechanical stimulation [22]. | 33 |
| 2.16 | Measurement of rotation angle from the ImageMeter Pro application [22]. | 34 |
| 2.17 | Setup for observing nanogap circuit using the monitoring system [22]. | 34 |
| 2.18 | Bioreactor Model [23]. | 35 |
| 2.19 | Experimental steps [23]. | 36 |
| 2.20 | Results on the mechanical and biochemical stimulation of MSCs [23]. | 36 |
| 3.1 | Electrode montage types and the detected action potentials in each configuration [30] | 41 |
| 3.2 | Commercial EMG Devices | 42 |

| | | |
|------|---|----|
| 3.3 | Hardware architecture of the EMG probe | 45 |
| 3.4 | Software architecture of the EMG probe | 46 |
| 3.5 | Overvoltage protection circuit | 47 |
| 3.6 | Differential High Pass Filter with 30 Hz cut-off frequency [31] | 48 |
| 3.7 | INA321 configuration circuit [32] | 48 |
| 3.8 | Multiple-feedback Low Pass Filter Circuit | 49 |
| 3.9 | Sallen-Key based Low Pass Filter Circuit | 49 |
| 3.10 | 3.6 V boost step-up voltage regulator | 50 |
| 3.11 | Block diagram of PPI | 50 |
| 3.12 | Graph representation of the overall system | 51 |
| 3.13 | Synchronization process of the whole system | 51 |
| 3.14 | Block diagram of FIFO | 52 |
| 3.15 | Brief comparison of the 3 prototypes of the system | 53 |
| 3.16 | Synchronization of two slave nodes | 54 |
| 3.17 | Different working modes of slave nodes | 55 |
| 3.18 | Raw data from the sEMG measurement | 56 |
| 3.19 | Envelope data from the sEMG measurement | 57 |
| 3.20 | ATC data from the sEMG measurement | 58 |
| 3.21 | Graphical User Interface for controlling master node | 59 |
| 4.1 | Drug administration errors | 62 |
| 4.2 | Typical Electrochemical Cell configuration [39] | 62 |
| 4.3 | Typical Electrochemical experiment | 63 |
| 4.4 | ChronoAmperometry(CA) [40] | 63 |
| 4.5 | Cyclic Voltammetry(CV) [39] | 64 |
| 4.6 | Differential Pulse Voltammetry(DPV) | 64 |
| 4.7 | Block representation of the whole system [41] | 68 |
| 4.8 | Block representation of the software architecture | 68 |
| 4.9 | Schematics of the custom board [44] | 70 |
| 4.10 | Graphical User Interface of the electronic system [41] | 71 |
| 4.11 | Work flow of the micro-controller | 73 |
| 4.12 | Command packet for CA | 73 |
| 4.13 | Command packet for CV | 74 |
| 4.14 | Command packet for DPV | 74 |
| 4.15 | Data packet for the measurement results | 75 |
| 4.16 | Composition of the start tag | 75 |
| 4.17 | TCP Server running RPi | 77 |
| 4.18 | The MATLAB GUI for remote controlling of the pump | 77 |
| 4.19 | IoT based anesthesia monitoring [45] | 78 |
| 4.20 | Work-flow charts on the patient and doctor side [45]. | 78 |
| 4.21 | Sketch of the RPi based electronic system for Anesthesia monitoring [47] | 79 |
| 4.22 | Electrochemical test parameters during the measurements [48] | 79 |

| | |
|--|-----|
| 4.23 ChronoAmperometry test on APAP using Screen Printed Electrodes [48] | 80 |
| 4.24 Cyclic Voltammetry test on APAP using Screen Printed Electrodes [48] | 80 |
| 4.25 Differential Pulse Voltammetry test on APAP using Screen Printed Electrodes [48] | 81 |
| 4.26 Comparison of the calibration curves [48] | 81 |
| 4.27 Scan rate analysis for CV and DPV measurement of APAP [48] . . | 82 |
| 4.28 Pencil Graphene Electrodes [51] | 83 |
| 4.29 Test parameters for the CV and DPV measurements [47] | 84 |
| 4.30 CV and DPV measurement of Propofol and DPV of APAP and the calibration curves for each measurement [47] | 85 |
| 4.31 Scan rate analysis for CV and DPV measurement of Propofol and DPV of APAP [47] | 86 |
| 4.32 Experimental setup for the injection test with TCI pump [52] . . . | 86 |
| 4.33 Example of the dose injection [52] | 87 |
| 4.34 Dye test with TCI pump [52] | 87 |
| 4.35 pH test: dose injection and measurement of concentration [52] . . . | 88 |
| 4.36 APAP test with TCI pump [52] | 88 |
| 5.1 Four fundamental circuit variables (a) [63] and the hysteresis curve of a memristor (b) [63] | 94 |
| 5.2 Applications of memristive structures ref to [68][70] | 95 |
| 5.3 Hysteresis response of the memristive nanowires before (1) and after (2) the bio-functionalization [77] | 96 |
| 5.4 Hardware architecture of Memristive Biosensing Platform | 100 |
| 5.5 More detailed hardware architecture of the system | 100 |
| 5.6 Software architecture of the system | 101 |
| 5.7 Chip holder board [78] | 103 |
| 5.8 Signal conditioning front end [78] | 103 |
| 5.9 GUI for controlling the measurement | 104 |
| 5.10 Work flow of the central control block | 105 |
| 5.11 Voltage sweep during measurement | 107 |
| 5.12 The first prototype of biosensing control system | 108 |
| 5.13 The complete memristive biosensing platform | 109 |
| 5.14 Hysteresis curve of the bare memristive nanowire chip | 110 |
| 5.15 Voltage gap of the bare memristive nanowire chip | 110 |
| 5.16 Hysteresis curve of the bio-functionalized memristive biosensor chip | 111 |
| 5.17 Voltage gap of the bio-functionalized memristive biosensor chip . . . | 111 |
| 5.18 Comparison of hysteresis for 3.3 and 330 fM PSA | 112 |
| 5.19 Comparison of voltage gaps for 3.3 and 330 fM PSA [78] | 112 |
| 6.1 Internal blocks of a biosensor [83] | 117 |
| 6.2 Simplified hardware architecture of the overall system | 123 |

| | | |
|------|---|-----|
| 6.3 | Detailed hardware architecture of the GBIB Platform | 124 |
| 6.4 | Software architecture of the GBIB system | 125 |
| 6.5 | GBIB Interface pinout | 126 |
| 6.6 | Sensing and Actuation. | 127 |
| 6.7 | Schematics of the bipolar voltage to current converter | 127 |
| 6.8 | GUI for controlling the whole system | 129 |
| 6.9 | First prototype of the system. A) amperometric biosensors B) Ion-Sensitive biosensors C) Memristive biosensors D) GBIB Platform . | 130 |
| 6.10 | A) CV acquisition from GBIB system B) CV acquisition from Autolab C) Comparison of calibration lines obtained for CV measurements of six increasing concentrations of APAP (50;100;150;200;250;300) μM | 132 |
| 6.11 | Comparison of lithium ion detection with a commercial Autolab potentiostat (A) and with our GBIB system (B). The small insets show the time trace during successive solute additions, while the main graphs display the corresponding calibration curves. | 133 |
| 6.12 | Comparison of voltage gaps on bare memristive nanowires between A) Memristive Biosensing System [78] and B) Memristive Electronic Biosensor (Figure 6.9.C). | 133 |

Chapter 1

Introduction and Thesis aims

1.1 What is an Embedded System

Ever since the first-generation computer is invented, the computer technology has evolved substantially. There have been the year of vacuum tube, the creation of first transistor and then the integrated circuit before the invention of the microprocessor in 1970. The invention of the microprocessor has been the main reason for the invention of the personal computer (PC) and also for graphical user interface(GUI) development. In the meanwhile, the microprocessor invention has also led the development of an another type of computer system, the task-specific computer system, also called an Embedded System [1].

1.1.1 Definition

Embedded system is a microprocessor or rather a micro-controller based system that is composed of hardware and software designed for specific purposes or tasks. Its definition can be more clear by comparing it with the PCs. The PC is a general-purpose platform that can execute a generic type of operations that user wants. For example, the PC can be a music player; it can be a text editor; it can be a calculator; it can be an audio or video recorder; it can be a data transmitter or data logger; it can be an image visualizer and editor, etc [2].

An embedded system receives inputs from the user, processes it and carries out the specific operations. A possible structure of an embedded system can be as shown in Figure 1.1.

So, an embedded system can contain inputs to receive commands or signals from external environment. It contains a real-time operating system (RTOS) that continuously executes the software loaded inside the hardware and the RTOS is responsible for carrying out different operations based on the inputs. It can contain outputs that can be processed data, specific signals or commands, etc. It can also

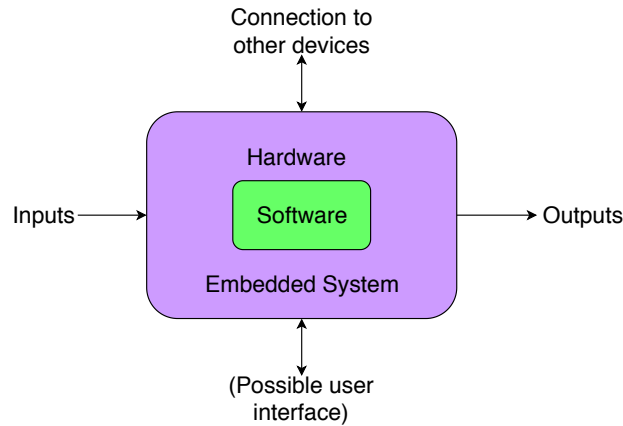


Figure 1.1: Block representation of an embedded system.

contain a user interface in order to receive control commands from the user. It can also be connected to other devices for other purposes.

Generally, an embedded system hardware can contain a microprocessor, a memory and peripherals. The microprocessor executes the operations defined by the software written inside the memory. The memory can be used for storing the software and also the data. The peripherals can be used for specific aims such as providing clocks, generating signals, processing signals, etc. Some examples of the embedded systems include: micro-controller, expended micro-controller, microprocessor based embedded systems, board based embedded systems, and so on [3].

As mentioned earlier, the embedded system is dedicated to limited number of operations. For example, a washing machine can contain a microprocessor or a micro-controller based embedded system for starting and stopping the washing, setting up the temperature, setting up the rotation speed, selecting the operation type and so on. But a washing machine cannot execute other generic types of operations, such as heating a food, capturing a picture or displaying an image, etc. A car washer can be based on an embedded system that is dedicated to selecting the water speed, water temperature, washing control, etc. So, these examples well explain that an embedded system is designed for a specific task or set of tasks and it cannot work as a general-purpose platform like a PC.

1.1.2 Embedded System Types

The embedded systems can be divided into three groups based on the performance:

- Sophisticated
- Medium scale

- Small scale

According to the functionality requirement and performance, they can be divided into following groups:

- Stand alone
- Real-time
- Mobile
- Networked

Sophisticated embedded systems

These are embedded systems with 32 or 64-bit microprocessors or micro-controllers and the complexity of software and hardware are very high. They contain enormous hardware resources and are dedicated to cutting edge applications where scalable, parallel and configurable processors are needed.

Medium scale embedded systems

These embedded systems usually contain 16-bit or 32 bit microprocessors or micro-controllers with external ROM and RAM so that they can carry out medium complexity jobs. They support high level programming languages such as Java, C, C++, Visual C++, RTOS, etc.

Small scale embedded systems

Such systems include 8-bit or 16-bit microprocessors or micro-controllers and they are dedicated to simple tasks. They can be used for developing battery powered electronic systems.

Stand alone embedded systems

These types of embedded systems are electronic systems that don't need a host computer and can carryout defined operations by themselves. They can accept analog or digital input signals, then process these signals and finally transmit these signals to other peripherals for display or for further post-processing purposes. They can also execute tasks according to the internal software without having input signals. Some examples can be the microwave oven, washing machine, etc.

Real-time embedded systems

From the name, it can be inferred that these types of embedded systems are those that can carry out operations within a dedicated time and they usually contain high performance micro-controllers or microprocessors with complex peripheral resources. Examples can be the traffic surveillance systems, video processing platforms, etc.

Mobile embedded systems

These types of embedded systems are extensively used in portable devices, such as mobile phones, smart phones, digital cameras, etc.

Networked embedded systems

These are electronic systems dedicated to the networking applications. They can provide access to network resources and the network can be internet or LAN or WAN.

1.1.3 Advantages of Embedded Systems

Embedded systems have the following advantages [2]:

- They can replace the discrete logic-based circuits thanks to the flexibility of their internal software.
- They can provide functional updates without changing the system hardware.
- They can provide easy maintenance upgrades.
- They can provide improved mechanical stability and performance.
- They can provide better intellectual property rights protection.
- They can replace the traditional analog circuits.

1.1.4 Challenges in Embedded Systems

Embedded systems are specific purpose platforms that carry out a single or a set of operations. So, they usually have very limited hardware resources. This can result in performance constraints, real-time constraints, resource constraints and power consumption constraints. They are also sensitive to the cost and the price of a single component can affect the cost of the overall system. The software failure is more common than other general purpose platforms and the development of software needs specific debugging circuitry, software development environment and

tools. So, these challenges should be taken into consideration when an embedded system is designed for a given application [3].

1.2 Embedded System Design Process

When designing embedded systems, an individual designer or design team usually follow some processes or approaches in order to carry out the design in a systematic way. A general steps that are included in the embedded system design process are shown in Figure 1.2.

As it can be seen from the Figure 1.2, the design process starts with the require-

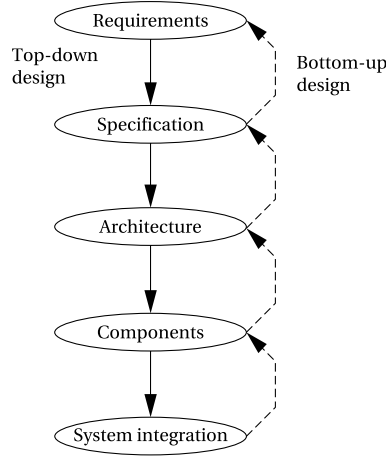


Figure 1.2: Major steps involved in the embedded system design process [4]

ments that indicate what is needed as a final goal. Then there is the specification that describes in details how the system behaves. Then there is the architecture design step that decides the system architecture in terms of blocks. Then the hardware and software components are analyzed and selected. Once the components are chosen, then they are designed in more details and integrated into the system in the final step.

The design process can follow the top-down approach or the bottom-up approach. In the top-down approach, the design is started from the most abstract level of the system and then goes to the concrete details of the system. While the bottom-up approach is exactly opposite and the design starts with known components. Then the functionality and specification are decided according to the design. Then it goes to the architecture level and so on. This approach is necessary when there is not enough information about the outcomes of the design process and also about the possible functionality that the final system can have at the end [4].

1.2.1 Requirements

Before the embedded system design process is started, it is important to know what should be the final goal of the design, such as the functionality that the system should have and the operations it should carry out. These information can be collected based on the needs of the user.

Besides having the basic functional requirements of the system, it is also important to have the nonfunctional requirements that include:

- *Performance*: The performance of the system can affect the usability and also its final cost. it is related to whether an embedded system can perform a required operation within a given time.
- *Cost*: The cost is one of the major consideration in the design. It contains two types of costs: 1) the manufacturing cost that is composed of component and assembly cost 2) nonrecurring engineering cost that includes the personnel and other costs of the design.
- *Physical size and weight*: The physical dimension and weight of the embedded system are dependent on the application and they affect the usability of the system. Both are important factors especially in the design of an implantable or wearable embedded systems.
- *Power consumption*: In the battery-powered embedded systems, the power consumption is an an important factor to consider as it directly decides the operational lifetime of the system.

1.2.2 Specification

Specification is the bridge between the requirements and architecture of the system. it is the detailed description of the user requirements and it helps the designers understand exactly what they are building. Specifications indicate clearly the type of inputs and outputs of the system, the exact operations to be carried out to meet user requirements, other relevant operations needed to keep the system running properly.

1.2.3 Architecture

Although the specifications indicate what tasks an embedded system does, they don't indicate how the embedded system carries out these tasks. The architecture design can indicate how the embedded system carries out operations and define what types of functional blocks are needed in order to carry out the specified operations. It also indicates how these functional blocks interact with each other and exchange data or information between them.

The architecture design includes both the hardware architecture and software architecture designs. The hardware architecture indicates what kind of hardware is needed for a specific operation, while the software architecture indicates how the operations are executed in the hardware architecture.

The functional and non-functional requirements should be both met during the architectural design. Besides all the functional requirements are present in the block diagram of the architecture, the other requirements such as power, performance, cost, speed and other constraints should also be taken into account during the architectural description. This can be done by considering the properties of the components in the diagram [4].

1.2.4 Hardware and Software Components Design

However, the architectural design is still in the abstract level and it does not indicate the exact types of components that are required for the design. These components are built in details in the hardware and software components design step. During the hardware components design, a proper ready-to-use hardware is selected or a hardware component is designed in order to meet the architecture requirement and specifications. During the software components design, the software module is selected or is developed for the correct operation and functional requirements of the software architecture.

1.2.5 System Integration

After the hardware and software components are ready, they need to be integrated to build a working embedded system. It is not just placing the software and hardware components together. But there is the need to guarantee that the hardware design components are able to carry out the software operations, as well as the software design components can control correctly the hardware resources. Usually there are the compatibility issues between the hardware and software, as well as hardware and software bugs. These problems can be addressed in component design phase by carrying out independent debug and test operations on individual hardware and software components [4].

1.3 Design Methodology

As it can be seen that, the embedded system design process includes several steps. When designing complex and sophisticated embedded systems, the functional specifications can be very complex and these specifications should also comply with other requirements on performance, cost, power, etc. So, there is a need

to follow some design flows or methodologies during the design of large systems. The design process is important because it is related to the delivery of the embedded system products. When designing simple embedded systems, following the previously mentioned general design process maybe feasible. But when it is a complex embedded system, many teams might involve in the process and it is important for them to be explicit and be well-organized and coordinated during the design process.

Besides the delivery of the useful product, the design process also aims at functionality, performance and power of the system. Besides that, the design process also focuses on other goals that include the time-to-market, design cost and quality.

However, the design process changes over time. It can change due to internal or external forces. Customers, the requirements, products and also the available components can change. Therefore, it is necessary to follow a good design methodology in order to build an embedded system that works as expected. This is extremely important in the health care, aerospace and automotive systems as serious safety problems can arise due to the bugs in the design process [4].

The common design methodologies include:

- waterfall model
- spiral model
- successive refinement model
- hardware/software design model, also called the concurrent model

1.3.1 Waterfall Model

The waterfall model is initially created for the software development purposes. It follows a top-down approach. In the requirements step, the basic characteristics of the system are analyzed. In the architecture step, the functionality of the system is decomposed into major components. In the coding step, the detailed software components are written and integrated. In the testing step, the software bugs are addressed and fixed. In the maintenance step, the software system is deployed in fields and is regularly updated. The waterfall model assumes that the designer has well understanding in the details of the system in the early stage of the design. However, this is not realistic during the design of complicated systems, because it is not possible to know all the details of the system. Besides that, there is limited feedback from lower design layer to higher abstract layer as the design follows one-way work and information flow.

A typical waterfall model in the software development is shown in Figure [1.3](#).

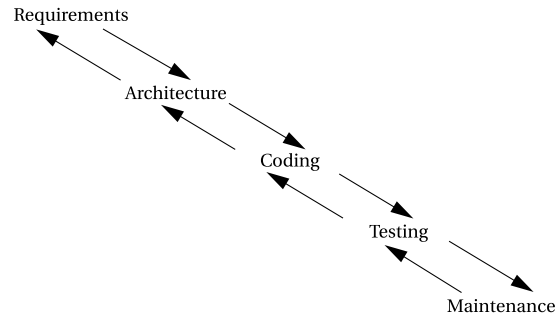


Figure 1.3: Waterfall model methodology in software development [4].

1.3.2 Spiral Model

In the spiral model, multiple versions of the system are developed. Starting from simple versions of the systems at the beginning, designers can optimize and improve their intuitions and experiences with the system. Then as the design process continues, more robust and sophisticated systems can be built. Each level of design includes requirements, design and testing phases. This model is more preferred than the waterfall model, as after several iterations of the design, it is possible to include all the functional details and achieve the goal of designing of a complete system. In the cases when there is a strict design time requirement, the spiral model may not be very appropriate as it might take more time with the design process when the systems get more complicated with more spirals. The Figure 1.4 demonstrates the flow of the spiral model.

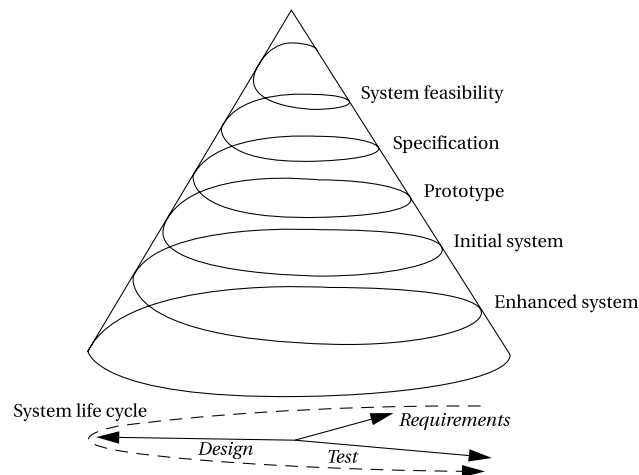


Figure 1.4: Spiral model design methodology [4].

1.3.3 Successive Refinement Model

In the successive refinement model, the system is built several times. An initial prototype system is designed, then is further refined by building successive models of the system. This methodology can be used when the designer is unfamiliar with the application environment. By building an initial system, one can find out what architecture and design techniques can be used, can figure out the existing problems in each step of the design and can also understand the responses of the system for the given inputs. In the design of the next version of the system, the designer can address these problems and optimize the system.

The typical design flow of a successive refinement model is shown in Figure 1.6.

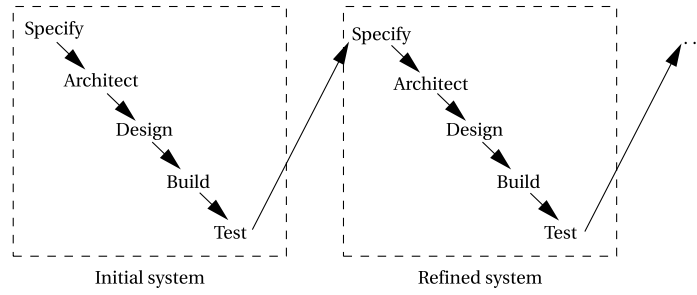


Figure 1.5: Successive refinement model design methodology [4].

1.3.4 Concurrent Model

The design of embedded systems include both the hardware design and software design. The software/hardware design model, also called the concurrent model is a design methodology where the hardware and software design are considered simultaneously during the design process. The Figure 1.6 shows the involved steps in the concurrent model. The requirements and specification, architecture steps consider the hardware and software in parallel. In the system integration and test stages, again both the hardware and software are considered together. In the design stage where the detailed hardware and software components are designed, they can be carried out independently.

This design methodology is extremely useful when designing a large complex system. The development teams can work in parallel while reducing the design time. It can also be very useful to keep track of the complete design flow and optimize it. The concurrent model includes several elements:

- *Cross-functional teams*

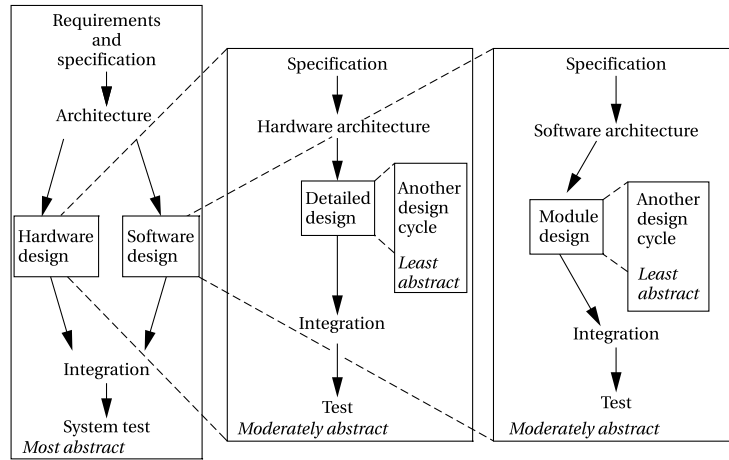


Figure 1.6: Concurrent engineering model design methodology [4].

- *Concurrent product realization*
- *Incremental information sharing*
- *Integrated project management*

1.4 Embedded Systems in Biomedical Applications

Embedded systems are being widely used in biomedical applications and are playing important roles in health care industry. The recent advances in embedded systems technology are transforming the health care solutions rapidly and making it possible to design smaller, wearable, smarter and connected medical devices in medical applications. During the development of these medical devices, the embedded systems have been part of them and one of the reasons for the improvement in the technology [5]. These medical devices are more portable and smaller. Smart devices like glucose monitors and blood pressure monitors are giving the patients the possibility to continuously monitor their health conditions at home without going to the hospitals [6] [7]. Furthermore, shrinking in size makes it possible for medical devices to be implanted inside the patients for long term monitoring [8]. The thesis focuses on the application of embedded systems in the following fields:

- regenerative medicine
- therapeutic drug monitoring
- cancer diagnostics

- rehabilitation therapy

The decision of targeting these four different applications was due to their huge market potential and their important roles in the health care. They are sufficiently broad to give the possibility of exploiting the several possible solutions given by embedded systems, challenging diversified implementation methods, with the goal of demonstrating the effectiveness of the use of embedded solutions for these important application domains.

1.4.1 Embedded Systems in Regenerative Medicine

Regenerative medicine is being recognized as an important research field that could revolutionize the patient care in 21st century. There are great scientific, public and commercial interests in the massive health care markets, such as chronic metabolic diseases or neurological conditions, cardiovascular diseases which are potentially addressed by regenerative medicine [9]. According to the report from *Markets and Markets* website (<https://www.marketsandmarkets.com>), the Regenerative Medicine Market is expected to reach USD 38.7 billion by 2024 from USD 13.3 billion in 2019.

In regenerative medicine, during the culturing of the cells in vitro, the ambient environment of the cell plays critical role in the growing of the cells, as the cells are instructed by various kinds of stimuli that simulate the condition of the cells in vivo. The stimuli can be chemical, mechanical or electrical. The electrical and mechanical stimuli play important role in the cardiac related applications [10].

The embedded systems can be ideal candidates for the design of electrical and mechanical stimulation signal generators and several studies have been done on the development of electrical and mechanical bioreactors for stem cell stimulation. Mantero et al. have developed an electrical and mechanical bioreactor for skeletal muscles [11]. Pavesi et al. have developed a cell culture platform for cardiac tissue application [10]. However, these systems have large dimensions, high costs, low output load current and are not flexible or customizable in order to fit requirements of a specific stimulation application. Besides that, these systems lack the capability of monitoring the status of the stimulated cells. So, there is the need to develop an easy-to-use, low-cost, portable, flexible and accurate electrochemical stimulation system with monitoring capability for the cell stimulation applications.

1.4.2 Embedded Systems in Rehabilitation Therapy

Rehabilitation therapy aims at regaining or restoring the neurocognitive functions that are lost or diminished in patients that have suffered from neurological accidents. The physiotherapy market is expected to reach USD 165.73 billion by

2023 according to the market research report by *IndustryARC*.

Embedded systems are playing important roles in developing instruments for the rehabilitation therapy. Such instruments can be used for monitoring the movement of the patients, activity of their brain, stimulating the muscles of the patients as well as assisting them with their movements.

During the rehabilitation therapy, clinicians and researchers record the muscle activities of the patients and analyze the defects in their movements, then address proper methods for curing them. One of the commonly used embedded devices for the monitoring process are the EMG devices, such as COMETA, FreeEMG, Consensus, Shimmer, etc. These devices support multi-channel acquisition and also a continuous signal monitoring of up to 12 hours.

In some cases, the clinicians might need a long-term monitoring of the patient that require acquisitions of one to several days. The available EMG devices in the market cannot fulfill this long-term acquisition requirement. Furthermore, another factor that limits the usage of these devices is the high cost. So, there is the need to design a low power, low cost embedded system for the EMG monitoring.

1.4.3 Embedded Systems in Therapeutic Drug Monitoring

The therapeutic drug monitoring (TDM) is a branch of clinical pharmacology and clinical chemistry. It specializes in measuring concentration of drugs in blood [12]. The aim of the TDM is to improve the patient care through the adjustment of the dose. It is based on a priori clinical, demographic and pharmacogenetic information, and/or on the posteriori measurement of blood concentrations of drugs (pk/pd monitoring) [13].

According to the market report from *Markets and Markets* website, the therapeutic drug monitoring market is expected to reach USD 1.63 billion by 2023 from USD 1.16 billion in 2017.

Medical devices based on embedded systems are being widely used in the TDM. For example, immunoassay analyzers and mass spectrometry are widely used in centralized laboratories for TDM. Continuous-flow anaesthetic machine, bispectral index monitors, heart rate and blood pressure monitors are used by anesthesiologists during surgeries for continuous monitoring and anesthesia delivery.

In anesthesia delivery, anesthesiologists deliver the anesthesia to the patients according to specific delivery models that consider parameters such as age, weight, sex and height, as well as the Bispectral index and blood pressure of the patient. However, due to the patient variability and the metabolic process, it is difficult to accurately decide the amount of dose that needs to be delivered to the patient during surgery and excessive or insufficient amount of dose could produce severe problems to the patients.

So, an embedded system for continuous monitoring and delivery of anesthesia is

needed in order that the correct amount of anesthesia can be delivered to the patient during the surgery.

1.4.4 Embedded Systems in Cancer Diagnostics

According to the released reliable data about the global epidemiology of cancer by World Health Organization (WHO), cancer is listed as of the most common diseases. There are as many as 14 million new cases and around 8.8 million deaths around the globe due to the cancer.

Cancer diagnostics aims at detection of cancer and the early stage cancer detection is very importance in cancer diagnostics. More treatment options can be adopted when the cancer is in its early stage.

In recent studies, memristive biosensors are being used as a new way of detection of the cancer and have demonstrated ultra-high sensitivity in prostate cancer detection. These biosensors are used together with commercial probe stations and parameter analyzers [14].

However, although the memristive biosensors exhibit the high sensitivity for cancer detection, the measurement setup is very bulky, hard to use and the measurement takes too long time. Besides that, the processing of the measurement data is all manual and is processed separately. This adds further delays to the availability of the detection results. These problems could be addressed by designing an embedded system platform that hosts the memristive biosensors, carries out the measurement and data processing automatically. So, there is the need to develop an embedded biosensing platform that is easy to use, programmable, portable, has low cost and low power.

1.5 Research Challenges

As mentioned earlier, the thesis focuses on designing embedded systems for biomedical applications in different areas listed above. Due to the huge diversity of these areas, a single embedded system might not be able to meet all the requirements and specifications of these applications. So, a specific embedded system has to be designed in each application scenario.

Furthermore, in each application, the embedded systems are complex and the design process includes several teams to collaborate. Each design project may have different requirements and specifications, different design and test teams, different completion cycles. Last but not least, some of these designs have to be carried out in parallel.

However, the design of these systems cannot be random, but it has to follow proper design approaches or methodologies. Through the right design methodology, at the end of the design, one can guarantee the reliability and usability of the system and

the designed system might be able to meet all the requirements and specifications of the target application. The collaboration among different teams can be managed efficiently and design time could be optimized.

So, the key challenge is how to choose a proper design methodology or approach in order to design an embedded system for a given application. The selection of the methodology could depend on the complexity of the embedded system, amount of available information from the possible application, requirements and specifications of the biomedical application, experience of the design teams, affordable cost for the development, time to market and lifetime of the embedded system, available resources and technology for the design and production of the system, maintenance and upgrading requirements, etc.

1.6 Thesis Outline

In this chapter, the concept of the embedded system is introduced. The common types of embedded systems are analyzed. The design process is explained and several design methodologies are presented. The main goal of the thesis is to demonstrate how these design methodologies are applied successfully in designing complex systems for the biomedical applications and relevant results are presented and discussed.

The following chapters of the thesis are organized as follows:

- In Chapter Two, the state-of-the-art in regenerative medicine and tissue engineering is introduced. Then the challenges and research goals are presented, followed by the analysis of the project and selection of the design methodology. Then the detailed steps of the design approach are explained. Finally the test results are presented and discussed.
- In Chapter Three, a wearable wireless low power surface EMG system is presented. The system is implemented using the successive refinement model and relevant results are presented.
- In Chapter Four, an electrochemical sensing platform for continuous monitoring of anesthesia is presented. The design process of the system has followed the hardware and software design model and several electrochemical experiments have been carried out in order to validate the design of the system.
- Chapter Five is about a novel point-of-care memristive biosensing platform for cancer detection. The system is designed using the hardware and software design model and test results related to the measurement of Prostate Specific Antigen are presented.

- Chapter Six presents a general purpose interface bus system that supports any type of electronic biosensors and provides a interface bus standard. In this design, the hardware and software design model is used. For the validation of the generality of the system, three types of electronic biosensors are designed and relevant tests are presented.
- Chapter Seven is the conclusion of the whole thesis and it presents the future work.

Chapter 2

Electromechanical Bioreactor System Design

2.1 Introduction

2.1.1 Regenerative Medicine

Regenerative medicine is one of the new disruptive technologies that are attracting more focus in recent years. It includes the tissue engineering, biomedical engineering techniques, gene therapy, cell therapies and also other treatments involving biology, pharmaceuticals and devices. The main aim of the regenerative medicine is to replace or regenerate the tissues, human cells or organs for the patients that have undergone some diseases or injuries that have caused the permanent damage of their tissues or organs [15]. This can help with therapeutic treatments where the current methods are inapplicable.

In the regenerative medicine, the cell therapies and tissue engineering enable the delivery of safe, consistent and efficient therapy. The human body can be modeled as a complex micro-fluidic system which can regenerate or repair its organs or tissues through stem cells which can be found in those organs or tissues. The regeneration and repairing is done through evolution of the stem cells, so the contribution of stem cells for the regeneration medicine is vital [16].

2.1.2 Stem Cell Differentiation

In the beginning of 19th century, scientists have discovered that the different types of blood cells in the human body were originated from a particular cell, called 'stem cell'. Becker et al. (1963) discovered that these stem cells had the capability of self-renewal and differentiation into various cell lineages. Under certain physiological conditions, with the right stimulation signal, these stem cells can convert

into specific cells of the body, such as cardiac cells, muscle cells, liver cells, tendon cells and so on.

The physiological conditions are created using scaffolds. Scaffolds are special mechanical structures with biodegradable materials and they can host the stem cells, can interact with the stem cells and facilitate cell attachment allowing great structural biomimicry [17]. The scaffolds are similar to the extra-cellular matrix which exists in all mammalian organs and tissues [18].

On the other hand, the biofunctional stimulation signals can be generated through signal generation units and are applied to the scaffolds on which the stem cells are immobilized or tethered. So, the communication between the extra-cellular environment and stem cells can be modulated through scaffolds [19]. Therefore, the key challenges are to design engineered scaffolds and electronic systems that can generate the right stimulation signals.

Tendon injury is common among elderly people and athletes. One way to cure the injury is to use healthy tendon cells to replace the damaged tendon tissues. However, these tendon cells come from the donation, and are very limited in amount. Tendon tissue engineering has paved the path to culture new tendon cells in vitro using specially designed tendon scaffolds [20].

2.1.3 Research Objective

The objective is to design a system that generates stimulation signals and also hosts stem cells. As the natural functions of the tendon require mechanical stimulation for the stem cells, the system has to be capable of generating mechanical stimulation. Furthermore, if the system generates also electrical signals, then the system can be used for the cardiac tissue engineering, where the hosted stem cells are differentiated into cardiac cells through applied electrical and mechanical signals. Besides that, the system has to have a low cost, be robust and portable. Besides that, there is the need to keep the system running continuously for several days and also a continuous monitoring of the cells might be necessary. In the mechanical signal generation, a stepper motor is adopted. So, it is also necessary to guarantee a safety operational condition for the motor. Therefore, the system has to perform tasks in real-time for the monitoring and motor control.

2.2 Project Analysis

As it is stated in the previous section, the aim is to design an electronic system for cell stimulation and monitoring. Electrical and mechanical stimulation signals should be generated from the system and the platform has to be able to carry out real-time monitoring. However, it is not yet clear how the electrical and mechanical

stimulation effects the cells and how the cells change. So, it is preferred to have an initial prototype of the system in order to have some feedback regarding the system requirements and validate the design concept. Then, in the next version of the system, the possibly encountered problems can be addressed. Besides that, further functional requirements would be added to the system during the design and test steps. So, the successive refinement model is suitable for the design process of the system.

2.3 Model Implementation

This section describes how the design steps of the successive refinement model are implemented. After the first complete cycle that includes steps from requirements to the system integration. The first prototype of the system is complete. After the test and validation, the design techniques, hardware and software blocks are optimized and refined in the next cycle of the system design.

2.3.1 Requirements

The functional requirements of the electromechanical stimulation and monitoring system are following:

- Voltage signal should be generated for the electrical stimulation.
- The voltage should be AC type with an amplitude in the range of 0.2 to 5V.
- The voltage signal should not have an DC offset.
- The voltage should be a square wave with a frequency of 1 Hz for human cells and 3 Hz for mice, and a pulse duration of 1-3 ms.
- There is only one stretching motor used for the mechanical signal generation.
- It would be great to monitor the stem cells in real-time during the stimulation.
- Safety operation should be guaranteed for the motor as it is tied to the scaffold.

The non-functional requirements can be as following:

- The system should monitor the cells in real-time.
- The system should be cost-effective.

- The system should be portable, should have a proper physical dimension and moderate weight.
- The system should be reliable and should operate as expected.

2.3.2 Specification

After the requirements are written, the next step is to specify in more details the needs of the actual application and also to translate the needs into the design requirements of the system. For the electrical stimulation, a voltage signal is needed, so there should be a functional unit that can generate the voltage signals. Besides that, the voltage signal is an AC type square wave voltage signal with a fixed frequency, with a variable amplitude and pulse duration. So, the functional block of the electrical stimulation should be able to generate a voltage signal that can be tuned. The output of the voltage signal is without a DC offset, so the functional unit should be able to generate an AC voltage signal without an offset. The voltage signal has a fixed frequency, so the timing requirement should be respected when the signal is generated.

The mechanical stimulation signal comes from the motor, so there should be a functional block that can drive and control the single motor according to the needs of the stimulation. The motor is connected to the scaffold, so it is important to have a safe operating status of the motor and its movement should be precisely controlled.

The monitoring of the cells in real-time is also part of the goal of the system. So, there should be a functional block with integrated camera for the monitoring. It should also respect the real-time monitoring requirement, so this functional unit should have a fast image processing capability and a display or monitor is needed.

2.3.3 Architecture

After the specifications, the next step is to design the architecture of the system. As it is stated earlier, there is the need to have a real-time monitoring capability. So, the system should be a real-time embedded system with high performance microprocessors or micro-controllers. The design of the architecture is composed of two parts: hardware architecture and software architecture.

The hardware architecture has to contain functional blocks that generate electrical signals, drive and control motors, monitor cells in real-time. Besides that, there has to be a central control block that takes control of all other hardware blocks and interacts with the user input. So, a possible hardware architecture with these functional blocks can be as depicted in figure 2.1. The software architecture should contain the functional blocks that carry out the correct operations, such as

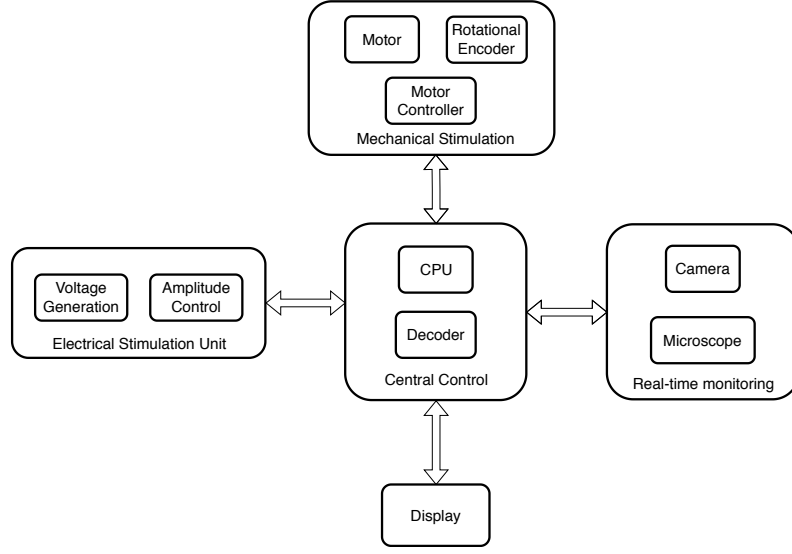


Figure 2.1: Block representation of the hardware architecture of the system.

generation of expected voltage signals, precise movement of the motor, real-time monitoring of cells and correct interaction with the user. The software architecture can be as depicted in figure 2.2.

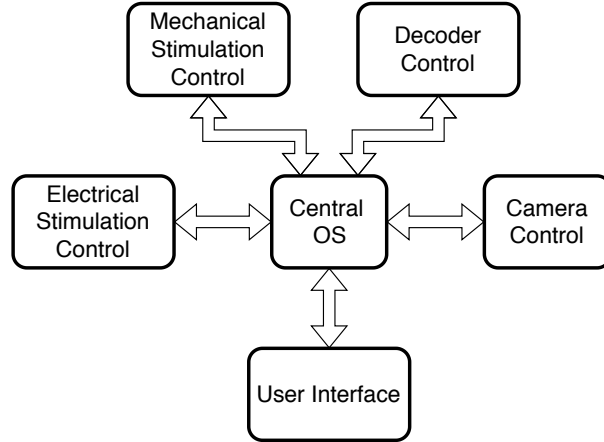


Figure 2.2: Block representation of the software architecture of the system.

2.3.4 Components Design

In this components design step, both the hardware and software architectural designs are decomposed into detailed hardware and software components. The selection of the components in this step is based on the functional and non-functional

blocks in the architecture design. They can be chosen from the ready-made components, or they need to be designed by the designer.

Hardware Components Design

A) Central Control Block. The central control block is composed of the Raspberry Pi (RPI) 3 Model B Microcomputer. The RPi contains Raspbian OS and it can be used as a computer. Besides that, it has several advantages as Quad-core, 1GB RAM, HDMI Port and 40 GPIO pins [21].

The RPi communicates with the electrical stimulation block through the I2C interface. While it controls the mechanical stimulation block through the GPIO interface and through its camera port it controls the real-time monitoring block. The user can control the system through the USB port and can setup the test parameters through the monitor which is connected to the RPi through HDMI cable.

B) Electrical Stimulation Block. As it is mentioned earlier, the electrical stimulation block generates the voltage signal necessary for the cell differentiation and it should be configurable for the waveform amplitude and pulse width.

So, the Digital to Analog Converters (DAC) and digital potentiometers are deployed to meet all these requirements. The sampling frequency can be set by controlling the writing interval of the DAC. The amplitude of the waveforms can be controlled through the value of the digital values of the DAC and the amplitude range can be set through the digital potentiometers. The bipolar waveform can be generated through two DACs with complementary voltage outputs. The MCP4275 DAC is selected for the digital to analog conversion as it has a 12-bit resolution, can work between 2.7V and 5.5V. It can also be controlled through the I2C interface and can easily be controlled by external devices.

C) Mechanical Stimulation Block. The mechanical stimulation block generates the mechanical stimulation signals through the interaction between the polymer materials of the 3D scaffold and a mechanical motor. The 3D scaffold hosts the stem cells, while the motor generates the movements. Besides that, the rotational encoder is attached to the motor so that it can generate electrical encoding outputs for each rotational position of the motor.

There are usually 3 types of motors, such as DC motors, servo motors and stepper motors. The DC motor is used for applications where the continuous rotation is required. While the servo motor can generate very high torque with accurate rotation angle. The stepper motor is used in applications where a slow periodic movements are needed. The mechanical stimulation signal is generated through the rotation of the motor, so a highly precise motor control is necessary for the safety of the stimulation of the cells. In this design, the NEMA 11 11HS12-0674S stepper motor is chosen. It has the rotation accuracy of 1.8 degree, can generate high torque and

can be controlled through its driving circuit which can be interfaced easily to external embedded systems. The Figure 2.3 shows the prototype of the mechanical stimulation unit that is composed of a stepper motor, a rotational encoder, and a 3D scaffold.

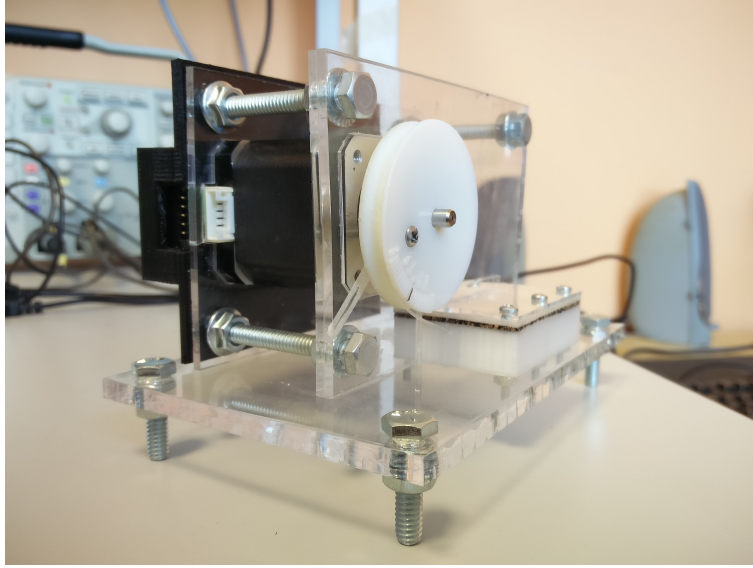


Figure 2.3: The motor and scaffold connection [22]

D) Real-time Monitoring Block. Real-time monitoring of the stem cells can be helpful for the observation of the stem cells. A properly designed monitoring system can keep track of the cells under stimulation. For this, we have developed a digital microscope using the RPi camera, standard 20X microscope objective and custom holders. The RPi camera module is equipped with 8MP optical sensors and can be connected to the RPi through the CSI interface. The Figure 2.4 shows the RPi camera with its connection to the RPi: In order to integrate the RPi Camera module with the microscope objective, we have removed the lens of the camera module and placed the camera module directly on top of the microscope objective. In this way, the amplified objects can be sensed directly by the camera module and can be visualized inside RPi. Then we have designed specific holders for the camera module and the microscope objective in order to fix them on the metallic holder. Figure 2.5 shows the first prototype of the RPi camera based digital microscope. The RPi contains the libraries for capturing videos and images and also for real-time display. So, there is the possibility to monitor the stem cells under stimulation in real-time thanks to the camera libraries inside the RPi.



Figure 2.4: The Raspberry Pi camera [22]

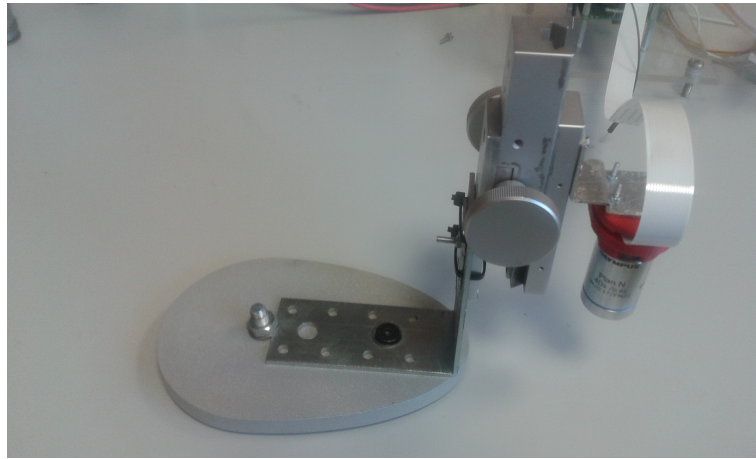


Figure 2.5: The Raspberry Pi camera based microscope [22].

Software Components Design

According to the specification of the bioreactor system, the generated electrical and mechanical signals should be configurable in terms of frequency, amplitude and waveform type. So, in order to make the system configurable, a user configurable software application is developed inside the Raspbian OS running inside the RPi. The main task of the software application is to control the electrical stimulation unit, mechanical stimulation unit and camera monitoring unit, to establish the communication between these units and RPi, and also to carry out data analysis and generate commands inside the RPi.

The software is developed in QtCreator 5.3 using the C++ programming language and also the Qt libraries. The advantage of using the Qt software development environment is that, once the application is ready, it can run on Windows, Linux and MAC, so the application will be a cross-platform application supporting all

types of main operating systems.

In this section, the detailed software components of the whole system is explained. it is composed of electrical stimulation, mechanical stimulation, camera monitoring and decoder control blocks. The overall software architecture is shown in Figure 2.6.

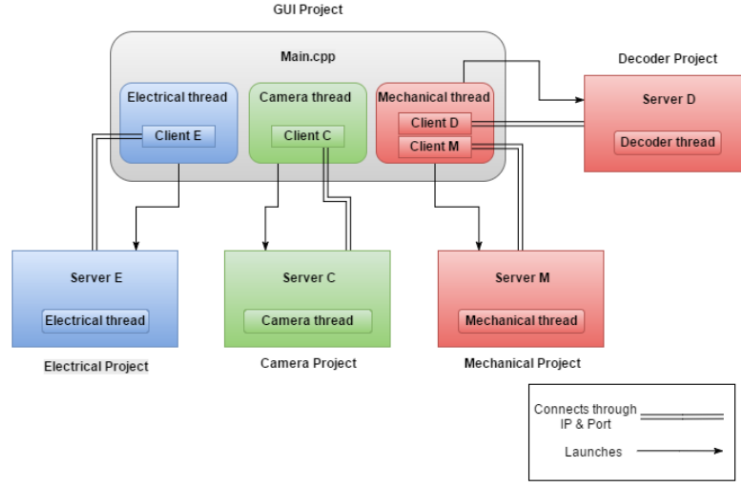


Figure 2.6: Software architecture of the bioreactor system [22].

A) GUI. It can be seen that the software application of the system is composed of five different projects: Graphical User Interface(GUI) project, electrical project, mechanical project, camera project and decoder project. The GUI project is the core of the all projects and it controls the whole application. It contains a user interface that configures the experimental parameters for the electrical and mechanical stimulation and also controls the RPi camera. The communication between the GUI project and other projects are based on TCP/IP communication as there are QTCP clients that correspond to the electrical stimulation, mechanical stimulation, decoder control and camera monitoring inside the GUI. While in each of the electrical project, mechanical project, decoder project and camera projects, there are corresponding QTCP servers that communicate with the clients inside the GUI through given IP and ports. The clients and servers in these projects run on individual threads, so that the mechanical stimulation, electrical stimulation and camera control tasks can be carried out independently. The Figure 2.7 shows the graphical user interface used to control the whole bioreactor stimulation and monitoring system.

B) Electrical Stimulation Block. As it is mentioned earlier, the GUI project

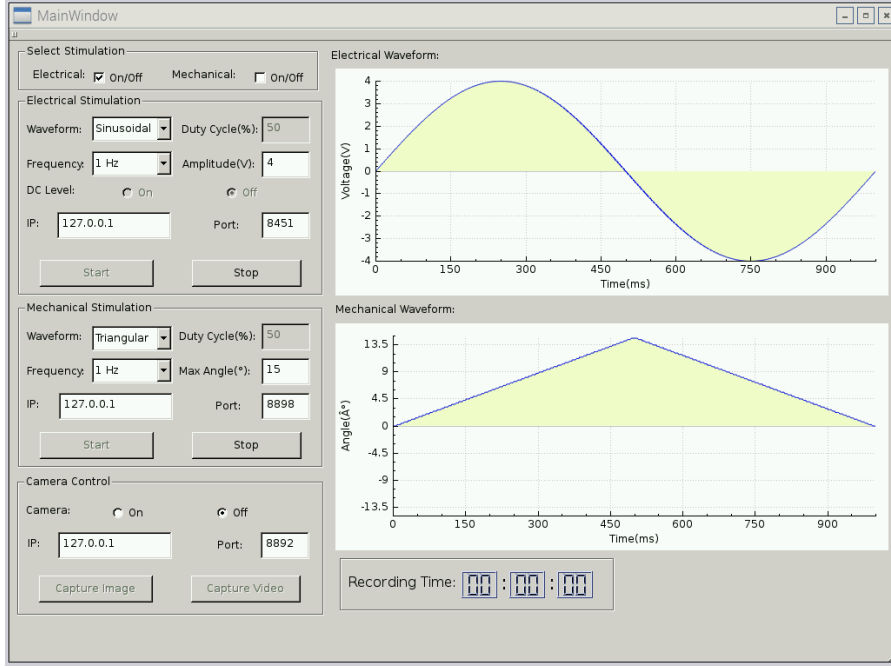


Figure 2.7: Graphical User Interface of the bioreactor system [22].

contains the thread that controls the electrical stimulation and interacts with the electrical project. This thread contains a TCP client that communicates with the TCP server inside the electrical project.

After the test parameters for the electrical stimulation are set, the user clicks the start button in the electrical stimulation panel. Then the electrical thread will create a process and run the electrical project by forwarding the test parameters. After the parameters are received, they will be extracted inside the electrical project and the DAC samples will be generated from these parameters. Then TCP server inside the electrical thread will be ready for the communication with the GUI project and wait for the TCP client connection from the IP address and port parameters.

When the TCP/IP communication is established, electrical project will send back the digitally created samples to the GUI project in order to confirm that the parameters are received by the electrical project. Then the GUI project will send the start command and the electrical project will start sending the samples to the DACs and generate the desired electrical signals. The Figure 2.8 shows the detailed work flow of the electrical thread inside the GUI project and the Electrical project.

C) Mechanical Stimulation Block. This part explains the firmware related to the mechanical stimulation. The mechanical thread created inside the GUI

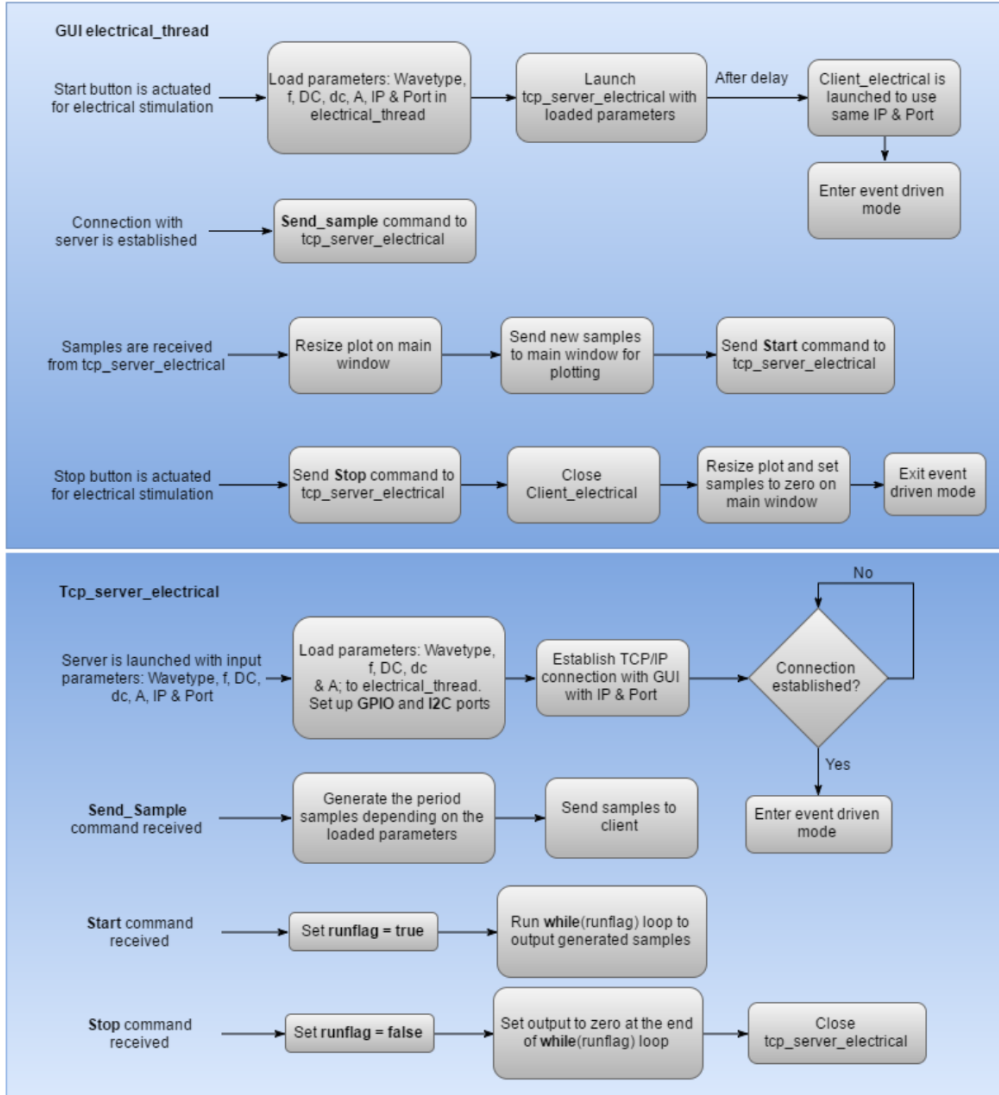


Figure 2.8: Work flow of the electrical stimulation process on the client and server side [22].

project contains two clients, one for communicating with server inside the mechanical project, one for the server inside the decoder project.

After the test parameters are set in the mechanical stimulation panel, the mechanical thread creates two processes for the mechanical project and decoder project. The mechanical project controls the rotation of the motor through the motor driver, while the decoder project controls decodes the incoming electrical signals from the optical encoder and sends the rotation position to the mechanical project as a feedback. In this way, the mechanical project can track in real-time the rotation of the motor and can guarantee a safe operation of the motor. Figure 2.9 displays how

the mechanical thread works inside the GUI project. The Figure 2.10 explains the

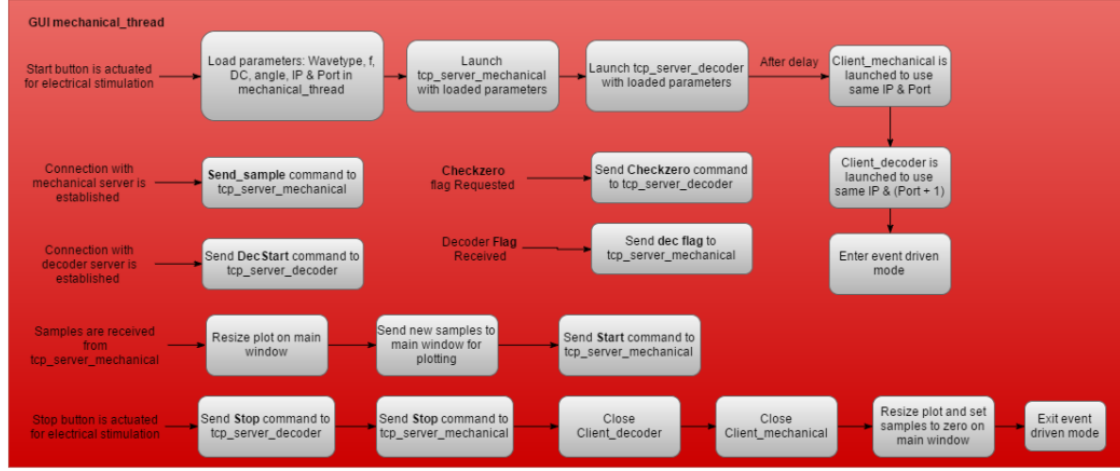


Figure 2.9: Work flow of the mechanical thread on the GUI project [22].

work flow on the mechanical project.

D) Decoder Block. Figure 2.11 explains the work flow of decoder block. The project measures the rotation angle of the motor and then gives a feedback to the mechanical project in order to guarantee a safe rotation range of the motor.

E) Real-time Monitoring block. The camera project controls the camera and captures images, videos, displays the observation of the microscope objective in real-time.

The different operations can be executed through the TCP/IP communication between the camera thread inside the GUI project and the TCP server inside the camera project. When the video recording is on, the elapsed time will also be displayed on the panel. In Figure 2.12 is depicted the work flow of the camera thread inside the GUI project, while Figure 2.13 shows the work flow of the camera project.

2.3.5 System Integration

In this step, the hardware and software components are placed together and the complete system is built. Figure 2.14 presents the first prototype of the bioreactor system that is capable of generating electrical and mechanical signals, and can also carry out real-time monitoring of the cells inside the 3D scaffold.

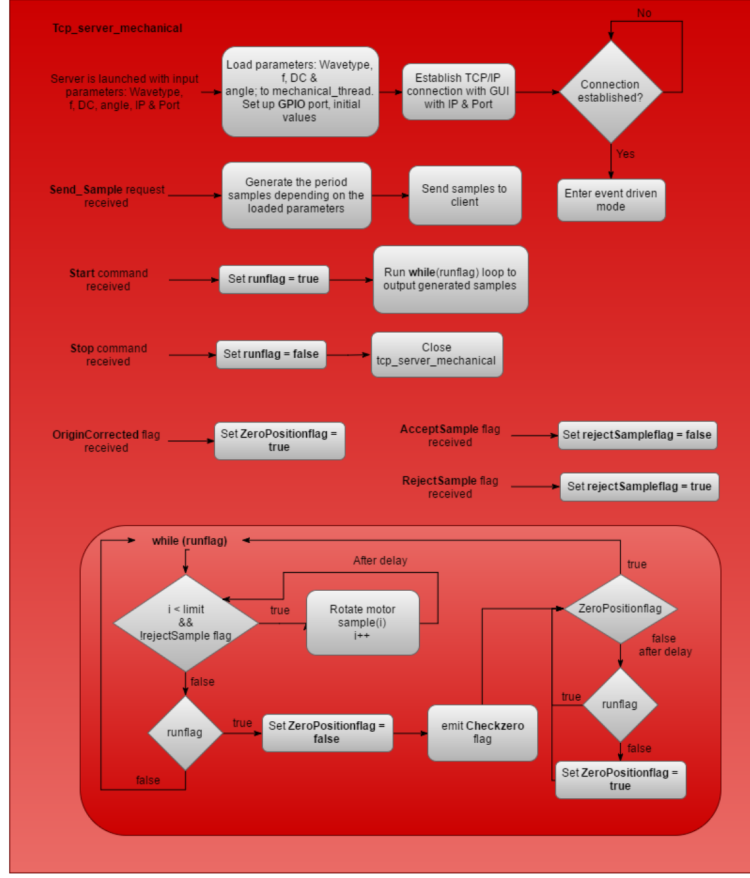


Figure 2.10: Work flow of the mechanical project [22].

2.3.6 System Refinement

As previously mentioned, during the design, the successive refinement approach is adopted. After the design of the first prototype, the hardware and software functional blocks are tested and the design techniques are validated. The improvements in each functional block are described in this section.

Central Control Block

The main update in this block in the new version is the usage of more powerful Raspberry Pi (RPi) 3, as it has higher performance with more robust internal hardware resources.

Electrical Stimulation Block

In the first prototype of the system, the electrical stimulation hardware block generates only a square wave voltage, while in the new version, besides the square

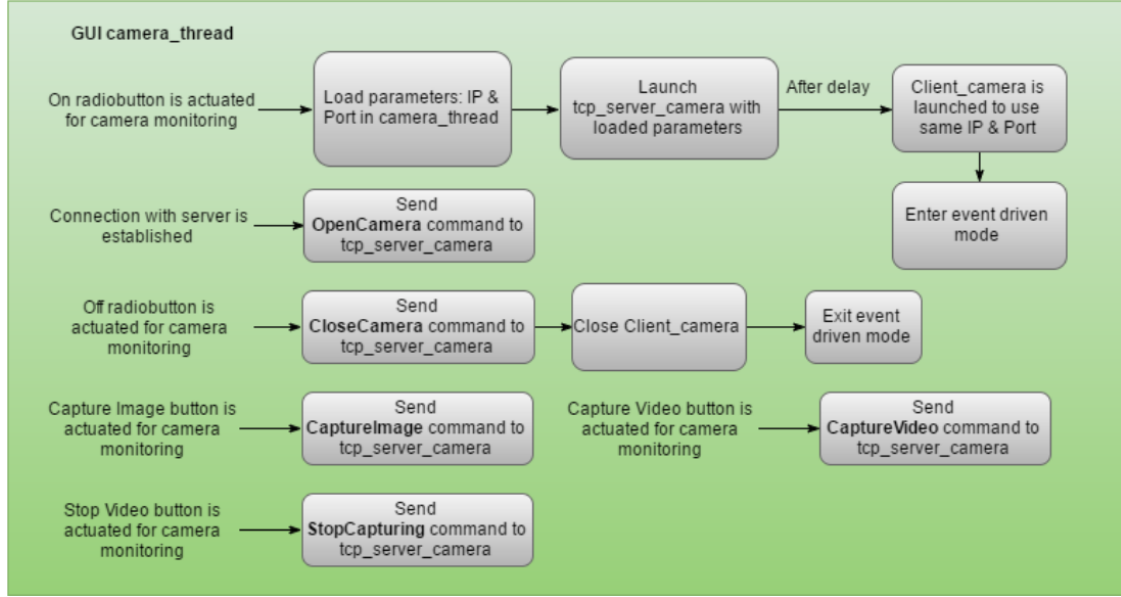


Figure 2.12: Flow chart of the camera thread inside the GUI project [22].

Real-time Monitoring Block

In the new version, the monitoring of the camera is based on the GPU of the RPi and it supports much higher frame rate and there is the possibility to capture images and videos. The other change is in the microscope holder and it is very light with better usability.

2.4 Validation of the System

In the previous sections, the different units of the bioreactor system were explained. After the design of the system, the next step is the validation of the system to check if it could carry out the tasks specified during the documentation of the overall system and function correctly, according to the configuration set through the user interface.

2.4.1 Electrical Signal Generation

This section contains the validation for the electrical signal generation unit. As indicated before, the electrical stimulation unit should be able to generate different shapes of waveforms, such as Sinusoidal, Triangular, Square, Gaussian 1st derivative, Gaussian 2nd derivative and ECG (an artificial reproduction of an ElectroCardioGraphic signal). Besides that the system should be able to generate each

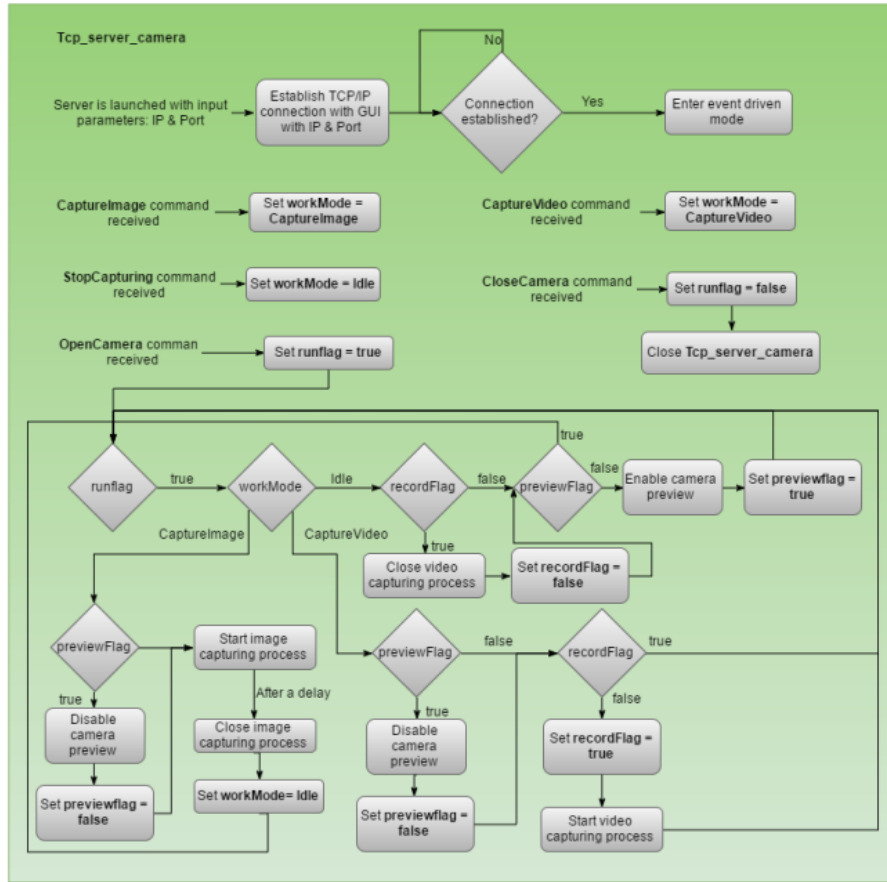


Figure 2.13: Flow chart of the camera control process on the server side [22].

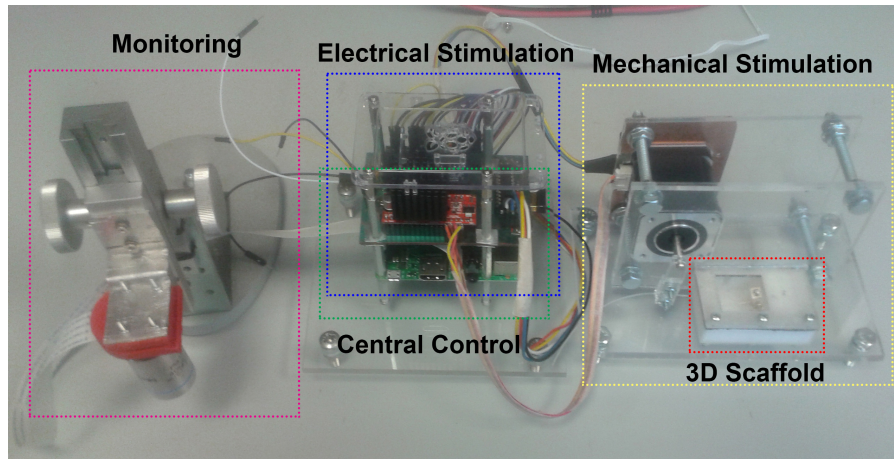


Figure 2.14: First Prototype Electrical-Mechanical Stimulation and Monitoring System [22].

type of the waveform with the frequency and amplitude indicated in the user interface.

2.4.2 Mechanical Signal Generation

In this section, the validation is carried on the mechanical signal generation unit. According to the requirements on the mechanical stimulation, the mechanical stimulation unit should be able to generate mechanical movements that vary in the sinusoidal, triangular and square forms.

In order to carry out the validation, the mechanical waveform parameters are set and the mechanical signal generation starts. In order to check if the mechanical movement corresponds to the assigned frequency of the setup, the rotational encoder output is measured. As the movement is periodic, the output of the encoder will also be periodic and its output signal can be displayed in the oscilloscope. Then we can measure the period of the waveform and compare it with the preset value. Figure 2.15 shows the output channels of the encoder and it can be seen that the movement of the motor is periodic. By measuring the repetition period of the waveform we can measure the frequency of the rotational movement of the motor.

Besides the frequency, the next parameter is the amplitude of the mechanical wave,

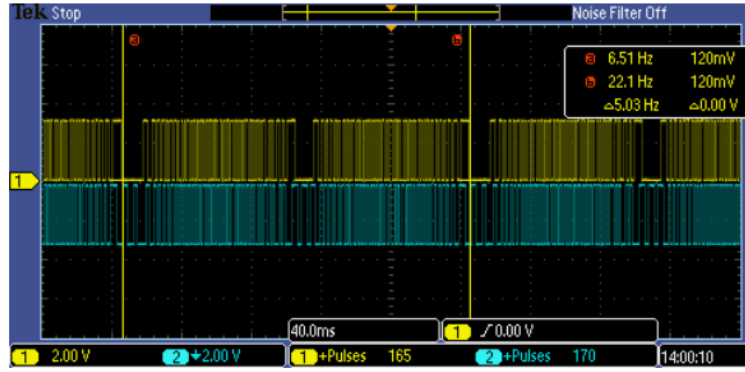


Figure 2.15: Encoder output at the mechanical stimulation [22].

or let us say the maximum rotation angle of the waveform. This can be measured through the ImageMeter Pro application. Here in the Figure 2.16 below is the angle measurement from ImageMeter Pro and it displays the maximum rotation angle of 30.2 degrees, which is quite close to the preset amplitude of 30 degrees.

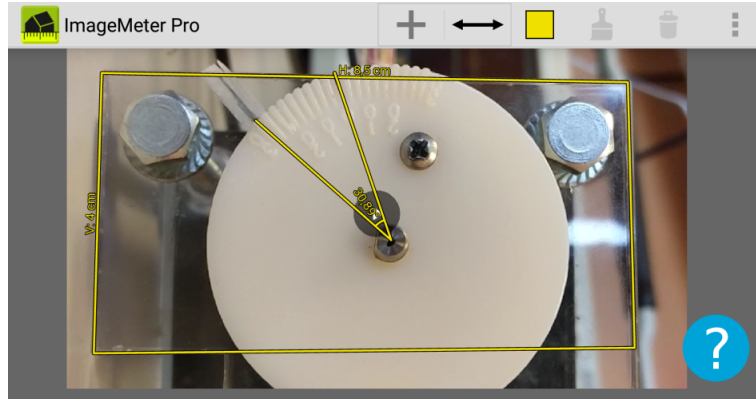


Figure 2.16: Measurement of rotation angle from the ImageMeter Pro application [22].

2.4.3 Real-time Monitoring

This section includes validation on the monitoring unit. The Figure 2.17 shows the setup of the test and there is the nano gap circuit placed under the custom designed microscope. The objective is the standard 20X one, which amplifies the nano gap circuit by 20 times. The focus of the microscope can be adjusted manually in order to have best resolution of the monitoring image.

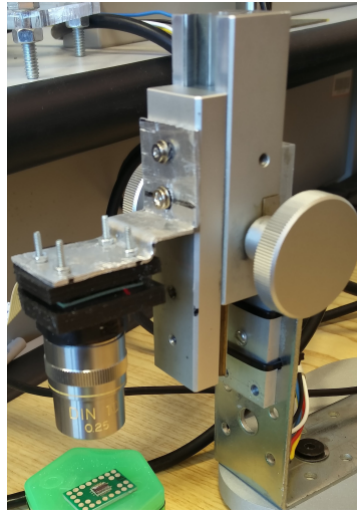


Figure 2.17: Setup for observing nanogap circuit using the monitoring system [22].

2.5 Experimental Results

This section presents some results on the system regarding the differentiation of Mesenchymal stem cells (MSCs) into tendon cells using mechanical and biochemical stimulation. Figure 2.18 shows the bioreactor model [23].

In this figure: A) demonstrates the schematics of the bioreactor function and purpose. After mounting the samples into the bioreactor system, stimulation is carried on under tensile cycle load in order to perform dynamic culture of the cell and improve cell proliferation alignment. B) shows the Raspberry Pi based electronic circuit that drives the stepper motor and stimulates the scaffolds through a wire. C) is the chamber model designed in SolidWorks. D) presents a PMMA model which is designed to minimize the working volume and maintain the sterility. In E), the samples were loaded in the chamber and stimulated mechanically for 7 days (4 hours/day). F) shows the mounting of the scaffolds into the bioreactor system, incubation and culturing under dynamic condition [23]. In Figure 2.19, the de-

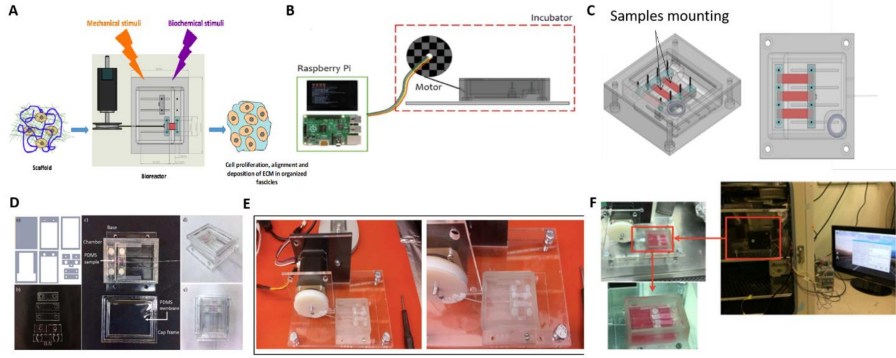


Figure 2.18: Bioreactor Model [23].

tailed steps involved in the cell differentiation are shown. The detailed explanation of each step can be found in [23]. The Figure 2.20 shows the stimulation of cells under Static Condition (SC) and Dynamic Condition (DC) in 7 days. In static condition, no mechanical stimulation is applied.

Figure 2.20.A) shows the fluorescence images of the cell cytoskeletons after 7 days of culture and we can see the cell alignment in the direction of the stretching for the scaffolds stimulated mechanically, while cells cultured under static conditions show random orientation.

Figure 2.20.B) shows the alignment of cells quantitatively and reports upto 40% cell alignment in the direction of the strain under mechanical and biochemical stimulation.

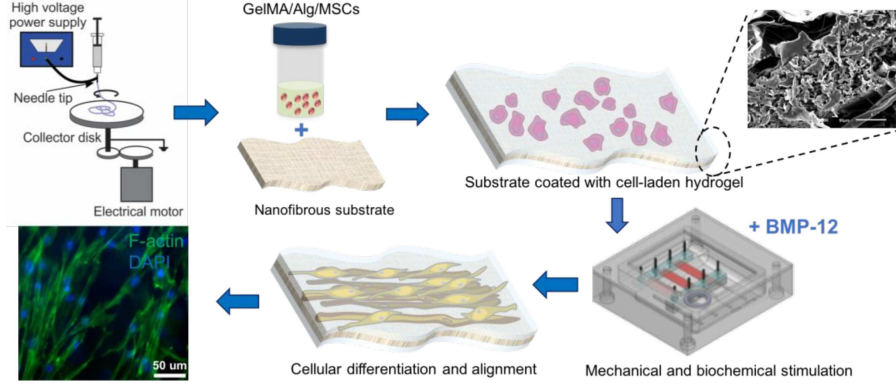


Figure 2.19: Experimental steps [23].

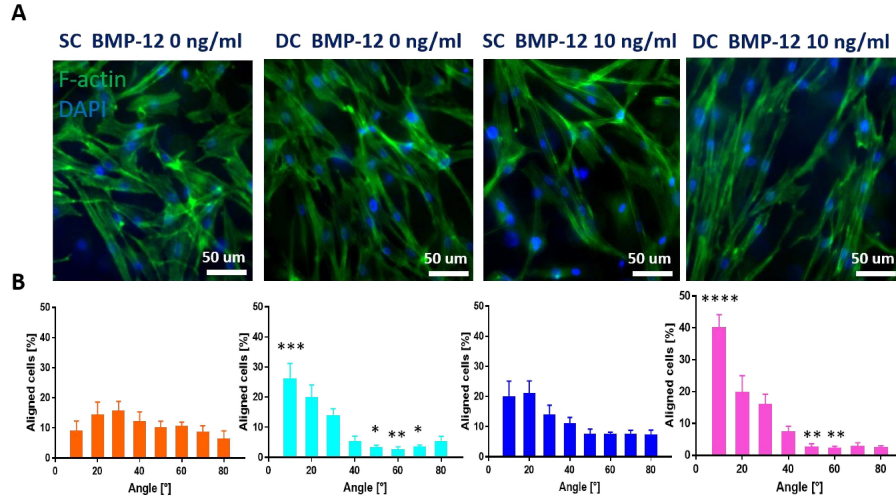


Figure 2.20: Results on the mechanical and biochemical stimulation of MSCs [23].

2.6 Discussion and Conclusion

In this project, a novel type of smart, flexible and easy-to-use bioreactor system is designed and validated. Starting from the requirements and specification of the system, choosing the architecture, the components, designing the hardware, validating the system and carrying out experiments, we have strictly followed the successive refinement model design procedure.

The system is smart, because it can carry out operations without the involvement of the user, such as the controlling of the motor, automatic tracking of the motor rotation, estimating the safety status of the motor and carrying out corrections. In this version, machine learning algorithms have not yet been implemented, but there are plenty of libraries available inside Raspberry Pi 3 and they will be studied and integrated into the system in order to make it more smart.

The system has been successfully tested on the generation of tendon cells in the Khademhosseini Lab at MIT premises in Boston, and we were able to differentiate the stem cells into the tendon cells by providing proper physiological environment and a mechanical stimulation from our system. The relevant results were recently accepted as publication in the ACS Journal on Biomaterials Science & Engineering.

Chapter 3

Wearable Wireless Surface EMG System Design for Muscle Synergies

3.1 Introduction

3.1.1 Muscular System

Brain is an organ which is center of the nervous system in all living animals and human. Its function is to control other organs of the body. A neural accident such as a stroke or traumatic brain injury or spinal cord injury can cause changes in motor functions of the patient which include physical, social and mental disabilities. This maybe caused by a compromised nervous system that results in damaged motor nerves and it can be also due to the interruption of the communication between the central neural system and different parts of the body [24].

In human body, the muscular system cooperates with other organ systems such as skeletal system and neural system in order to carry out movements of the body, posture and stability control, blood circulation, heat production and help in digestion. The movement is generated from the muscular system when an electrical stimulus is received from central nervous system. This stimulus is called action potential and it creates voluntary or involuntary movements of the muscles.

The muscular system is composed of three types of muscles:

- **Skeletal Muscle:** The muscle is attached to the bone through tendons and it carries out movements such as locomotion, posture, facial expressions and other types of voluntary movements of the body [25].
- **Cardiac Muscle:** This muscle exists in the walls of the heart and this muscle works in autonomous and rhythmical way [26].

- Smooth Muscle: This muscle exists in blood vessels, internal organs and other parts that carry out involuntary movement [26].

When the voluntary movements of the human body are carried out through the contraction and relaxation of the skeletal muscle, electrical signals are generated. These signals are controlled from the central nerves system and are dependent on the type of the skeletal muscle [27]. So, measuring these signals can help clinicians understand the disorders of the motor control in the patients that suffered neural accidents. The technique used for the measurement of these signals is called Electromyography (EMG).

3.1.2 Surface Electromyography (sEMG)

The EMG technique can be divided into two types: Surface EMG and the intramuscular EMG. The surface EMG carries out the assessment of the muscle function by recording from the surface on the skin the muscle activity. The intramuscular EMG records the electrical signals by inserting the electrodes into the target skeletal muscles.

Once the EMG data is available, the next step is to calculate muscle synergy data using Non-Negative Matrix Factorization (NNMF) method. In this way, the contribution of muscles in each synergy can be obtained and therefore, it is possible to evaluate the activity of each muscle from the calculated synergy data [28].

In this research, the surface EMG is studied as it has following advantages:

- It can give information on the duration, on the moment, on the activation entity of a muscle during movements;
- It is possible to provide indications on the overall activity of a muscle group or an individual muscle;
- It can demonstrate the maximum degree of relaxation or contraction of muscles or muscle groups of the patient, which is also called the Bio-feedback;
- It can provide analysis on the muscle in a non-invasive approach;
- It can be used for controlling other devices;
- It is possible to carry out long-lasting and dynamic tests with this technique;
- It is easy to carry out and is painless.

So, with all these advantages, it has become a very popular technique in the clinical and rehabilitation applications [29].

Currently, there are ways of setups in recording the sEMG signals, depending on the

materials, detection configurations and dimensions. Materials that are mostly used for fabricating sEMG electrodes are silver chloride (AgCl), gold (Au) or silver (Ag) or mix of silver and silver chloride (Ag/AgCl). The main reason for using these materials in the fabrication is that the polarization of the electrodes can be avoided, the surface potential sensitivity to the movement artifacts of the electrode can be reduced and the electrode-skin interface stability can be increased by interposing a conductive gel layer [30].

Besides the differences in the materials, the sEMG recording can be different also based on the montage of the electrodes. There are commonly two types of recording: a) monopolar and b) bipolar. The Figure 3.1 shows the two different types of electrode configuration: It can be seen from the Figure 3.1 that, in the monopolar

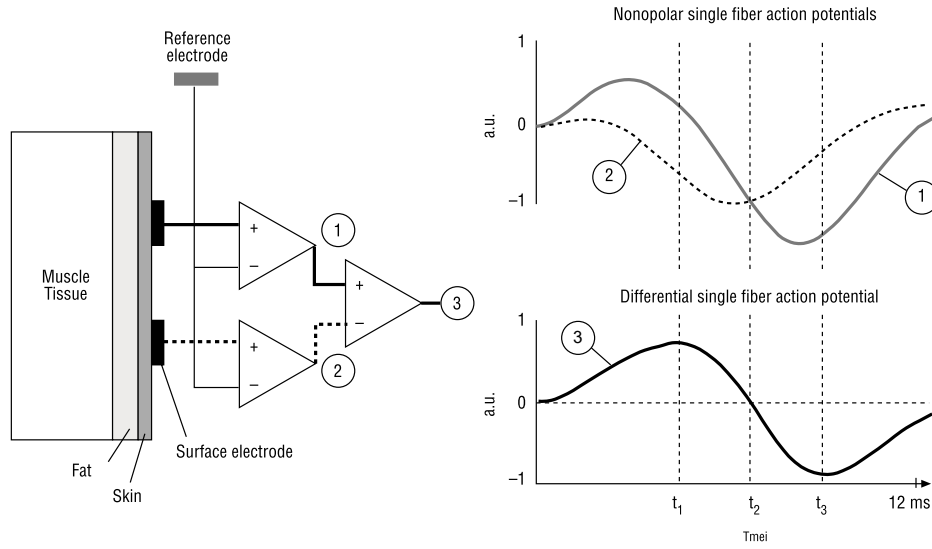


Figure 3.1: Electrode montage types and the detected action potentials in each configuration [30]

configuration there are two electrodes: a reference electrode and a single surface electrode. In the bipolar configuration, there are three electrodes: a reference electrode and two surface electrodes.

The monopolar configuration has large sampling volumes and is very susceptible to the disturbances. It also keeps all the information in the captured signals with no spatial filtering. The bipolar configuration has a reduced sampling volume and is less susceptible to external disturbances. Therefore it can provide a more clean and stable signal compared to the monopolar configuration [30].

3.1.3 Commercial EMG Devices

There are many existing commercial EMG devices for recording surface EMG signals. Some popular ones are FREEEMG, PicoEMG, DataLITE sEMG.



Figure 3.2: Commercial EMG Devices

- FREEEMG: This device is produced by BTS Engineering and it supports upto 20 probes for simultaneous signal recording. It has a battery life of 6 hours for a continuous acquisition. It has a dimension of $41.5 \times 24.8 \times 14mm$. However, it does not support a uSD Card storing.
- PicoEMG: This device is produced by Cometa and it is based on two monopolar electrode configuration. It can support synchronous acquisition of upto 32 devices and it can support upto 12-hour continuous signal acquisition with wireless transmission and 8-hour data logging with memory on board.
- DataLITE sEMG: The DataLITE sEMG is produced by Biometrics ltd. It has adimention of $42 \times 24 \times 14mm$. It can support upto 8-hour continuous signal acquisition.

3.1.4 Research Objective

As it is reported in section 3.1.3, all these available sEMG devices cannot last beyond 12 hours for a long term monitoring. Therefore, it is necessary to develop a low-power sEMG system that supports multiple channel acquisition with a long lasting battery life as possible.

3.1.5 Project Analysis

In this project, the aim is to design a low-power surface EMG that could last as long as possible for a continuous measurement on a single charging of a battery. Besides that, the system should be wearable, synchronous among probes and wireless.

So, the challenges are on the power consumption, dimension, wireless communication, timing and of course the cost. All of these constraints put limits on type of the electronic system, selection of components, design approach and techniques.

From the goal of the system, what is needed is a stand-alone low-power embedded system that can work continuously for the expected amount of time, such as several days. Therefore, for the design of the system, it is necessary to follow the embedded system design methodologies thanks to the advantages of such approach described in Chapter 1.

Regarding the designing of the system, the idea is to select an architecture, define the technology, design the first prototype and then improve the system step by step. So, the successive refinement model is the right choice for designing and validating the design concepts and techniques then refining it in the next versions of the design.

3.2 Model Implementation

The section is dedicated to how the steps are realized in the successive refinement model. In this model, the first step is to describe the requirements of the system, then list all the possible specifications followed by the architecture. Then the implementation of hardware and software components is described with system integration at the end. After the first prototype is ready, the next cycle starts with the improvements in each step and so on.

3.2.1 Requirements

The requirements of the system include both the functional descriptions and non-functional descriptions. The functional requirements can be summarized in the following list:

- Measurement of surface EMG signals;
- Simultaneous recording from up to 16 measuring probes;
- Long-term monitoring;
- Wearable system;
- 1KHz signal sampling frequency;
- Local storage of data;
- Clean and stable EMG signal
- Wireless control of measurement probes.

Non-functional requirements can be summarized in the following list:

- Affordable cost;
- Data collection and processing capability;
- Reliable wireless communication between the controlling and measurement nodes;
- Battery powered;
- Acceptable design time.

3.2.2 Specification

After the description of the requirements, the next step is to list all the specifications of the system. The specifications bridge the requirements of the user and the implementations of the designer. The specifications that can be extracted from the requirements can be summarized in the following list:

- The recorded signals are the electrical signals measured from skeletal muscle contraction;
- The system should be able to filter the recorded signals in order to obtain the signals of interest;
- All measurement probes should record signals synchronously;
- There should be functional blocks that keep a stable working environment of the system under a battery;
- The dimension of the measurements probes of the system should not be very big;
- The system should have a signal sampling unit that can sample at a frequency of 1KHz;
- The system should have local storage units that can store the recorded signals;
- The recording signals should be clean and insensitive to movement artifacts;
- The central control probe should be able to communicate wirelessly with all measurement probes without packet loss;
- The system should not cost too much in terms of component selection and design;

- The system should have internal data processing units that can process and store or transmit processed data;
- The system should be able to work under low voltage supplies;
- A proper design process should be followed in the design.

3.2.3 Architecture

After the system specifications are listed, the system should be designed at architectural level. Since the embedded system contains hardware and software, the architecture design should consider both cases.

Hardware Architecture

A possible hardware architecture that could meet the specifications can be following as shown in Figure 3.3.

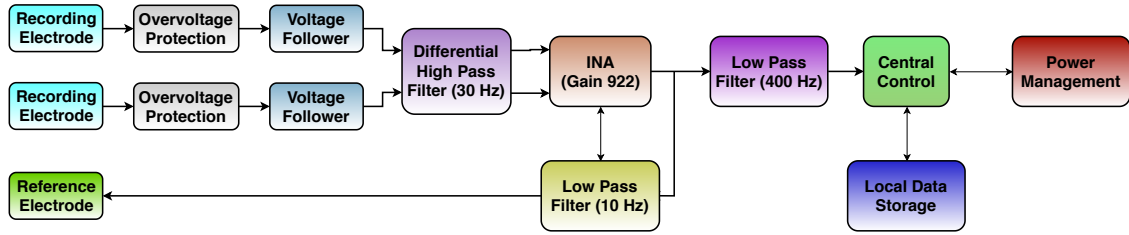


Figure 3.3: Hardware architecture of the EMG probe

A) Central Control. The Central Control Unit can sample the signals with 1KHz frequency. It can process the signals coming from the EMG Analog Front End unit. It can communicate with central control probe and exchange data packets. It can also store the processed data into local storage unit.

B) EMG Analog Front End (AFE). The EMG AFE unit has the functionality of removing spikes from recorded signals, buffering the recorded signals, providing bipolar electrode configuration, filtering out the noise and movement artifacts from the captured signals and finally adjusting the processed signals into measurable signal ranges.

C) Local Storage. The Local Storage unit contains μ SD Card data storing block and it is used for local data logging.

D) Power Management. The power management unit is responsible for conditioning the battery voltage and supplying the whole hardware with a stable operating voltage.

Software Architecture

Besides the hardware architecture, there is also the need for the software architecture considering the specifications of the system. The software architecture can be following as shown in Figure 3.4.

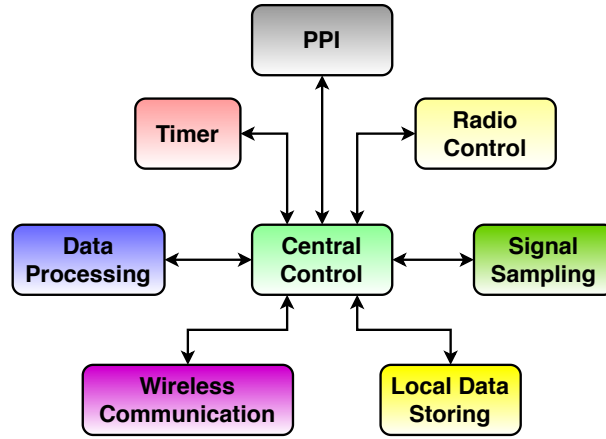


Figure 3.4: Software architecture of the EMG probe

3.2.4 Components Design

The next step is to implement the detailed design according to the functional blocks inside the hardware and software architectures. During this step, hardware components that meet the functional requirements of the hardware architecture are selected if they are ready to use, otherwise they are designed.

Hardware Components Design

A) Central Control Unit. From the specifications of the system, there is a strict timing requirement on the synchronous acquisition of signals from each measurement node. The communication is wireless, which means there should be a radio transceiver hardware. Besides that, there are many types of wireless communications, such as WiFi, Bluetooth Low Energy(BLE), ANT, Lora, Zigbee, etc. So, it can be very helpful if there is a hardware platform that could support

multiple communication standards so that a proper, reliable communication type with acceptable synchronization accuracy can be selected through software when the system is complete. The low power consumption requirement should also be respected. So, the nRF52832 micro-controller is selected as the central control unit and it has following advantages compared to other stand alone embedded systems:

- Multiple wireless communication standards
- In-built high performance Microprocessor
- Rich in hardware resources and communication interfaces
- Small dimension
- Exceptionally low power consumption

It has many types of hardware interfaces, such as SPI, I2C, I2S, UART, etc. It also has plenty of well-written software libraries with many examples. Besides that, it contains 12-bit Analog to Digital Controller with adjustable sampling frequency. So, the nRF52832 can be a good choice for the design of the initial prototype of the system.

B) EMG Analog Front End. The detailed design of the AFE is based on the hardware architecture shown in Figure 3.3. The overvoltage protection block is added in order to avoid possible voltage overshoots so that the recorded input voltage will be limited in a safe range. The detailed circuit design is shown in Figure 3.5.

In this design, Zener diodes of the model ESD5Z3.3 are selected as they have

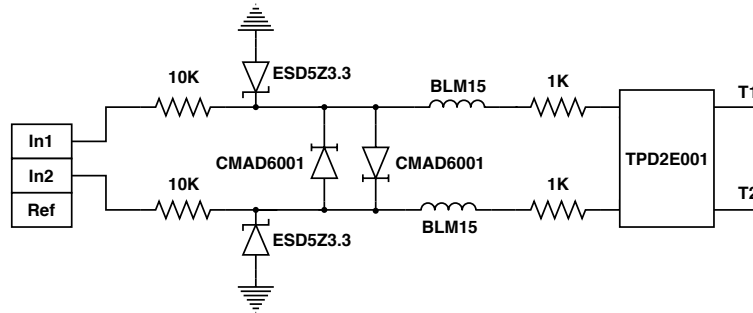


Figure 3.5: Overvoltage protection circuit

small dimension, very low leakage current and fast response time. Besides that, BLM15AX102SN1 ferrite bead is selected for additional protection. The TPD2E001 is selected as it is composed of double channel transient protection diode array. The voltage follower is composed of an OPA2347 operational amplifier as this chip

has a very low quiescent current (0.034 mA maximum). Then comes the high pass filter composed of passive components and the schematics is shown in Figure 3.6. The instrumentation amplifier is based on an INA321 that has an adjustable gain

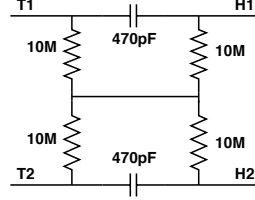


Figure 3.6: Differential High Pass Filter with 30 Hz cut-off frequency [31]

between 5 to 1000 V/V. The gain can be set through the connection of two resistors R10 and R11 to the chip, shown in Figure 3.7. The formula for the gain is: $G = 5 + 5(R11/R10)$. However, with the commercially available resistors, it is possible to reach a gain of 922 instead of 1000. In order to filter out the low-

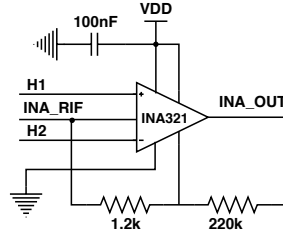


Figure 3.7: INA321 configuration circuit [32]

frequency voltages coming from INA reference voltage, a low pass filter with cut-off frequency 10.43 Hz is designed and connected to the reference voltage input pin 5 of the INA. The low pass filter is based on a multiple-feedback architecture and the actual design of the filter is shown in Figure 3.8.

Besides the low-pass filter for the INA321 feedback, there is a need to implement another low pass filter for processing the measurement signals. This filter is based on Sallen-Key architecture and its implementation is shown in Figure 3.9.

Then the output of the filter is connected to the ADC input of the nRF52832 Micro-controller. In both cases, the OPA333 operational amplifier is selected for the design due to its minimum Common Mode Rejection Ratio of 106 dB. It has a typical quiescent current of 17 uA, a wide supply voltage range between 2.7 V and 7 V. It also has a low input voltage noise of $0.3\mu V_{pp}$ in the frequency range from 1 mHz to 1 Hz.

C) Local Storage. The Local storage unit is responsible for storing the data locally. So, there is a need for a memory chip that can store the data and provide an easy to read access. Therefore, a μ SD Card slot is selected in the design as

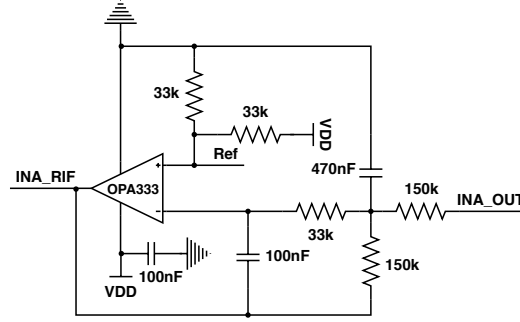


Figure 3.8: Multiple-feedback Low Pass Filter Circuit

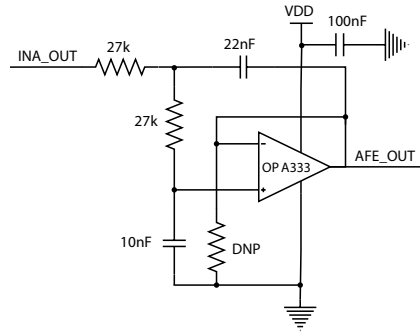


Figure 3.9: Sallen-Key based Low Pass Filter Circuit

the normal PCs contain a μ SD Card reader so that the measurement data can be fetched easily. In this research, the 16 GB Apacer Micro SDHC Class 4 Memory Card is used for storing the measurement results or processed data.

D) Power Management. The power management unit supplies the whole system with a stable operating voltage. Since the embedded system is powered by a coin battery, the output voltage of the coin battery drops as time passes by. So, it is necessary to design a voltage supply block that can produce a stable output voltage regardless of the drop of the input voltage. This means that it is necessary to use a step-up boost voltage regulator. There is also a need to prevent a reverse connection and a diode would be necessary for this purpose. The typical operating voltage of the μ SD Card is 3.3 V, so it might not work properly if the voltage level is lower than this due to the voltage drop in the circuit. Therefore, an output voltage of 3.6 V will guarantee the normal operation of μ SD Card. The actual design of the voltage regulator block is shown in Figure 3.10.

Software Components Design

A) Central Control. This software unit is responsible for initializing the whole software and hardware by calling corresponding initialization functions. It

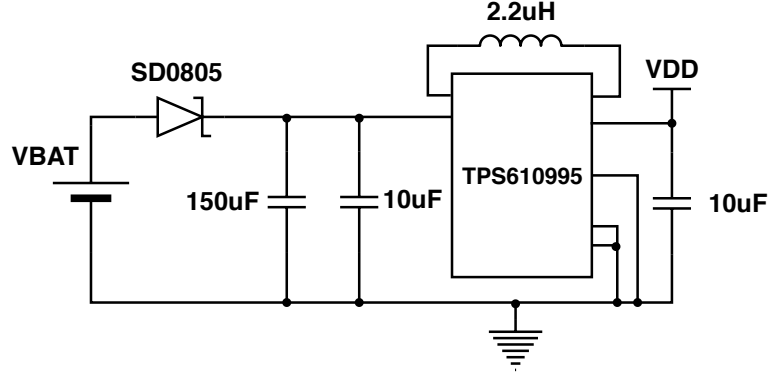


Figure 3.10: 3.6 V boost step-up voltage regulator

also handles interrupts and calls specific operations based on the interrupt flags.

B) Peripheral Programmable Interconnect (PPI). One of the amazing features of the nRF52832 is the Peripheral Programmable Interconnect system. It can enable interconnection between peripherals with each other using tasks and events without the need of CPU. It can also allow synchronization between peripherals to meet timing constraints of the applications [33].

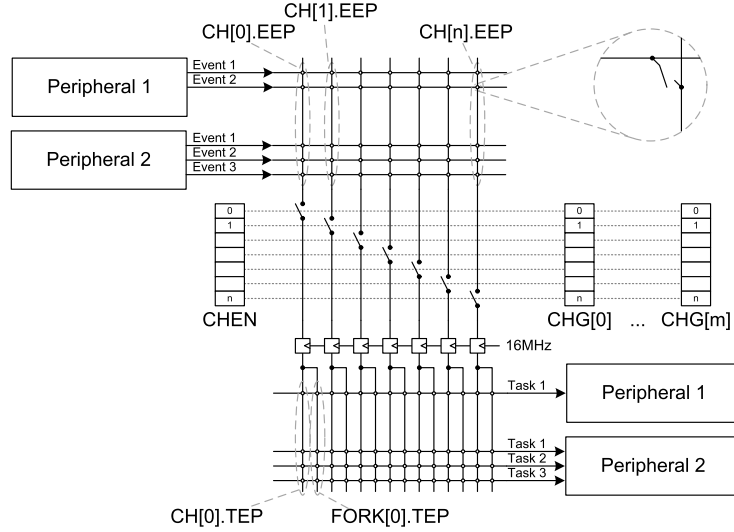


Figure 3.11: Block diagram of PPI

C) Timer. The timer unit contains the setup and relevant operations carried out by the timers. Two high frequency timers with 16 MHz and one Real-Time Counter (RTC) with 32.768 KHz frequency are used. One of the high frequency

timer(let us call it radio timer) controls the radio block inside the nRF52832 micro-controller for the wireless communication, while the other one controls the synchronization of the node(let us call it synchronization timer). The RTC timer is also used for controlling the radio block.

In Figure 3.12, graph representation of the whole system shown. It includes the central node (also called master node) and measurement nodes (also called slave node). The master node controls all the other slave nodes, so they communicate

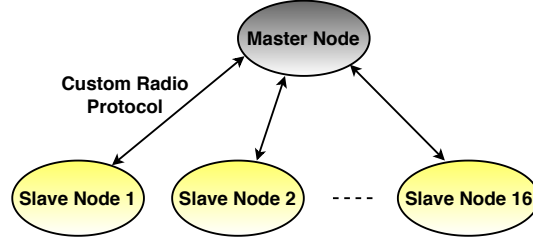


Figure 3.12: Graph representation of the overall system

via custom radio protocol. Since the recording of EMG signals on each slave node should be synchronous, the idea is to synchronize the synchronization timer in the slave node with the one in master node. Once the timers are synchronized on both master and slave node sides, then the recording of signals can be synchronized as the recording is controlled by the synchronization timer. The synchronization process is shown in Figure 3.13. In the first step, the master node is in transmission

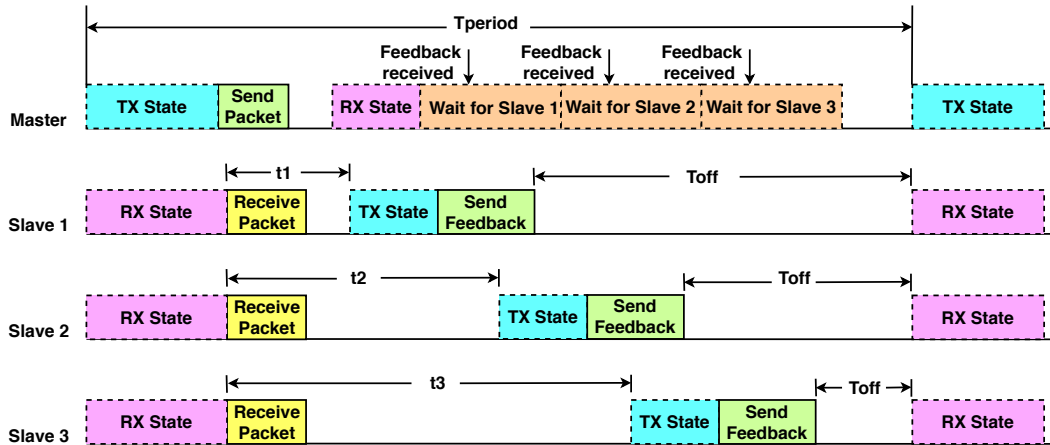


Figure 3.13: Synchronization process of the whole system

mode, while all the slave nodes are in reception mode. The master sends its clock information via the 2.4 GHz Enhanced Shock Burs (ESB) wireless radio protocol then it switches to the reception state and waits for the feedback from each slave node in a time duration of 30 ms. Once the slaves have received the packet from the

master, they adjust their synchronous timer with the one of the master and they in turn change their status from reception to transmission state. Then they send their feedback to the master node. After the master node receives the feedback of all slave nodes, then it can send the start measurement command and the slave nodes can start recording signals.

D) Signal Sampling. The sampling of the signals is carried out through the internal 12-bit Analog to Digital Converter (ADC) of the nRF52832 and the ADC is controlled through the synchronization timer in order to guarantee a precise 1 KHz synchronous sampling.

E) Local Data Storing. The data storing is based on the FatFs library of the nRF52832 and corresponding data storing operations are called when the central control block wants to write the measurement data into the local μ SD Card. This unit also contains an FIFO with 7 internal buffer blocks in order to guarantee an independent signal capturing and data storage. On one side, measured or processed data enters from the top; on the other side, the data inside the FIFO is shifted to the local μ SD Card. This can optimize the memory utility in the micro-controller. The block diagram of the FIFO is shown in Figure 3.14.

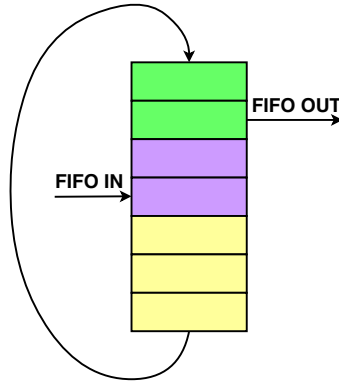


Figure 3.14: Block diagram of FIFO

F) Wireless Communication. The master node and slave nodes communicate with each other using a custom radio protocol called Enhanced Shock Burst Protocol. This protocol provides a reliable and configurable wireless communication. The data rate, maximum packet size, communication frequency, transmission and receiving power, device address and other relevant parameters can be set through this library.

3.2.5 System Integration

The final step is the integration of the hardware and software components. After the software library is downloaded into the nRF52832 micro-controller, the next step is to debug and test each individual hardware and software block. After the individual tests, final tests on the complete system are carried out by synchronizing the overall system, starting the measurements on the slave nodes, storing the data locally and then stopping the measurements.

3.2.6 System Refinement

After the test and debugging of the first version, it is necessary to address possible issues in the new version of the system. The previously described design methodology steps are improved in order to design more refined system. So far, three prototypes are designed and the differences between these versions can be seen from Figure 3.15.

So, step by step the final system is optimized in each cycle of the successive re-

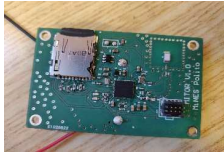
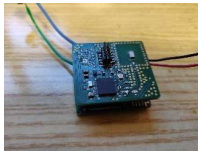

| | 1 st Version | 2 nd Version | 3 rd Version |
|-----------------------------|--|---|---|
| System Image |  |  |  |
| CPU | nRF52832 | nRF52832 | nRF52840 |
| Area | 57x37x10mm | 29x27x11mm | 57x32x11mm |
| Hardware improvement | Mainly designed for debug and test, may include additional components | Step-up boost regulator is implemented, PCB stack architecture is applied. Area is optimized. | Additional ATC hardware feature is added. |
| Software improvement | Basic custom radio communication protocol is implemented. High synchronization accuracy is achieved. | More stable ESB custom radio protocol is included. Serial port library is added. External GUI is designed to control master node. Software Envelope, ATC libraries are implemented. | Still under test. |

Figure 3.15: Brief comparison of the 3 prototypes of the system

finement model and a more robust, more stable system is designed. More hardware and software functionalities are introduced in each cycle. For example, from the

first version to the second version, besides the improvements in the hardware, several additional software libraries are implemented for the different working modes of the slave nodes and also for the serial port communication. A Graphical User Interface (GUI) is designed in order to control the master node.

3.3 Experimental Results

In this section, the test results are presented in order to validate that the system meets the requirements and specifications. The tests are done on the synchronization, wireless data transmission, signal acquisition and also on graphical user interface.

3.3.1 Synchronization

During the synchronization process, the master node sends its clock information periodically to each slave node and the slave nodes adjust their internal synchronization timer. The synchronization accuracy depends on how often the master node sends its clock. With a 1 second synchronization interval, the clock difference in the synchronization timer of two slave nodes is obtained from oscilloscope and the accuracy is 625 nanoseconds. In order to see if there is a drift in the synchronization accuracy, the master board and two slave boards are left in the synchronization process and after 16-hour continuous test, the accuracy is still kept at 625 nanoseconds. In Figure 3.13, a screen shot is captured from the synchronization process:

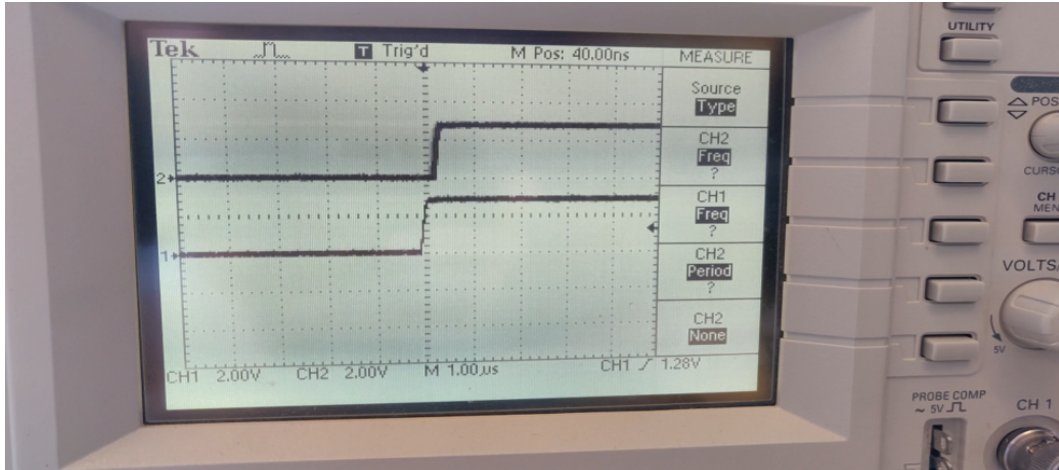


Figure 3.16: Synchronization of two slave nodes

3.3.2 Signal Acquisition

As it is shown in Figure 3.15, in the second version of the system, software libraries for different working modes of the slave nodes are implemented. Basically, there are three working modes as shown in Figure 3.17: Raw Data mode, Envelope mode and Average Threshold Computing (ATC) mode.

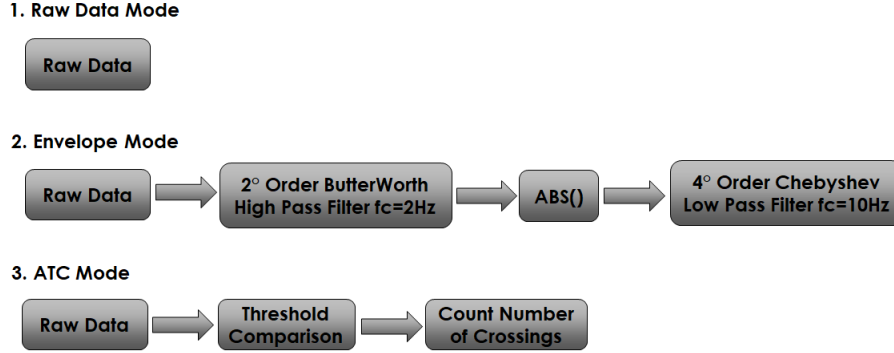


Figure 3.17: Different working modes of slave nodes

A) Raw Data

In this mode, the slave nodes do not carry out any post-processing on the ADC output data and store them on the μ SD Card. The figure 3.18 shows the acquired raw data from the Biceps during the measurement:

B) Envelope

In this mode, the output data of ADC first passes the 2nd-order Butterworth high pass filter in order to remove the DC components of the signal. Then the absolute value is calculated. After that, it passes through a 4th-order Chebyshev low pass filter in order to get the final envelope. In Figure 3.19, the intermediate data corresponds to the data before passing through the Chebyshev low pass filter. After the envelope is extracted from the original data, then by using Non-negative Matrix Factorization approach, it is possible to extract the muscle synergies.

C) ATC

In this mode, every 130 ms the output data array from ADC is processed in the Threshold Comparing algorithm and number of events where the signal level crosses the pre-defined threshold is counted and then is stored locally. The Figure 3.20 shows the obtained ATC counting values from the ADC output data. After the ATC data are obtained, the ATC envelope will be calculated and then using

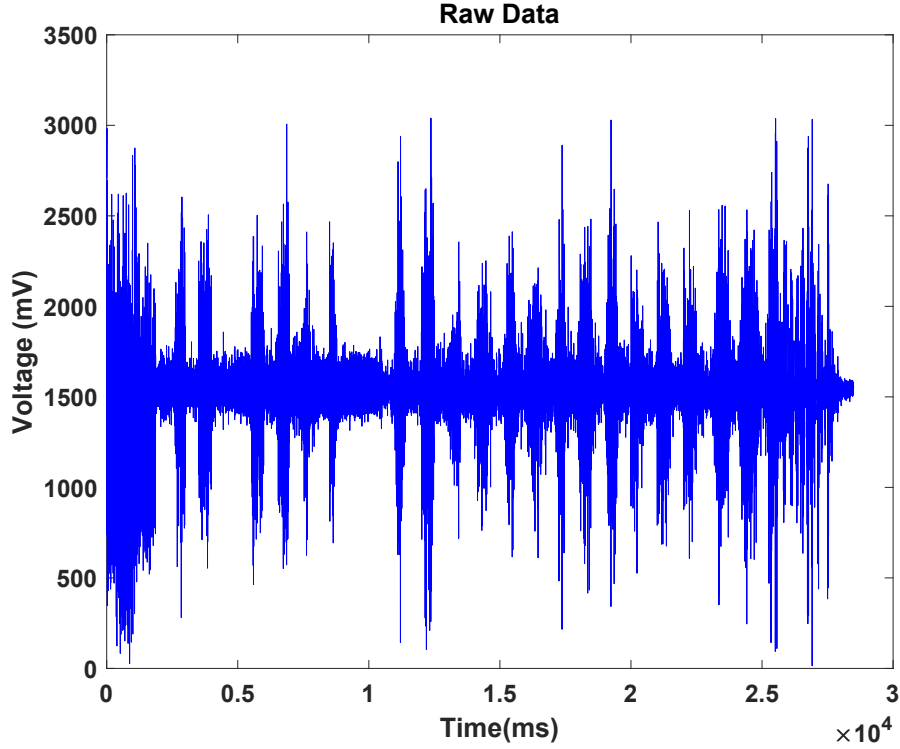


Figure 3.18: Raw data from the sEMG measurement

again Non-negative Matrix Factorization algorithms, the muscle synergies can be extracted.

3.3.3 Wireless Data Transmission

Besides storing the data into the local μ SD Card, the slave nodes can also send the measurement results wirelessly to the master node. In raw data mode, due to the fast sampling rate and huge amount of raw data produced on the slave node side, the master node can receive measurement data simultaneously from maximum 2 slave nodes and then transmits the data to the PC through serial port communication. In envelope or ATC mode, the master node can receive measurement results from all the 16 slave nodes since there is much less amount of data to be sent from slave node side in every second.

3.3.4 Graphical User Interface (GUI)

In order to control the master node from PC, a graphical user interface is developed and is shown in Figure 3.21.

The user interface contains a serial port library which enables a serial port com-

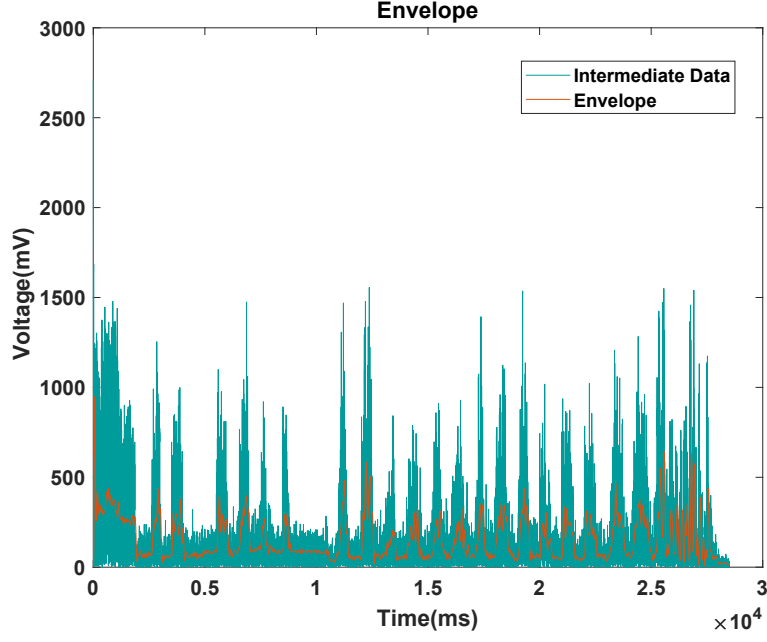


Figure 3.19: Envelope data from the sEMG measurement

munication between the PC and the master node. Each measurement types and working modes are tests are tested and command/packet exchange between the PC and the master node is successful.

3.4 Discussion and Conclusion

In this project, several versions of a wireless wearable sEMG system were designed following the successive refinement methodology, and the final system is

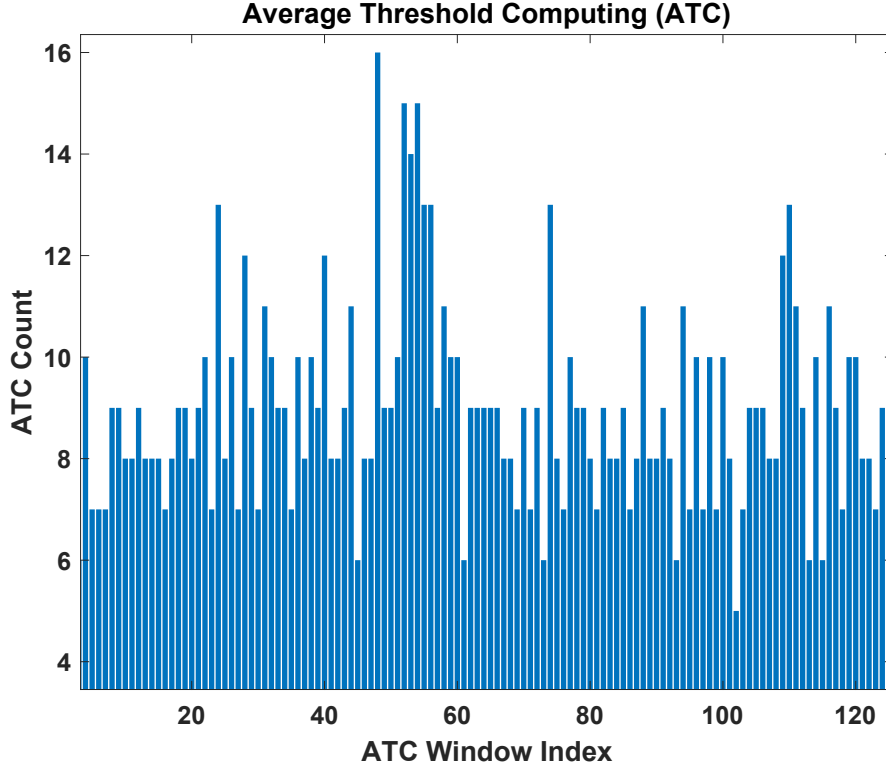


Figure 3.20: ATC data from the sEMG measurement

continuously optimized and refined. In the second version of the system, the following results are achieved with a 10-second synchronization period:

- Synchronization with $<10 \mu s$ resolution;
- Synchronization period is adjustable;
- Clock drift $<10 \mu s$ over 16 hours;
- Wireless transmission and local data storing
- Battery life can last up to 61.6 hours in ATC mode <12 hours (Cometa).

Additional tests are done on the current consumption in different working modes:

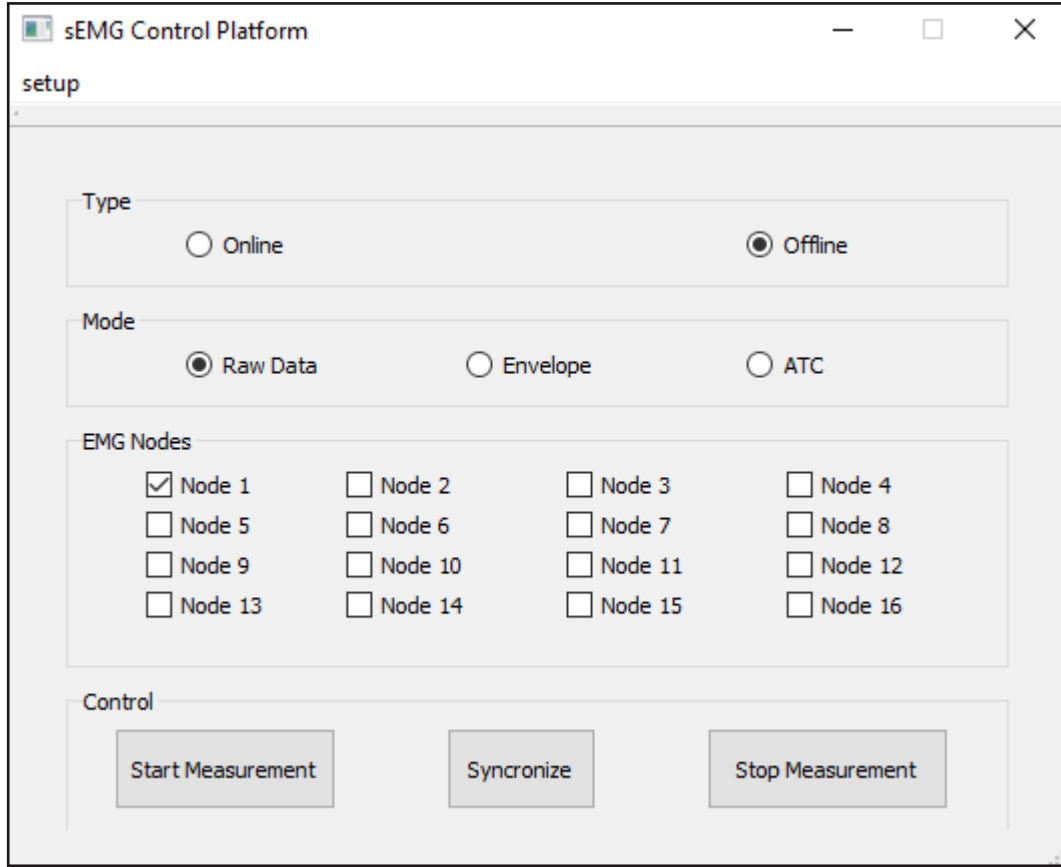


Figure 3.21: Graphical User Interface for controlling master node

Table 3.1: Current consumption test on different working modes

| | | |
|-----------------------|---|-------------------------|
| Operating conditions: | Battery Capacity = 450 mAh Sync Period = 10 seconds Sync Accuracy = 10 us Supply Voltage = 3.6 V | |
| Test Type | Current Consumption (mA) | Battery Life (h) |
| Raw Data | 14.0 | 32.1 |
| Envelope | 7.9 | 57.0 |
| ATC | 7.3 | 61.6 |

From the test results reported in Table 3.1 it can be seen that the designed sEMG system it is the very first wireless wearable sEMG system that can work in the three different modes mentioned earlier. It is also the most power efficient system compared to devices available in the market. Its wireless data transmission

and local data storage capabilities can allow the system to be used for both real-time and long-term muscle movement tests, inside or outside hospitals.

The designed system is smart as it can carry out operations in a smart way: automatic synchronization of clock signals, peripheral to peripheral control without CPU involvement, automatic data processing, filtering and storing, interrupt based smart power management.

Chapter 4

Electrochemical Sensing Platform for Continuous Monitoring of Anesthesia Delivery

4.1 Introduction

Recent studies show that the effect of a drug is strongly patient dependent, as it changes with age, gender, metabolism, living environment and health status of the patient [34]. So, the correct delivery and therapy of the drug can be very challenging due to these factors. Personalized Medicines (PM) try to address these problems by providing patient dependent solutions in order to deliver the right drugs and limit the side effects of the drugs [35]. This is extremely important for the case of Anesthesia, as it is a very powerful and fast acting drug that could endanger the life of the patient if not carefully monitored [36]. So, there are anesthesiologists that are responsible for the administration order, dose balance and delivery time. However, there are cases when the wrong dose is delivered or a wrong drug is given to the patient as shown in the Figure 4.1.

4.2 Drug Monitoring with Electrochemical Sensors

Due to the potential risks with the drug delivery stated in the previous section, the monitoring and measurement of the drug in patient needs to be very precise and Therapeutic Drug Monitoring(TDM) can be the key to do this [37]. The electrochemical sensors are ideal candidates for the measurement of drugs as they are very precise, low cost and very sensitive [38].

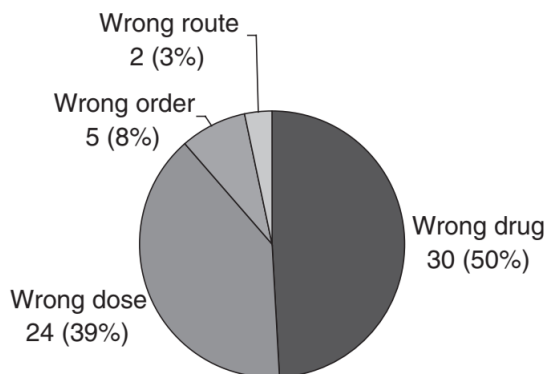


Figure 4.1: Drug administration errors

4.2.1 Electrochemical Sensing Techniques

Electrochemistry is the branch of chemistry which focuses on the interrelation between the electrical effects and chemical effects. It studies the chemical changes induced by the passing of electrical currents or electrons or vice-versa, where there is the change in current due to the chemical effects [39]. These electrical or chemical effects usually take place in the electrochemical cells, which consists of electronic conductors (electrodes) and ionic conductors (electrolytes). The most common configurations of the electrochemical cells are two-terminal configuration and three-terminal configuration shown in Figure 4.2. In the two electrode configuration, the

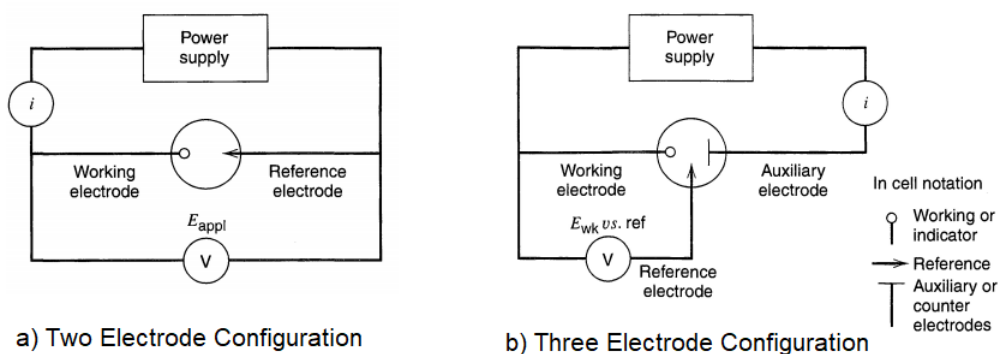


Figure 4.2: Typical Electrochemical Cell configuration [39]

electrochemical cell is composed of the Working Electrode (WE) where the electron exchange with the solution takes place, and the Reference Electrode (RE) which provides a stable reference potential for the measurement of the potential of other electrodes. This configuration is mostly used in applications where the voltage drop between the WE and RE is relatively small. In the three electrode configuration, there is an additional electrode, called Counter Electrode (CE), that enables the measurement of the faradaic current passing through the WE when a voltage is

applied between WE and RE [40]. The three electrode configuration is mostly used in applications where the voltage drop between WE and RE is relatively big. In the two electrode configuration, the RE works as supplier of the electrons and also as a reference potential, so it is very difficult to keep it stable. So, in this project, the three electrode configuration is adopted.

A typical electrochemical measurement is done by applying an excitation potential between the WE and RE, then measuring the generated current.

In order to monitor the concentration of the Anesthesia compound, the follow-

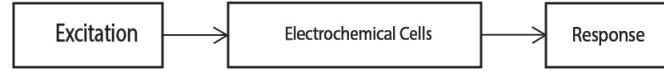


Figure 4.3: Typical Electrochemical experiment

ing electrochemical techniques are used in this project: ChronoAmperometry(CA), Cyclic Voltammetry(CV) and Differential Pulse Voltammetry(DPV).

ChronoAmperometry(CA)

In CA, a fixed potential is applied between WE and RE. Then the current change with respect to the variation of concentration of the drug is observed. The relationship between the concentration and current is expressed by the Cottrell equation:

$$i(0, t) = \frac{nFA\sqrt{D}C(0, t)}{\sqrt{\pi \times t}} \quad (4.1)$$

While the change of the current with respect to the metabolic concentration is given by:

$$\Delta i = \frac{nFA\sqrt{D}}{\sqrt{\pi \times \Delta t_0}} \Delta C \quad (4.2)$$

The typical curves for these equations are shown in Figure 4.4.

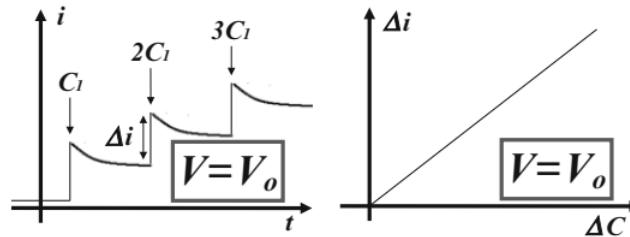


Figure 4.4: ChronoAmperometry(CA) [40]

Cyclic Voltammetry(CV)

In CV, a voltage sweep with a fixed voltage step is applied between the WE and RE, then the current response for each step is measured. A typical curve of the voltage scan and the current response is shown in Figure 4.5.

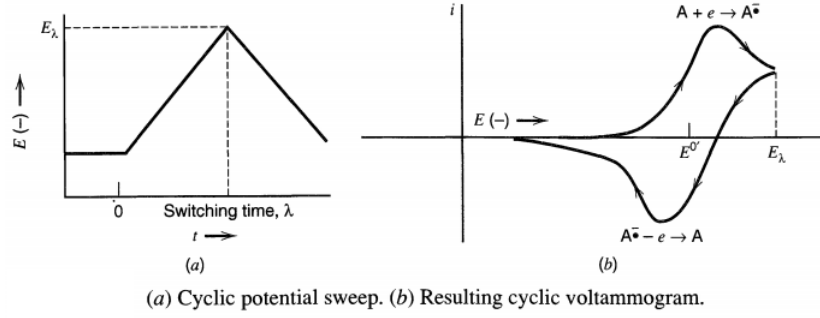


Figure 4.5: Cyclic Voltammetry(CV) [39]

Differential Pulse Voltammetry(DPV)

The DPV is a technique where a voltage pulse with an increasing step is applied and the current responses before and after applying the pulse are measured. A typical curve of the DPV voltage sweep and the expected voltage-current relationship is shown in Figure 4.6

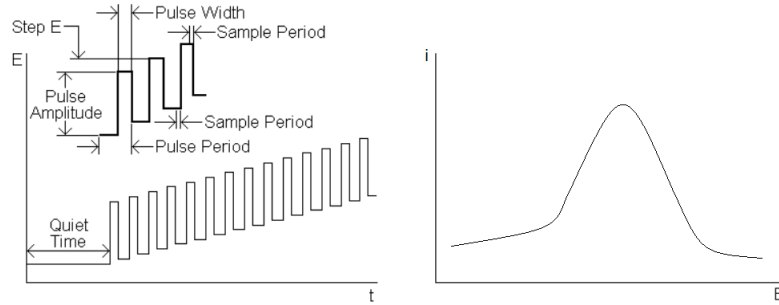


Figure 4.6: Differential Pulse Voltammetry(DPV)

4.2.2 Sensor Calibration

In the electrochemical applications, the sensors are designed and developed according to the requirements of the applications. The main common features of sensors are:

- Selectivity: the sensor is specific towards a desired analyte;
- Sensitivity: the ability of the sensor to detect the variations of analyte concentration;
- LOD: the minimum concentration of the analyte that a sensor could detect;
- Dynamic Linear Range: the ability of the sensor to follow the rapid changes in the analyte concentration.

So, before a sensor is used, it is needed to be calibrated. The calibration line of the sensor shows the relationship between the variation of the concentration of the analyte and the generated current.

4.2.3 Research Objective

The objective of this research project is to design an electrochemical biosensing platform that could carry out real-time monitoring and delivery of anesthesia compounds, such as Paracetamol (APAP), Propofol and Midazolam. Electrochemical techniques such as CA, CV and DPV should be supported by such platform. For the monitoring and measurement of anesthesia, the electrochemical sensors are deployed, while for the delivery of the drug, the TCI pumps are used. So, what is missing is the electronic system that controls the overall system, which includes the controlling of the interaction between the electrochemical sensors and anesthesia and also controls the TCI pump.

4.2.4 Project Analysis

The next step is design such biosensing platform that addresses the objective of the research. This platform contains some parts related to the electrochemical biosensors, also some parts that are for delivering the drug and also some that carry out the measurement. So, there are several parts that need to be integrated. In this case, the main challenge is to do the final integration of different parts and then create a fully working system. Besides that, the design is carried out by two design teams. So, it is important to optimize the design time and coordination between the design teams. For this reason, the hardware/software or concurrent design methodology is adopted during the design of the system.

4.3 Model Implementation

The design of the whole biosensing platform strictly follows the hardware/software design methodology. In this approach, the hardware and software components design are carried out in parallel. Since in this project, besides the electronics part of

the system, there are also the biosensing parts to design. So, there are several parts that can go in parallel and then are integrated at the end. The following sections explain how each design step is carried out.

4.3.1 Requirements

Requirements are the starting point in the design process and they include the information related to the needs of the actual application. In this project, the main target is to design a biosensing platform that monitors and delivers anesthesia in real-time. So, in details, the functional and non-functional requirements are following:

Functional Requirements

- The system should be able to measure and deliver the anesthesia.
- The system should be able to process data.
- The system should support Internet of Things (IoT) feature for the transmitting the measurement data.
- The measurement data should be less noisy and reliable.
- The system should be able carry out CA, CV and DPV for anesthesia.
- The system should be easy to use.
- The system should be able to carry out operations in real-time.

Non-functional Requirements

- The system should have low overall cost.
- The system should have high performance in data processing and real-time operations.
- The dimension and weight of the system should be moderate.
- The system should consume low power, if possible.

4.3.2 Specification

The specifications bridge the needs of application with designer. So, it is important to list out all the specifications of the system. They are following:

- The system should include biosensors that can detect the three anesthesia compounds.
- The system should be able to perform real-time operations.
- The system should be able to perform electrochemical techniques such as CA, CV and DPV.
- The system should be able to generate and sense signals from biosensors.
- The system should be able to deliver the drugs to the patient.
- The system should carry out the measurement of drugs and delivery in real-time.
- The system should be able to process the measurement data.
- The system should be able carry out measurements autonomously.

4.3.3 Architecture

Hardware Architecture

According to the requirements and specifications from the previous sections, the system should contain electrochemical sensors that are suitable for measuring anesthesia compounds. It should contain a central control block that is based on a high performance and low-power micro-controller to perform real-time measurements. The system should contain a voltage generation block in order to generate the excitation signals required in the electrochemical measurements. The system should be able to measure the generated current through a sensing block that is interfaced with electrochemical sensors. The system also needs a process data block and IoT interface for wireless transmission of data. In order to have a clean measurement signal, a possible filter block would be useful.

Such functional requirements can be realized with a possible hardware architecture shown in Figure 4.7.

Software Architecture

The software architecture includes the software operations that are executed in the hardware architecture. The functional blocks are defined in a way that they can guarantee a safe operating environment and realize the specifications. A possible

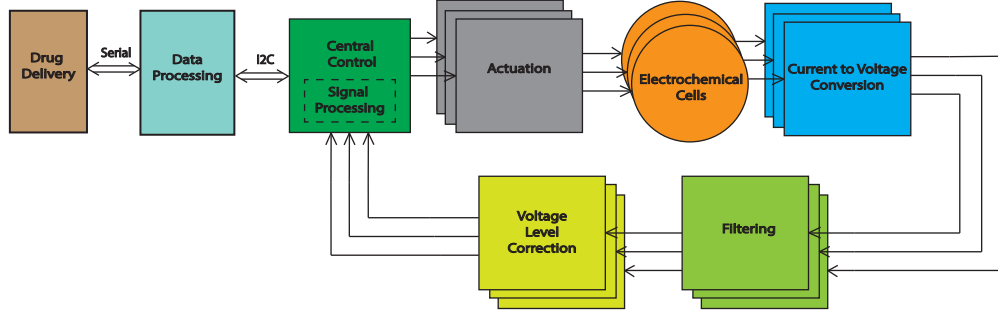


Figure 4.7: Block representation of the whole system [41]

software architecture can be following as shown in Figure 4.8.

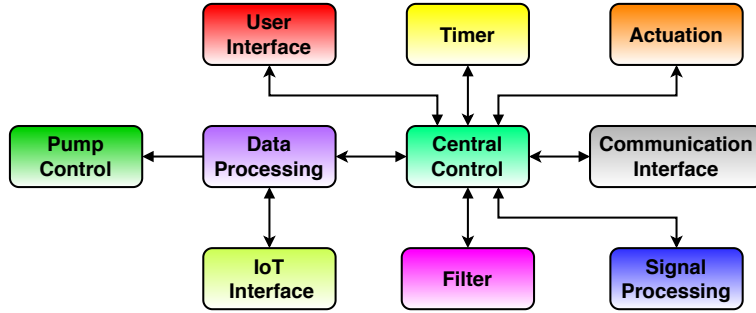


Figure 4.8: Block representation of the software architecture

4.3.4 Components Design

In this step, the hardware and software components are designed in parallel. The hardware of the whole system is designed using Altium Designer 16 and the software components are developed and tested in Atmel Studio 7.0.

Hardware Components Design

The hardware design implements step by step each block in the hardware architecture.

A) Central Control. The central control block contains the ATXMega32E5 micro-controller [42]. The micro-controller has an internal 32 MHz frequency micro-processor, a 16-channel/12-bit 300kSPS Analog to Digital Converter, several communication interfaces and high frequency timers.

This micro-controller controls the waveform generation in the actuation block and

processes the incoming signals from voltage level correction block. It also communicates with data processing block via I2C interface and exchanges data/command packets.

B) Data Processing. In this Data Processing block, the RPi is used for controlling the XMegaE5 micro-controller and also for processing and transmitting data over WiFi for the IoT Cloud Server. The RPi is the RPi 3 Model B+ and it contains Quad-core high performance micro-processors. It also has GPIOs that contain UART, Serial, SPI, I2C and general purpose Input-Output pins. So, it can communicate with other electronic systems through these available ports. Besides that, the RPi has Raspbian OS and it can work like a computer and supports connections with HDMI monitor, the keyboard and mouse. The RPi provides the Qt software development environment and software applications can be developed using Qt C++.

In this project, we have used the RPi to connect with the XMegaE5 micro-controller through its I2C port so that we can exchange data and command packets between the RPi and micro-controller. Besides that, a Graphical User Interface(GUI) is also developed inside the RPi and the user can setup the electrochemical measurement parameters and carry out the desired experiments.

C) Actuation. This block applies a voltage to the electrochemical cells and is composed of 3 independent DACs with SPI ports. The actuation, or waveform generation is done by writing to the DACs through the SPI port of the micro-controller. In this project, the 10-bit MCP4911 DAC is selected and for the OpAmp, the MAX4475ASA+ is used for the Control Amplifier in the excitation block.

D) Current to Voltage Conversion. The current to voltage conversion is done through the TIA stage in Figure 4.9 and the MAX4475ASA+ is used for the OpAmp. In this stage, the current coming from electrochemical cell is converted to a voltage signal and its DC voltage level is shifted to the half of the supply voltage in order to avoid the saturation at the output.

E) Sallen-Key Filter. The filtering block includes a 4th order Sallen-Key low pass filter and it has a cut-off frequency of 200Hz. The 4th order filter is composed of two cascaded 2nd order Sallen-Key low pass filters and the detailed design of the filter can be referred to [An IoT Solution for On-line Monitoring of Anesthetics in Human Serum Based on an Integrated Fluidic Bio-Electronic System.pdf]. This is a unity-gain filter and the input voltage signal amplitude doesn't change during the filtering stage. The reason behind using the Sallen-Key low pass filter is that the filter has a very flat response to the signals in the pass band. We have decided to use the 4th order filter, as it can give better noise filtering compared to lower order low pass filters.

F) Voltage Level Shifting. After the filtering stage, the next step is to adjust the level of the voltage signal coming from the filtering stage. Because the input voltage range of the 12-bit ADC of the XMegaE5 micro-controller is from 0 to 2V, so it is necessary to guarantee that the voltage signal is in this range in order to get a correct conversion values from the ADC.

The relationship between the generated current at the WE and the measured voltage at the input of ADC is following:

$$V_{out} = 1.65 + I_f R_f. \quad (4.3)$$

Once the V_{out} is measured, we can obtain the generated current I_f at the WE and from the Current-Concentration relation curve, we can obtain the corresponding concentration of the drug that we are monitoring.

G) Drug Delivery. In the anesthesia monitoring, after the concentration of the drug in the patient blood is measured through the electronic system, the next step is to estimate how much dose should be delivered to the patient and the delivery is done using a TCI pump. In this electronic system, the TMNE-1000 Programmable Single Syringe Pump [43] is used.

The overall electronic hardware of the sensing platform is shown in Figure 4.9.

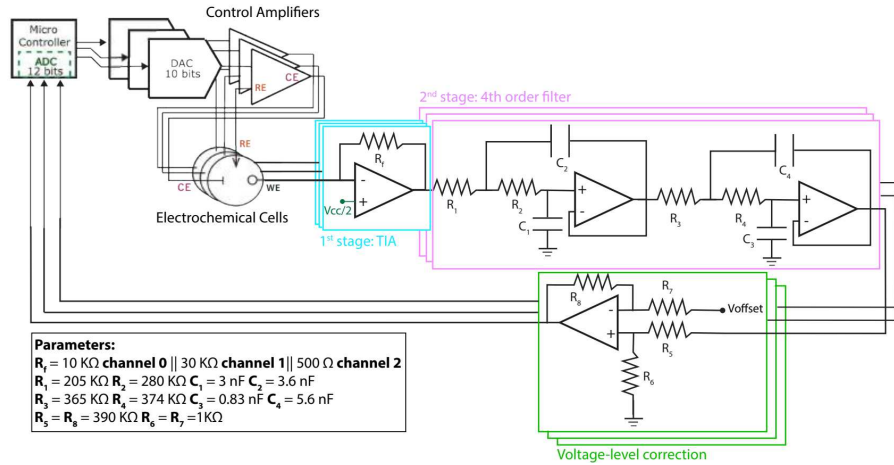


Figure 4.9: Schematics of the custom board [44]

Software Components Design

A) Graphical User Interface(GUI). After the hardware setup of the system is ready, a Graphical User Interface(GUI) is designed in order to configure

the electrochemical measurement and data processing. Figure 4.10 shows the steps included in setting up the GUI during the whole measurement: From the GUI a)

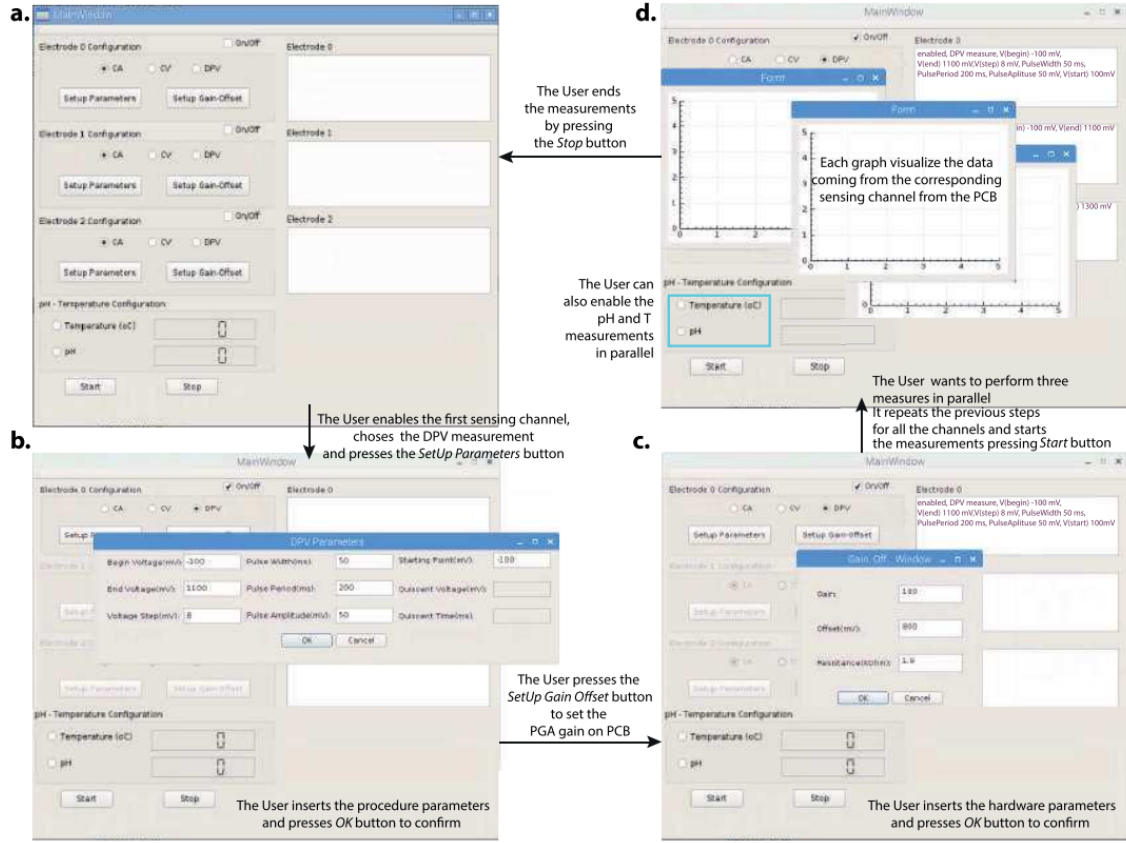


Figure 4.10: Graphical User Interface of the electronic system [41]

we can see that there are three configuration panels that are for Electrode 0, Electrode 1 and Electrode 2. This is because we have three independent electrochemical measurement channels and they can run in parallel if needed. In each configuration panel, there are three electrochemical techniques that can be chosen for each channel: CA, CV and DPV.

After the electrochemical technique is chosen for a given channel, the next step is to set the test parameters for that technique. When the CA is selected, what is needed to set is the apply voltage value and the sampling interval. When the CV is selected, the starting and ending voltage, voltage step, step width and starting point are configured. When the DPV is selected, the starting and ending voltage, the pulse amplitude, pulse width, pulse period, voltage step and starting point are configured. The measurement parameters differ from each other depending on the target drug and also the selected electrochemical sensing techniques.

After all the channels are configured, the measurement can be started by pressing the start button. These test parameters will be sent from RPi to the micro-controller through the I2C port. During the measurement, the curve of the applied voltage and generated current is plotted in real-time and measurement results are received from the micro-controller. Then the measurement can be stopped by pressing the stop button. Once the measurement is finished, the received measurement data are processed and then are stored in Microsoft Excel® files inside the RPi.

B) Central Control. As it is mentioned earlier, the micro-controller is responsible for controlling the sensing and activation block and also for exchanging data or command packets with the RPi through the I2C port. So, it is important to program the micro-controller for carrying out these operations. In the XMegaE5 micro-controller, there are three high frequency timers and they work independently from each other. Therefore, they can be used for waveform generation by sending samples to the three DACs at specific moments through SPI port and for voltage reading by sampling the input voltages with three ADC channels at desired moments. The work flow of the micro-controller is shown in Figure 4.11.

As it can be seen, after the initialization of the internal hardware blocks, the micro-controller remains in the while loop waiting for receiving commands through the I2C port from the RPi. Once the packets are received from the RPi, the micro-controller extracts the measurement parameters and configure again the internal hardware, such as the timer and ADC. Then the measurements start after the start command arrives and the data packet containing the measurement results will be sent back to RPi until a stop measurement command arrives.

C) Communication Interface. The RPi exchanges packets with the micro-controller through the I2C interface. So, it is important to set the data or command packet format in order to guarantee the reliable and configurable packet transmission. Here in the below, the packet formats for each electrochemical technique and measurement data are explained in more details.

D) ChronoAmperometry. The command packet for the CA measurement parameters is composed of 4 bytes: The set voltage byte contains the voltage value that needs to be written to the DAC of the corresponding channel for the CA measurement. The start tag and stop tag are added in order to indicate when the command packet arrives and when it is complete. The stop tag for all the electrochemical measurements is same and it is 0xBB.

E) Cyclic Voltammetry. The command packet for the CV measurement parameters is composed of 10 bytes: The Start Volt indicates the starting voltage of the CV measurement, while the End Volt indicates the ending voltage. The starting point indicates at which voltage value the CV measurement is started so

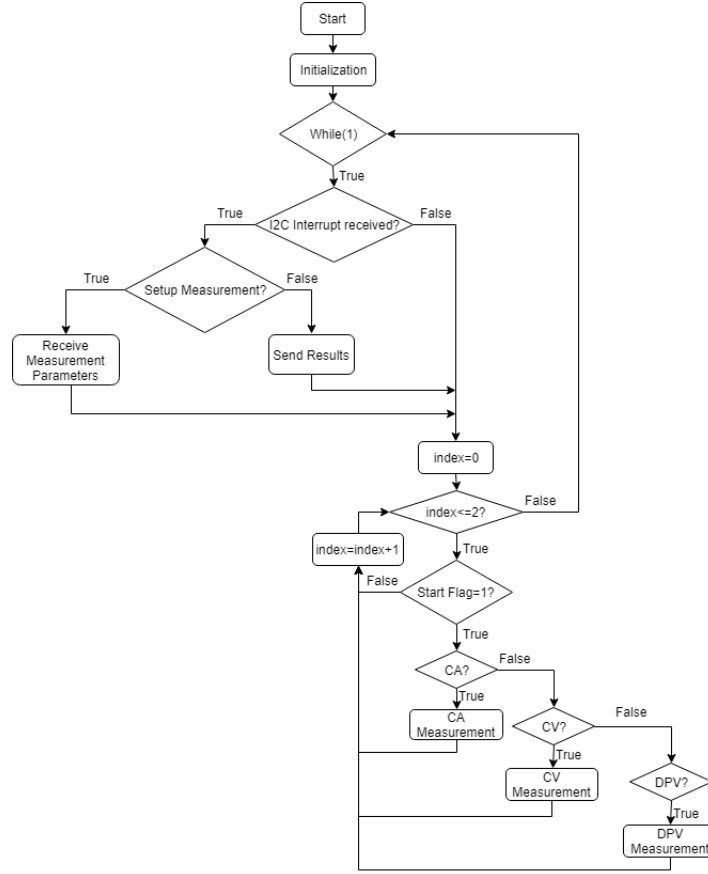


Figure 4.11: Work flow of the micro-controller



Figure 4.12: Command packet for CA

that we can start the CV measurement at any voltage value that is supported. The sweep time indicates how long each voltage step lasts.

F) Differential Pulse Voltammetry. The command packet for the DPV measurement parameters is composed of 16 bytes: The Start Volt, End Volt and the Starting Point has the same meaning as the ones in CV. The Pulse Amp indicates the height of the voltage pulse. The Pulse Width shows the duration of each pulse while the Pulse Period indicates the repetition period of each voltage pulse. The Volt Step indicates how much the applied voltage increases after each pulse period time.



Figure 4.13: Command packet for CV



Figure 4.14: Command packet for DPV

G) Measurement Results. The measurement results are composed of 6 bytes: They include the applied voltage, measured voltage, start tag and stop tag. The start tag contains the electrode index mentioned in the following section. Since there are three independent measurement channels, it is necessary to indicate which measurement channel is selected and what types of operations are to be executed. Besides that, it is also necessary to indicate whether we need to write the measurement configuration parameters to the micro-controller or if we want to read the measurement result from the micro-controller. So, all these operations are indicated in the Start Tag, which is 1 byte.

Depending on its upper 4 bits, we can select the types of electrochemical measurements.

By setting or clearing the D3 bit, we can indicate whether we want to write to the micro-controller or read from it. If D3=1, this means the RPi is writing configuration parameters to the micro-controller. If D3=0, then the RPi wants to read the measurement result from the micro-controller.

By setting the D2-D0 bits of the start tag, we can choose the measurement channel we want.

H) TCP/IP based Pump Control. The TMNE-1000 pump is connected to the RPi through the serial port and it can be controlled through the Qt software libraries provided by the manufacturer. After the measurement of the anesthesia compounds, the next step is to evaluate how much dose will be needed to the patient. The evaluation is done through MATLAB algorithms that models the human body and estimates the drug concentration in the patient brain in an external computer. After the amount of dosage is known, the value is sent to the RPi through WiFi using the TCP/IP communication. When the RPi receives the estimated dosage, it sends this information to the pump via serial port so that the drug delivery can be carried out. Figure 4.17 shows the TCP server running on the RPi in order to receive commands from the MATLAB application running on a laptop.

The Figure 4.18 shows the GUI in MATLAB that is used to communicate with

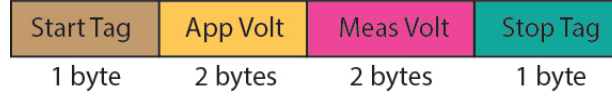


Figure 4.15: Data packet for the measurement results



Figure 4.16: Composition of the start tag

the RPi for sending the estimated dosage value to the pump. The MATLAB application can receive the real-time measurement values from the RPi, estimates the dosage needed to be delivered and sends the value back to the RPi.

I) IoT Interface. IoT based applications are being exploited more in the telemedicine and health care. It is gaining popularity as due to its convenience and the availability of large scale cloud network servers. The usage of IoT in health care can give the possibility of data sharing between any devices that are connected to the network. For example, in the hospitals, the IoT based medical devices can continuously track the status of the patients and send alarm to the doctors if there is any abnormal situation on the patient side.

For this reason, we also embedded the IoT capability into our electronic system for the continuous monitoring of the drugs. The idea is that, the electronic sensing platform continuously measures the concentration of the anesthesia compounds in the patient blood and sends alert to the doctors if the traced concentration exceeds the maximum safety level. This is done by establishing the TCP/IP based wireless communication between portable android devices and the RPi.

During the measurement, when the test results are received from the micro-controller, the RPi carries out the data processing and calculates the generated current values on the WE of the electrochemical cells. Then the calculated current values plus the applied voltage values are sent together to the portable android device through the PrYv cloud server. Then the doctor can see the concentration trend of the drug on the patient. The figure 4.19 shows a typical showcase of IoT based anesthesia monitoring.

So, it can be seen that, each electronic TDM system can communicate with the android application of the doctor through WiFi and the measurement results can be sent to the PrYv cloud server. Then these data can be processed further by other remote devices that are connected to the server.

On the patient side, the first step is to connect to the PrYv cloud server and allow data streaming with the doctor. At this point, the electronic system is ready for

| D7 | D6 | D5 | D4 | Hex | Type |
|----|----|----|----|-----|------------------|
| 1 | 0 | 1 | 0 | A | CA |
| 1 | 1 | 1 | 1 | F | CV |
| 1 | 1 | 0 | 1 | D | DPV |
| 1 | 1 | 0 | 0 | C | Stop Measurement |

| D2 | D1 | D0 | Electrode Index |
|----|----|----|-----------------|
| 0 | 0 | 0 | 0 |
| 0 | 0 | 1 | 1 |
| 0 | 1 | 0 | 2 |

data and event streaming with other devices connected to the cloud server.

On the doctor side, once a connection request is received from the electronic system on the patient side, the doctor accepts the connection, authenticates the credentials of the patient and then can start to receive the sensor data from the patient. There is also a possibility to send alarms to the doctor if the measurement detects unusual measurement values that are outside the safety range and then the doctor can carry out necessary steps to ensure the safety of the patients.

Besides connecting to the server on the doctor side, the electronic system of the patients can also be accessed through remote web applications that are connected to the cloud server.

With the IoT functionality, the designed electronic system can exchange measurement data and information of the patient with other cloud servers and can enable the doctors to remotely monitor and diagnose the patients, can be very useful in telesurgery and other medical services. In the rural areas where the medical conditions are poor, such system can be used for remote diagnostics where there are insufficient medical specialists for the health-care services [46].

4.3.5 System Integration

After the hardware and software components are designed, the next step is to carry out the integration of the two parts. In this step, every part of the system can be tested and debugged individually and also in groups so that possible bugs or problems can be addressed. An overview of the system is shown in Figure 4.21.

4.4 Experimental Results

In this section, The experimental results are reported for the drug monitoring, drug delivery and also for the IoT based data transmission tests. The drug monitoring test includes the measurement of the anesthesia compounds. The Drug delivery

```

pi@raspberrypi: ~
File Edit Tabs Help
pi@raspberrypi:~$ sudo ./Online_Monitoring_System/build_Debug/Online_Monitoring_System 0.0.0.0 50000
This is the online monitoring program!
Now system is waiting for a client connection...
A TCP connection request is received!
A client is connected to the online monitoring system.
Connection to pump is required.
Pump is connected.

```

Figure 4.17: TCP Server running RPi

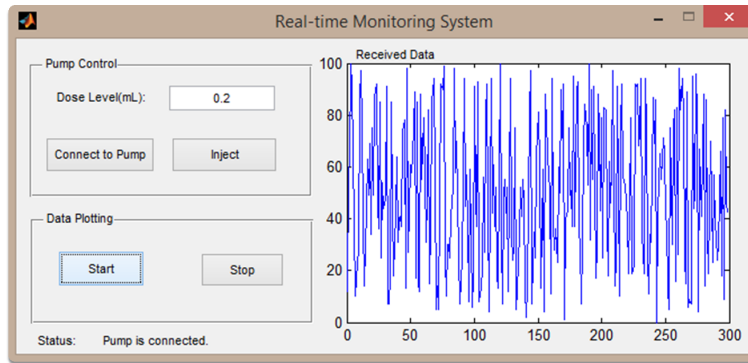


Figure 4.18: The MATLAB GUI for remote controlling of the pump

test includes the injection test of different solutions with the TCI pump. The IoT based data transmission test includes the data transmission between the RPi and android devices through the PrYv cloud server.

4.4.1 Test on Drug Monitoring

In this section, the test results for different electrochemical sensing techniques are reported and test is done on different anesthesia compounds, such as the Paracetamol(APAP) and Propofol. Besides that, measurement is done both using commercial sensors and also custom fabricated sensors.

1. Measurement of Paracetamol(APAP)

In this section, the measurement for the APAP is done using the electrochemical techniques CA, CV and DPV.

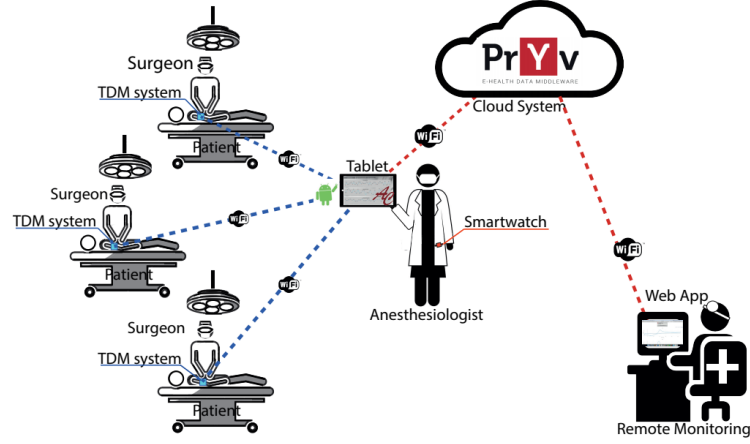


Figure 4.19: IoT based anesthesia monitoring [45]

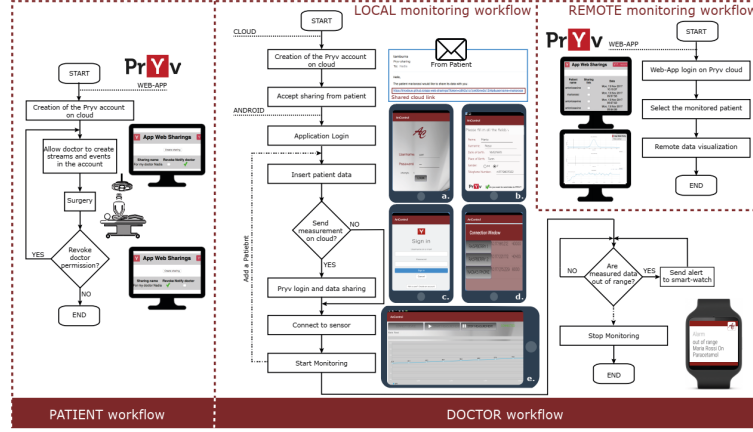


Figure 4.20: Work-flow charts on the patient and doctor side [45].

The measurements are done in vitro. During the experiment, standard Screen Printed Electrodes(SPE) from Dropsense (Spain) are used. The measurement is done by both the electronic sensing platform and also by the commercial Metrohm Autolab system (PGSTAT 302N) in order to compare and validate the results. The test parameters used in the following measurement for APAP are shown in Figure 4.22.

1) CA Measurement

In this measurement, the test is performed in PBS pH 7.4 with 10 mM concentration. The concentration of APAP is increased by [50 - 100 - 150 - 200] μM and the generated current from the WE is obtained. In this test, the applied voltage is fixed at 450mV and the measurement results are sampled at 500 ms period. The measurement results are shown in Figure 4.23.

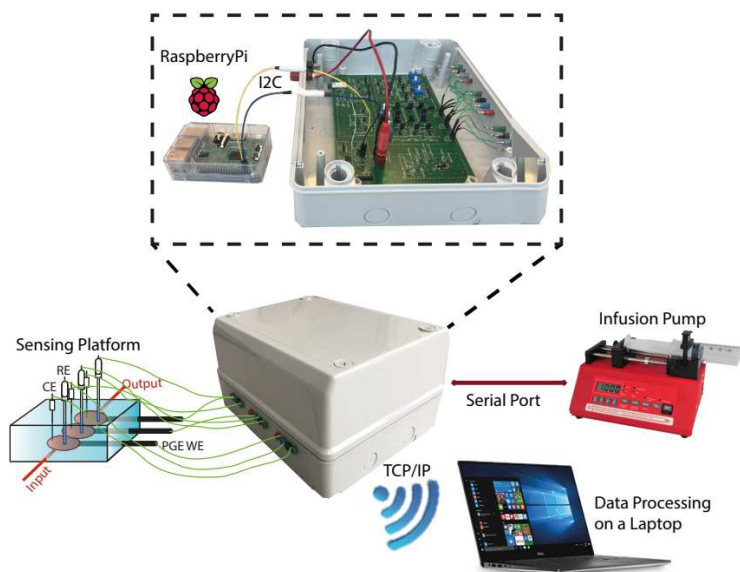


Figure 4.21: Sketch of the RPi based electronic system for Anesthesia monitoring [47]

| CV Measurements | | | | |
|------------------|------------------|----------------------|-----------------|-----------------|
| Start-V (mV) | End-V (mV) | V-Step (mV) | Step Width (ms) | Scan-Rate (V/s) |
| -100 | 1100 | 3.22 | 32 | 0.1 |
| DPV Measurements | | | | |
| Start-V (mV) | End-V (mV) | V-Step (mV) | | |
| -100 | 1100 | 3.22 PCB - 5 Autolab | | |
| Pulse-Width (ms) | Pulse-Ampl. (mV) | Pulse Period (ms) | | |
| 50 | 60 | 68 | | |
| CA Measurements | | | | |
| Appllied-V (mV) | | | | |
| 450 | | | | |

Figure 4.22: Electrochemical test parameters during the measurements [48]

2) CV Measurement

In this cyclic voltammetry test, the test is done with PBS pH 7.4 with 10 mM concentration. During the measurement, the concentration of the APAP is increased with the following values in each step: [50 - 100 - 150 - 200 - 250 - 300] μM . At the end of the measurement, the measurement results are processed with MATLAB and the peak current values for each concentration of the APAP are obtained. The test results are shown in Figure 4.24.

3) DPV Measurement

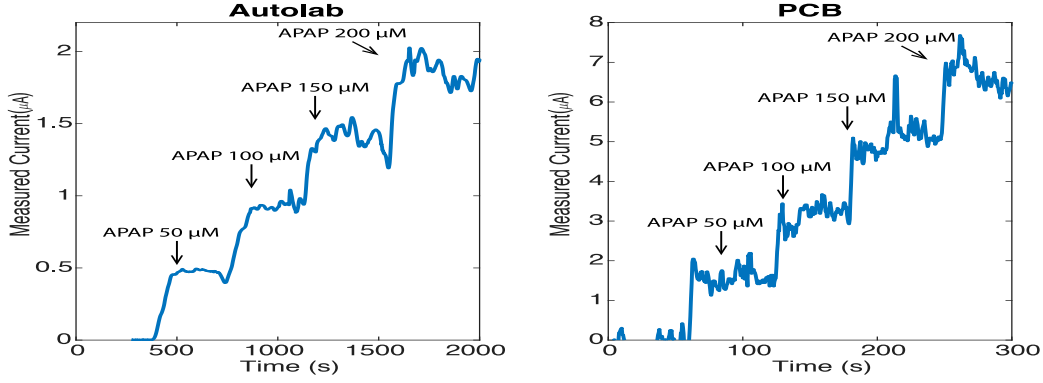


Figure 4.23: ChronoAmperometry test on APAP using Screen Printed Electrodes [48]

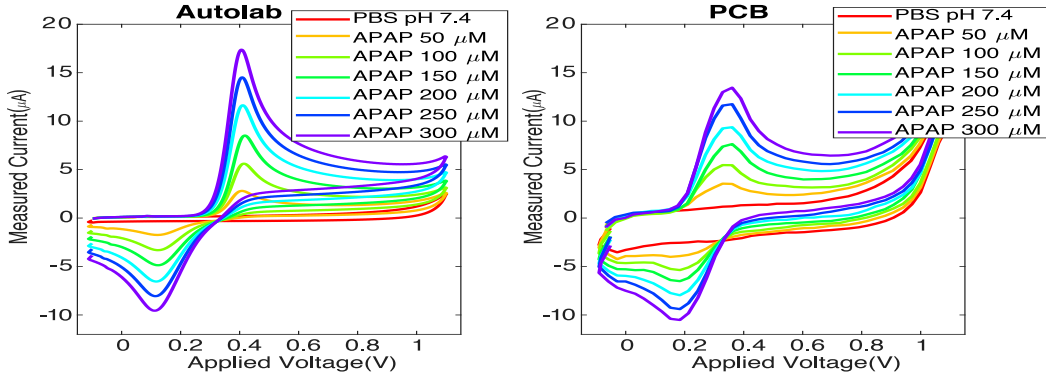


Figure 4.24: Cyclic Voltammetry test on APAP using Screen Printed Electrodes [48]

In this DPV test, we use again the PBS pH 7.4 with 10 mM concentration and we increase the concentration of APAP by the values: [50 - 100 - 150 - 200 - 250 - 300] μM . At the end of the measurement for each concentration, the peak current is obtained. The test results are shown in Figure 4.25.

4) Calibration Curves

After the CA, CV and DPV measurement for the APAP, the calibration curves are plotted in order to show the relationship between the peak current and concentration of the drug. The two sets of results coming from commercial Autolab system and the electronic system are plotted to have the comparison:

From the Figure 4.26, it can be seen that, the calibration curves are quite similar for the both systems and in CV and DPV measurements, our electronic system has better sensitivity as the corresponding curves have higher slopes.

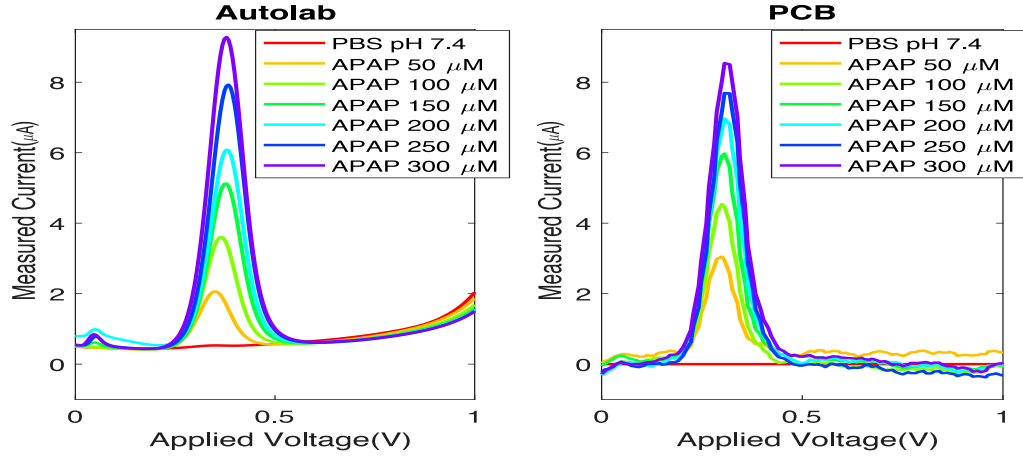


Figure 4.25: Differential Pulse Voltammetry test on APAP using Screen Printed Electrodes [48]

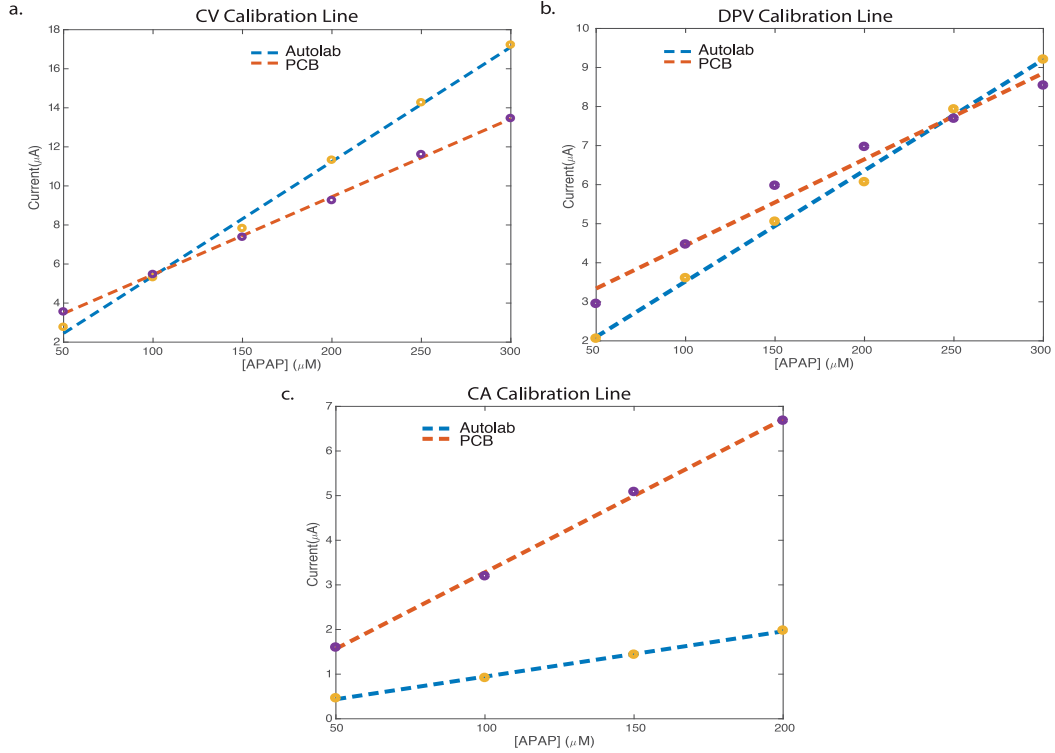


Figure 4.26: Comparison of the calibration curves [48]

5) Scan Rate Analysis

In order to test the performance of the electronic system, the scan rate analysis is carried out on CV and DPV measurements. For the CV measurement, the following scan rate values are tested: [0.16 - 0.11 - 0.09 - 0.08 0.07 -0.06] V/s, while for the

DPV measurement, the following scan rates are tested: [0.08 - 0.06 - 0.05 - 0.04 - 0.03 - 0.02] V/s, keeping constant the duty cycle at 73.5%. From the Figure 4.27, we

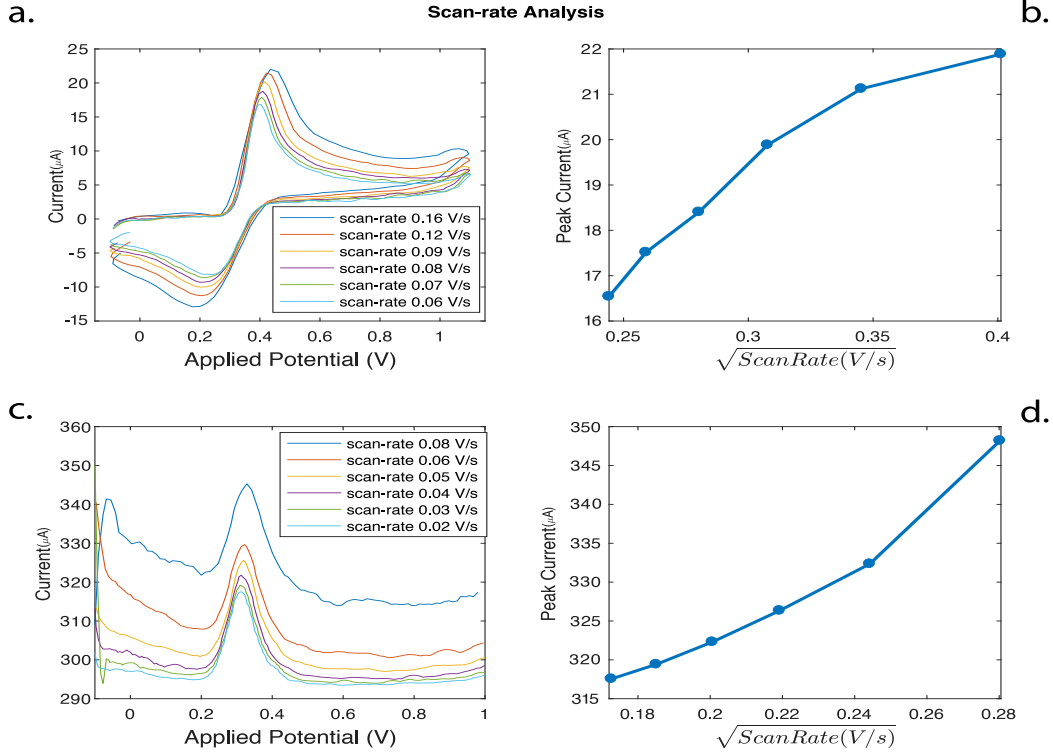


Figure 4.27: Scan rate analysis for CV and DPV measurement of APAP [48]

can confirm that, the Reduction-Oxidation reactions are possible in all the tested scan rates and there is an increase in the current peak with the increase of scan rate. From the CV scan rate analysis, we can see that there is a linear relationship between the peak current and the square root of the scan rate. Therefore, the reaction of the APAP is a diffusion-control process [49].

2. Measurement of Propofol

In this section, the electrochemical techniques of CV and DPV are carried out for Propofol and DPV is done for APAP. This time, the measurements are carried out using custom made electrochemical sensors. They are composed of Pencil Graphene Electrodes (PGE) as the WE, Ag/AgCl as the RE (K0265 105 - diameter 4 mm) and Pt wire from Princeton Applied Research - AMETEK as the CE. The PGE is disposable and it has excellent electrochemical reactivity that makes it highly sensitive. It also has very low cost, great mechanical rigidity, wide potential window, low background current, easy miniaturization and chemical inertness [50]. The electrochemical sensor used in the electrochemical sensing for the sensing

platform is shown in Figure 4.28.

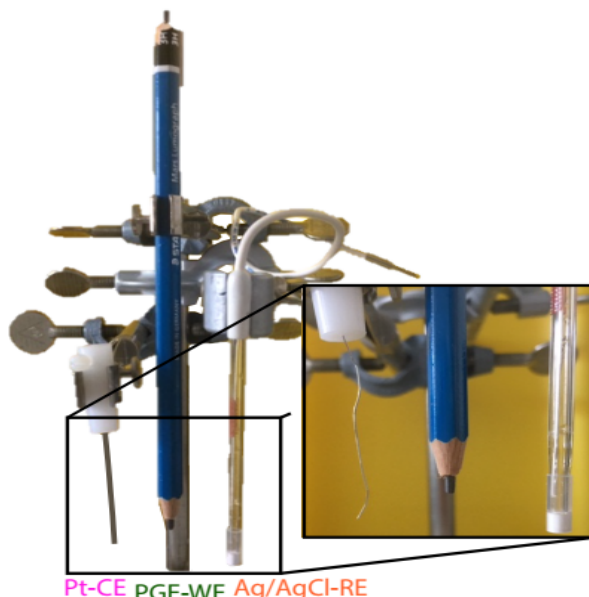


Figure 4.28: Pencil Graphene Electrodes [51]

The test parameters used during the CV and DPV measurements are shown in Figure 4.29.

1) CV and DPV measurements using PGE

In order to characterize the system for the Propofol measurements, the CV and DPV electrochemical techniques are used for the Propofol and the calibration lines are plotted (current peak versus the concentration).

Besides that, the DPV is done for the APAP in order to characterize how it behaves at the PGE interface.

2) Scan rate analysis

The scan-rate analysis is carried out in order to test the performance of the system in fast measurement conditions.

For the fast clearance drugs such as Propofol, the quick responding time of the system is very crucial. From the scan-rate analysis of CV for the Propofol, it can be confirmed that, the fouling effect didn't happen since the oxidation of Propofol was a diffusion-control process.

From these measurement results, we can confirm that the designed electronic sensing system can be used for reliable and robust anesthesia monitoring and therefore we can ensure a more personalized and safer dosing of anesthesia.

| CV Measurements | | | | | |
|-----------------|---------------|-----------------|----------------|--------------------|--------------------|
| Start-V (mV) | End-V (mV) | V-Begin (mV) | V-Step (mV) | Step Width (ms) | Scan-Rate (V/s) |
| 200 | 1350 | 210 | 3.22 | 32 | 0.1 |

| DPV Measurements | | |
|---------------------|-------------------------|----------------------|
| Start-V (mV) | End-V (mV) | V-Step (mV) |
| 0 | 1100 | 3.22 |
| Pulse-Width (ms) | Pulse Amplitude (mV) | Pulse Period (ms) |
| 50 | 60 | 68 |

Figure 4.29: Test parameters for the CV and DPV measurements [47]

4.4.2 Test on Pump Injection

In order to simulate the drug delivery process, the following setup as shown in Figure 4.32 is designed. The system can reproduce the time trend of a drug concentration in a given base volume of an analyzed solution. Through controlling the injection pump charged with the drug, the RPi can handle the dilution process that reproduces the PK trend of a drug. With a PK mathematical model in Matlab, the concentration level is evaluated [52].

In order to validate the system empirically, a dye is used, while the system is validated through experiments that include sensing the variation of pH and reproducing the Paracetamol trend.

In order to reproduce a concentration time-trend of the Paracetamol in the patient blood, the injection of dose is done under the continuous dilution of the base-volume which is executed by a peristaltic flow at a fixed and constant speed. In order to reach a target concentration, the injection volume of the drug is calculated using the initial concentration in a volume V with a flow rate Q . Then the actual concentration of the Paracetamol is measured using CV technique. From the Figure 4.33, we can see the time-trend of the target concentration and also the actual concentration. So, the two trends look quite identical in terms of concentration values [52].

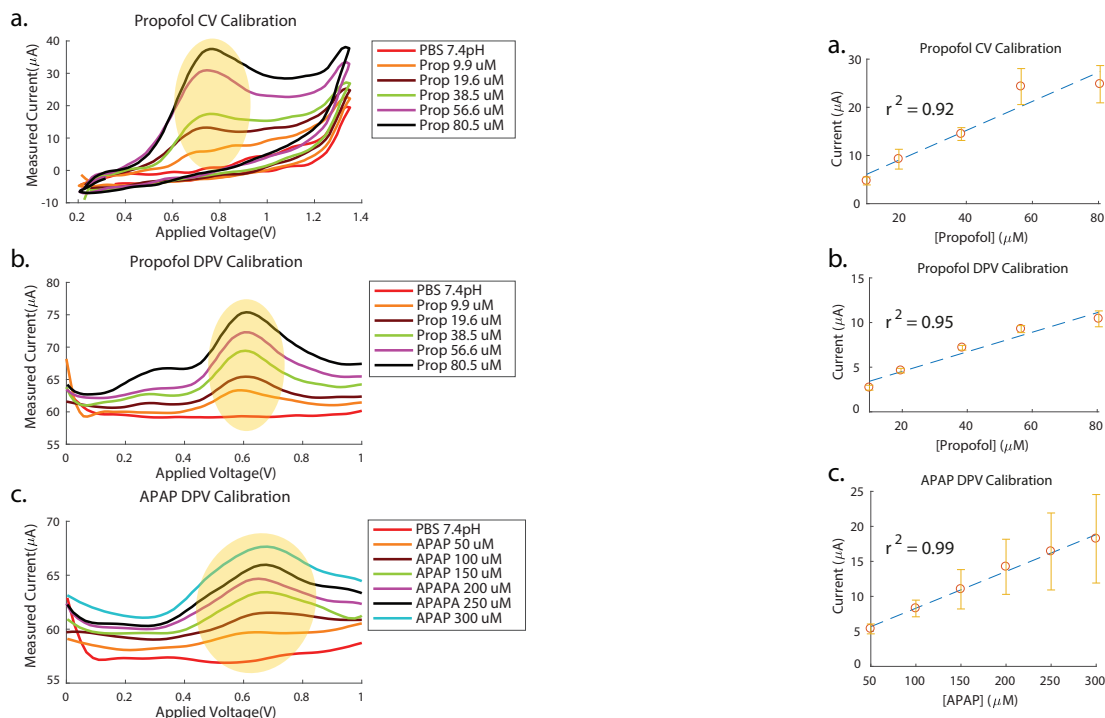


Figure 4.30: CV and DPV measurement of Propofol and DPV of APAP and the calibration curves for each measurement [47]

In order to see the change of the concentration visually, we used the green food dye in the water. The darkness of the green color is different with the different concentration of the dye in water. So, first the dye concentration is increased periodically with injection of dye and it becomes more dark. Then the dye solution is left to be diluted continuously. In this case, the dye concentration decreases in time and at the end, it becomes light green as shown in the Figure 4.34.

After the experiment with dye solution, the pH change in a given solution is observed. The main objective is to evaluate how the system increases or decreases the concentration of a drug quantitatively. This time, the distilled water is used as a neutral solution and the HCl acid is used for changing the pH. In order to measure the pH variations, we have used a commercial pH meter.

By injecting HCl into the solution, the pH is decreased and corresponding H^+ concentration is increased. So, the test is done by increasing the ion concentration fast in time and then leaving it decrease exponentially, as shown in Figure 4.35.

The last test with the flow-injection setup is done with Paracetamol (APAP). First the concentration of the APAP is increased in steps by injection and the APAP is left to dilute with time. Since the concentration of APAP can be measured using the PGE, the change of the concentration in time is plotted, as shown in Figure 4.36.

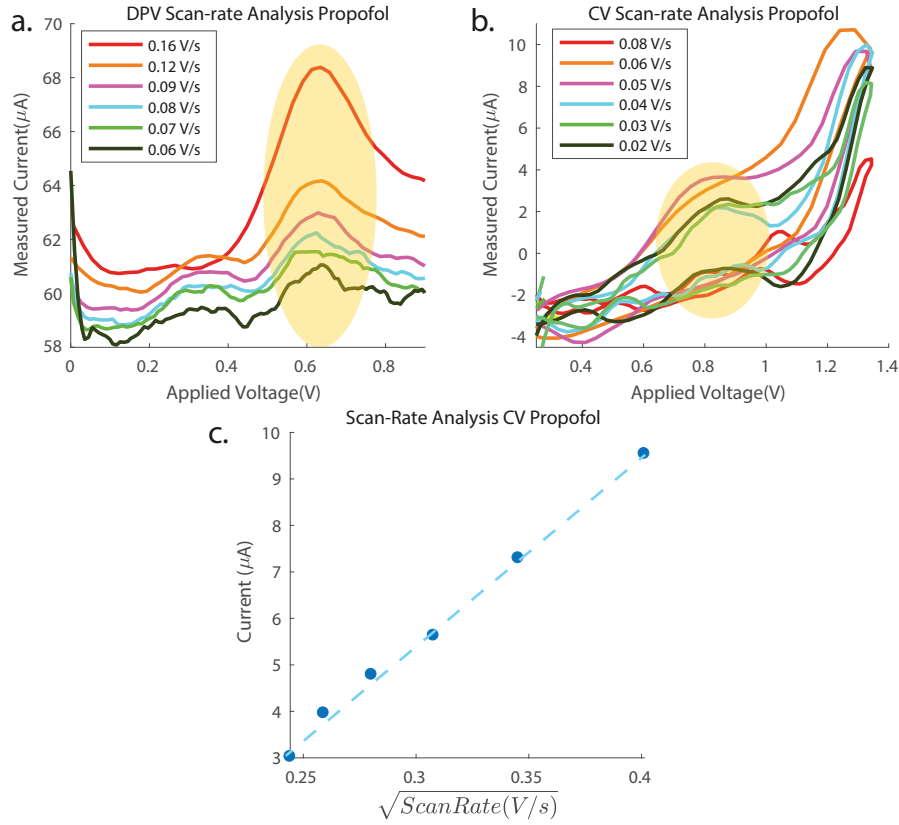


Figure 4.31: Scan rate analysis for CV and DPV measurement of Propofol and DPV of APAP [47]

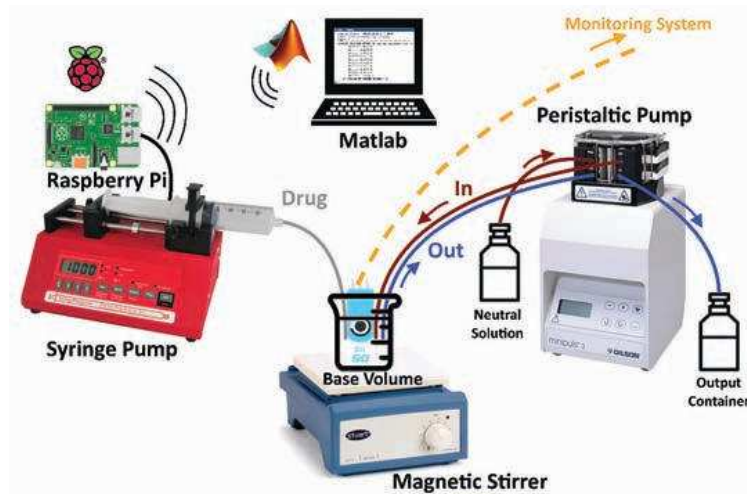


Figure 4.32: Experimental setup for the injection test with TCI pump [52]

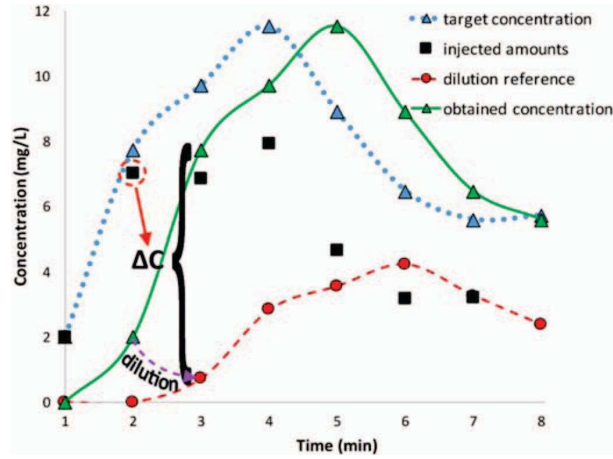


Figure 4.33: Example of the dose injection [52]

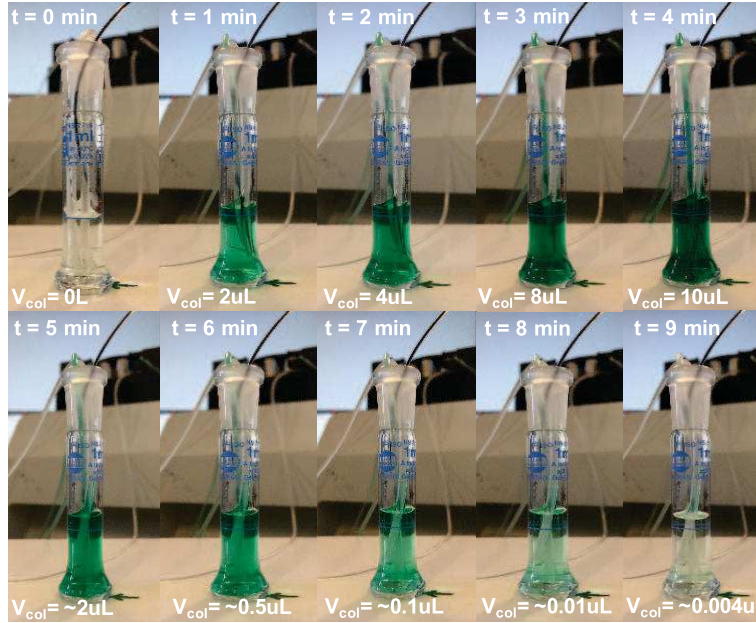


Figure 4.34: Dye test with TCI pump [52]

4.36. In this way, we can characterize the drug delivery system and identify the trade-offs between the drug injection speed, the peristaltic flow speed and the stirring condition of the system.

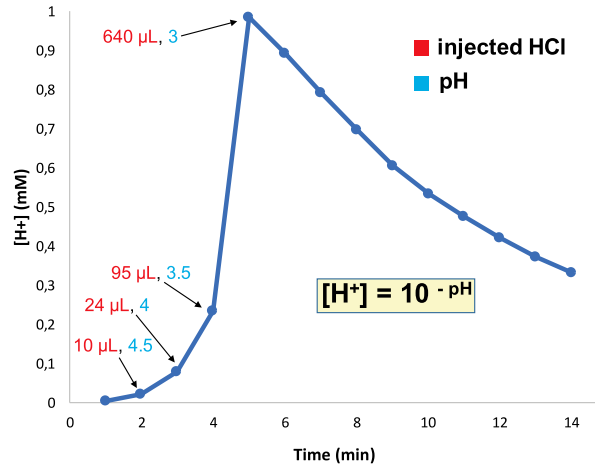


Figure 4.35: pH test: dose injection and measurement of concentration [52]

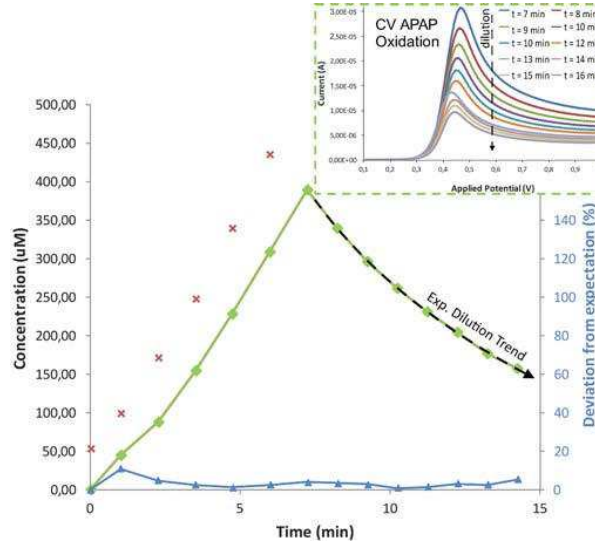


Figure 4.36: APAP test with TCI pump [52]

4.5 Discussion and Conclusion

In this chapter, an embedded electronic sensing platform has been presented for the anesthesia monitoring and delivery. The system is capable of detecting simultaneously and independently the compounds of anesthesia through different electrochemical techniques. The system has high sensitivity, fast response to the change of the concentration of the drugs.

The electronic part of the system consumes low power and is around 390mW. The design of the electronic part has followed strictly the embedded system design methodologies and the smart data analysis is realized in the firmware of the system.

The overall cost of the system is less than 150\$ and its size is 27 x 21 x 13 cm, and is portable. So, compared to the commercial Autolab system mentioned earlier, the has more advantages in terms of cost, sensitivity and portability. Besides that, with the IoT functionality, the presented system can have greater applications in telemedicine, remote patient monitoring and in smart hospital design.

Chapter 5

Portable Memristive Biosensing System for Cancer Diagnostics

5.1 Introduction

5.1.1 Prostate Cancer

The prostate is a gland with a walnut-size in the male reproductive system and is located below the bladder and in front of the rectum. The prostate cancer takes place in the prostate gland and it is a malignant tumor that is caused by the uncontrollable growth of the cells in the prostate gland.

The prostate cancer is a very common type of cancer and causes large number of death among men every year. The table 1.1 reports the predicted death rate of men due to the cancer and it can be seen that the predicted rate for the prostate cancer is around 10.6/100,000 in 2016, which is the third among men in Europe [53].

Table 5.1: Cancer related mortality [53]

| | Cancer type | Deaths in 2011 | Predicted deaths in 2016 |
|-------|-------------|----------------|--------------------------|
| men | Lung | 185,707 | 183,800 |
| | Colorectum | 90,412 | 95,600 |
| | Prostate | 72,330 | 75,800 |
| | Pancreas | 39,056 | 42,600 |
| women | Breast | 91,291 | 92,300 |
| | Lung | 79,474 | 89,700 |
| | Colorectum | 77,478 | 77,800 |

However, if the prostate cancer is detected in its early stage, it can be cured.

So, it is important to detect the cancer in its early stage. One of the most common method for detecting the prostate cancer is through using Prostate Specific Antigen (PSA). PSA is a 30 kDa kallikrein protein and is produced by cells of the prostate gland. it is one of the main cancer marker for prostate cancer.

5.1.2 Therapeutic methods for Malignant Diseases

In order to treat the prostate cancer, some of the common treatment methods are as follows: first, there is the active surveillance, then the surgery, radiopharmaceutical therapy and radiotherapy, chemotherapy, hormone-therapy and biophosphonate therapy. The drug treatment can be also an effective but chemically very invasive therapeutic approach, and is also called as chemotherapy. it is mostly used for the malignant disease treatment, such as the HIV and cancer. The drugs used in these cases are very toxic with severe side-effects, so the monitoring of these drugs is extremely critical.

In the treatment of prostate cancer and HIV, the Etoposide is one of the most commonly used drugs. However, the precise monitoring of the etoposide is very important as it has an effective therapeutic range and it ranges from tens of μM to several hundreds of μM [54][55], [56]. While a small portion of the drug is effective for the cancer, the remaining part goes to the other organs in the body and creates very undesirable side-effects such as hepatotoxicity, alopecia, myelosuppression, leukopenia, cardiomyopathy and so on.

Besides the etoposide, the Tenofovir is also another antiretroviral agent for treating the HIVD1 infection [57]. Its main function is the termination of the chain and it follows intracellular phosphorylation to triphosphate form and prevents the DNA from elongation and the HIV from multiplication. The therapeutic range of Tenofovir is from some nM to 860 nM.

The therapeutic drug monitoring is one of the mostly adopted therapeutic approach and it monitors the drug concentration over time in a closed loop system of the patient and aims at maintaining the concentration of the drug in the effective therapeutic range. This is a patient dependent approach and is based on the characteristics of the patient, and is also based on the drug characteristics used in the chemical treatment. So, it is very complex, has uncertainties when implemented, adopts invasive sample and require the detailed knowledge on the relationship between the profile of proteins and the responses of drugs. So, a cutting edge Point-of-Care approach is needed in order to address these problems existed in the drug monitoring.

5.1.3 Nanotechnology in Diagnostics and Therapeutics

Nanotechnology is drawing more attention of the researchers these years and is the combination of technology, science and other research fields. Its applications are exploited in many areas in the last ten years and in the medical field, nanotechnology is playing more important roles such as providing new approaches for clinical therapies and also for diagnostics [58][59][60].

In the nanotechnology, materials with nanometer scale are created or manipulated and these materials have comparable sizes to proteins, viruses, cells and other biological molecules. This offers a highly accurate sensing methods and it can be extremely useful for the detection and monitoring of the cancer. Therefore, these materials with nanostructures can be ideal candidates for high-sensitive biosensors. Such creation and manipulation of nanomaterials is possible thanks to the development of CMOS technology and small scale, low cost and sensitive, nanoscale biosensors can be produced and used in the medical applications, especially in point of care diagnostics, personalized medicines and self-diagnostics applications [61].

5.1.4 Memristive Phenomena

In the nanoscale, the nanostructures exhibit many interesting properties and some of them also show the hysteretic electrical property, also called the memristive phenomena. This phenomena is an important and unique signature of memory devices and such devices are also called memristors.

The memristor is first presented by L. Chua in 1971 as a fundamental passive circuit element with two terminals [62]. Its resistance depends both on its previous state and its present electrical conditions. The memristor is mathematically defined as a current-controlled device characterized by the memristance (M). For the linear elements, the memristance is constant and is same to the resistance. But when the memristance is dependent on the charge flowing through it, then in this case the memristance corresponds to a nonlinear circuit element and behaves like a resistance with memory and shows a frequency dependence, which is one of the key properties of memristive systems.

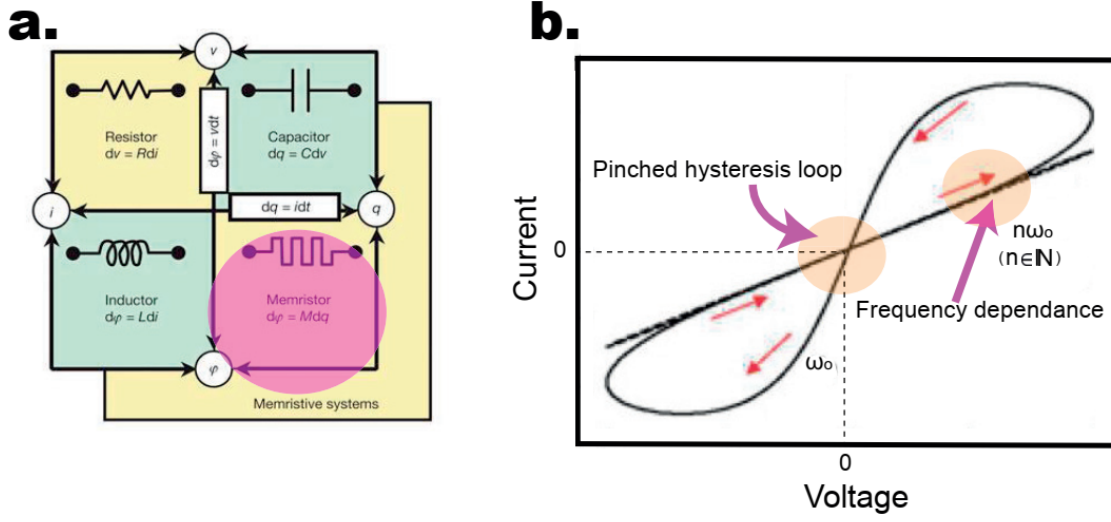


Figure 5.1: Four fundamental circuit variables (a) [63] and the hysteresis curve of a memristor (b) [63]

The mathematical expression for the memristor is following:

$$u = R(\omega)i \quad (5.1)$$

$$\frac{d\omega}{dt} = i \quad (5.2)$$

The u represents for the voltage and the i represents for the current. The ω is the state variable and the R represents the generalized resistance that is dependent on the state of the device.

Such memristance can have many potential applications in the design of memory devices, logic circuits [64], artificial synapses [65][66][67][68] and Resistive RAM memories [69].

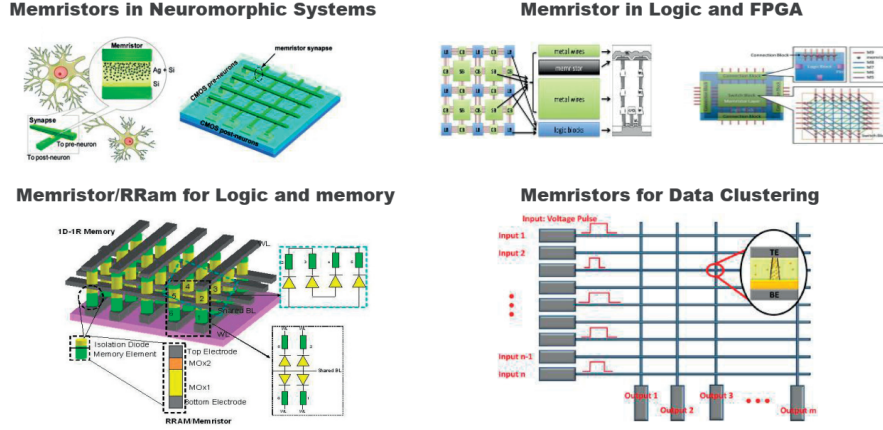


Figure 5.2: Applications of memristive structures ref to [68][70]

5.1.5 Memristive Biosensors for Cancer Detection

The nanobiosensing applications are attracting more attention as they provide real-time monitoring with minimally invasive approaches in the preventive treatments and personalized therapies [71]. Particularly, the one-dimensional silicon nano-wires can be best candidates for bio-sensing applications thanks to their quantum properties and large surface-to-volume ratio [72]. Furthermore, some of the nanofabricated devices such as the silicon nano-wires demonstrate the memristive phenomena mentioned in the previous sections [73]. The memristive effect is dependent on the rearrangement of the charge carriers at the nanoscale which is caused by the external perturbations [73]. In the recent studies, the possibility of creating such memristive silicon nanowires by combining modulated-gate nanowire transistors and redox active molecules is reported [74]. So, a novel-type molecular sensing using memristive nanowires functionalized with the bio-molecular thin films in dry condition is reported in literature [75].

In Figure 5.3 it is shown that the electrical response of the memristive nanowires before and after bio-functionalization is different and this can be used for the ultra-sensitive molecular detection [14], and also for the early stage prostate cancer detection [76].

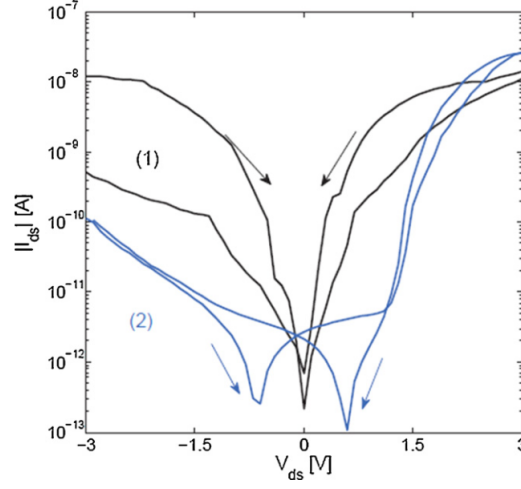


Figure 5.3: Hysteresis response of the memristive nanowires before (1) and after (2) the bio-functionalization [77]

In the curve (1), the voltage difference, also called voltage gap that corresponds to the current minima is zero, while after the bio-functionalization, in the (2), the voltage gap increases due to the gate modulation of the nanowire transistors from antibody charges [77].

5.1.6 Research Objective

The biosensors are devices that convert biochemical signals to measurable electrical signals. Therefore, they need to be combined with proper electronic systems. These electrical signals can be a current, voltage, temperature, humidity, capacitance etc. This is largely dependent on the type of biosensor due to their specificity. So, the bio/CMOS interface is also specific for a given type of biosensor. As it is explained before, the memristive biosensors exhibit the electrical response for the externally applied voltage and the memristive property can be used for the molecular detection. So, an electrical interface that stimulates the biosensors and senses the generated current would be necessary in order to relate the detection of molecules with the hysteresis. Besides that, the generated current signal needs a signal conditioning circuitry and then finally a signal processing block for the quantitative analysis of the measurement. So, the research objective is to design an embedded biosensing platform for cancer detection.

5.1.7 Project Analysis

In this project, the target is to develop an embedded biosensing platform for memristive biosensors and carry out some tests on cancer detection. So, it is important to follow a proper design flow during the implementation. The final system will contain parts related to electronics and also parts related to the memristive biosensors. Besides that, the system will also need some software functionalities to carry out some data processing and calculations. So, the design of these parts can be done in parallel and a final working system that could meet the basic requirements of the test for the detection of cancer could be sufficient. So, the hardware/software design methodology can be a good choice for the parallel design and also for coordinating between different research groups.

5.2 Model Implementation

In the hardware/software design methodology, the parts related to the hardware and software components design can be carried out in parallel. This section describes the implementation of each step and presents a fully working system at the end.

5.2.1 Requirements

The first step in the design is to find out the functional and non-functional requirements related to the project.

Functional Requirements

- The system should be able to interface with 12 memristive biosensors for applying the stimulation signals and sensing the generated currents.
- There are 12 memristive biosensors in each measurement.
- The memristive biosensors should have common stimulation signal from the system.
- The system should be able to provide the signal conditioning circuitry for the generated currents.
- The system should be able to process the output signals from the conditioning circuit.
- The system should be able to analyze the data in a given time.

- The system should be able to forward the data to remote servers if necessary.
- The measurement data should be clean and less noisy.
- The system contain a graphical user interface that can setup test parameters, start and stop operations and display the measurement data if necessary.
- The design time of whole system should not be very long.

Non-functional Requirements

- **Performance:** The timing requirement for a biosensing platform is important as it is related to how fast the system can cope with the biosensors in order to carry out a specific operation, how fast the acquired signals are processed and the data is analyzed, etc.
- **Cost:** The cost during the design of an electronic system is one of the important parameters that need to be taken into consideration from the manufacturing point of view and also from the design point of view.
- **Weight and Dimension:** The dimension and weight of an electronic system affect the usability of the system and they are mainly dependent on the type of the application. The dimension and weight of the system are very critical if when the system needs to be implanted inside the subject. The weight of the system also limits the usability or portability of the system in many scenarios. So, a careful design of the system with a proper dimension and weight is very important.
- **Power Consumption:** In the battery-powered applications, the power consumption is of the dominant factors that decide the lifetime of the system for a normal operation. For example, in the implantable electronic systems, it is not feasible to change the battery so often and it is very important for the system to be power efficient. In the applications where a portable electronic system is preferred, the power consumption is also very a important factor to be considered.

5.2.2 Specification

After the requirements from the application are listed, the next step is to specify in more details what the system functionalities and performances. The system has to have a connection interface to connect to a 12 V power adapter. It has to initialize all internal hardware after it is powered on and enter an idle mode for receiving commands from the serial port managed by the graphical user interface

(GUI) running in PC or other types of Embedded Computers. The GUI has to provide options for setting test parameters, starting and stopping the test operations, setting up, opening and closing the serial port. The GUI should display the test results if necessary and it has to process the data automatically. The signal conditioning block of the system has to process the generated signals from the biosensors and the system has to a data conversion block that can sample the signals from all the 12 memristive biosensors simultaneously or sequentially.

5.2.3 Architecture Design

After the specification step, there is the architecture design step that specifies how the system has to implement the requirements and specifications. The architecture design is composed of hardware architecture and software architecture design.

Hardware Architecture

So, the electronic system was designed to have the following hardware blocks to implement the required operations: 1) a mechanical block that interfaces the memristive biosensors with the rest of the system; 2) a block sensing and actuating the signals for the biosensors; 3) a functional block that can control the overall hardware; 4) a block for serial port communication; 5) a block for smart data analysis; 6) a block for cloud IoT interface for transferring the data. A possible hardware architecture can be as following as shown in Figure 5.4.

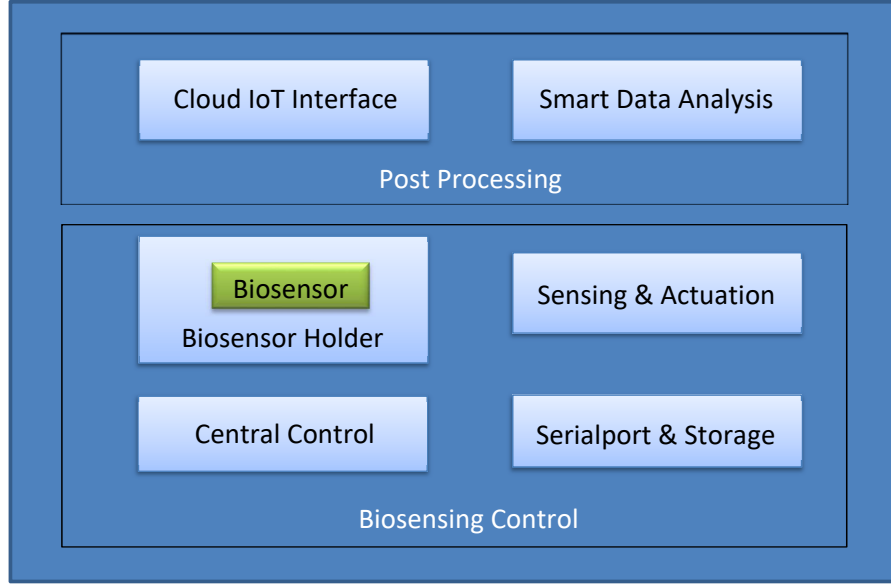


Figure 5.4: Hardware architecture of Memristive Biosensing Platform

It can be seen from Figure 5.4 that the biosensing platform is composed of two main blocks: 1) biosensing control and 2) Post processing block. The biosensing control block contains central control, biosensor holder, sensing and actuation, and finally the serialport and storage sub-blocks. The Post processing block is composed of cloud IoT interface and smart data analysis sub-blocks. A more detailed hardware architecture is shown in Figure 5.5.

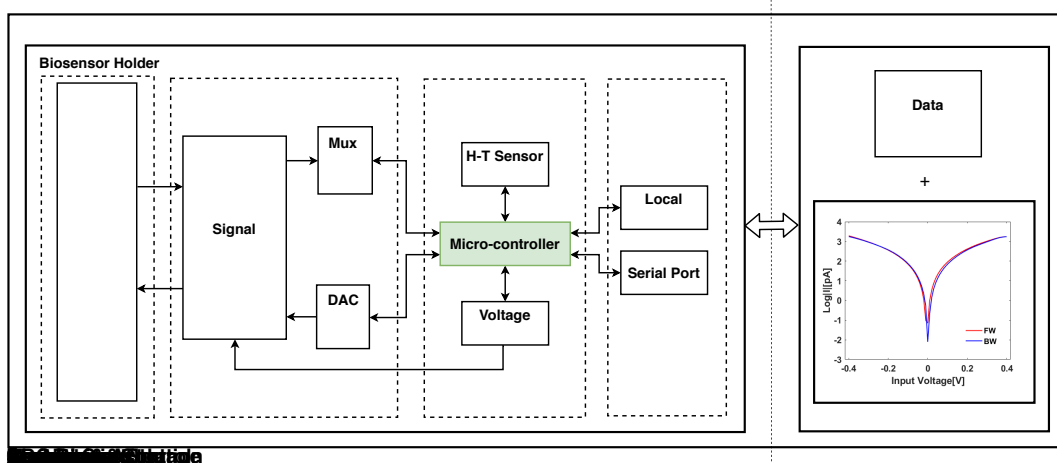


Figure 5.5: More detailed hardware architecture of the system

In the biosensor holder block, it is present a mechanical holder that hosts the

memristive biosensors and interfaces them to the rest of the hardware. In the sensing and actuation block, the signal conditioning block is responsible for processing incoming signals from the biosensors. The DAC and doubling block generates stimulation signals and amplifies by a factor of two. The Mux and ADC block multiplexes between 12 memristive biosensors and carries out measurements sequentially for each of them.

The central control block contains the micro-controller that executes software operations and also controls other blocks. The H-T sensor block is useful for measuring humidity and temperature, while the voltage regulators block shall regulate the input voltage and then powers up the rest of the hardware blocks except the data processing block.

It is present a local storage block that contains a μ SD Card holder for storing (in off-line mode) the measured data and the serial port block will be dedicated to the communication with a PC or an embedded computer. The data processing block post processes the data and forwards the data to IoT cloud server wirelessly. There is also a data visualization block that can plot the processed data if necessary.

Software Architecture

The software architecture contains the software blocks needed for the carrying out the operations of the system. A possible architecture is shown in Figure 5.6.

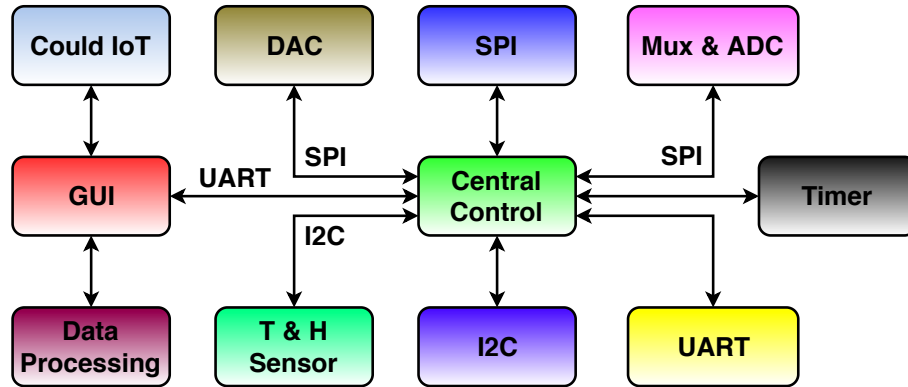


Figure 5.6: Software architecture of the system

In the software architecture, the central control block communicates with Graphical User Interface (GUI) block via the UART library, transmits data packets and receives test commands. It communicates with MUX and ADC block through SPI library, selects the input signal for ADC, triggers the conversion and then reads back the converted digital data. It communicates with DAC block via SPI library, writes digital samples to it to generate analog voltage signal. It communicates

with Humidity and Temperature block via I2C interface, reading the humidity or temperature of the environment. It sets up the timers for periodic operations. The GUI block contains the control panel for setting up the experiment and sends the parameters via UART port to the central block. It also receives the measurement data from central block, processes it and sends it to the Cloud server if needed.

5.2.4 Components Design

The components design step implements the blocks in the architecture design step and it contains hardware components design and software components design.

Hardware Components Design

A) Central Control. This block contains three sub-blocks: Micro-controller, H-T Sensor Module and Voltage Regulators. For the Micro-controller, the high performance STM32F446RE Micro-controller is selected. This micro-controller can reach 180 MHz frequency and it has 16 internal counters. It contains various types of communication interfaces, such as I2C, SPI, UART, etc. The H-T Sensor Module is composed of HDC1050DMBT and it is useful for measuring the environment humidity and temperature during tests. The voltage regulators produce different levels of output voltages: 2.5 V, 3.3 V, 5 V and 10 V. The 2.5 V is generated by ADR3425ARJZ as the 16-bit high resolution Digital to Analog Converter AD5686RBRUZ in the DAC & Amp block needs a highly stable 2.5 V reference voltage. The 3.3 V is generated from LD1117DT33 chip and it is supplied to the micro-controller. The 5 V is generated from LM22674MRE-5.0 chip and is supplied to operational amplifiers in the signal conditioning block. The 10 V is generated from MCP1804 chip and is also supplied to the signal conditioning block.

B) Biosensor Holder. The biosensor holder contains a sensing chip that includes 12 silicon nanowires with common excitation and independent outputs connected to the signal conditioning block. The biosensor holder has a dimension of 20x20 mm and it also has a connector that interfaces it to the signal conditioning block. The biosensor holder is shown in Figure 5.7.

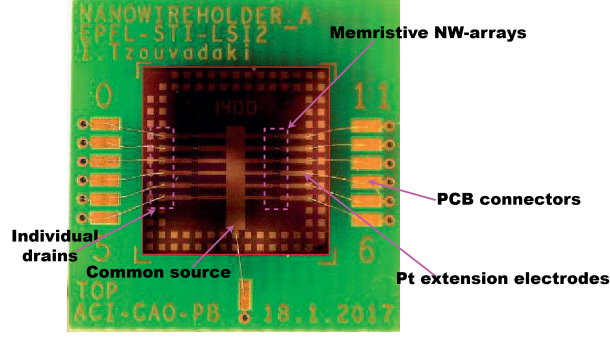


Figure 5.7: Chip holder board [78]

C) Sensing and Actuation. This block contains three sub-blocks: signal conditioning, mux & ADC, DAC & Amp. The signal conditioning block takes the input current from biosensor holder block, then converts the current to voltage through a transimpedance amplifier and then gives it to the Mux & ADC block. The detailed schematics of the signal conditioning block is shown in Figure 5.8.

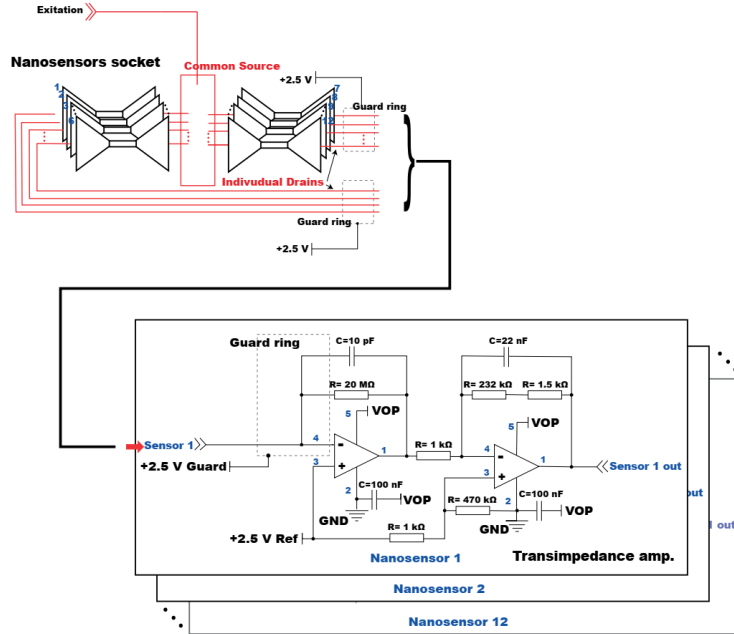


Figure 5.8: Signal conditioning front end [78]

The OpAmp is AD8641 and it has an input bias current of maximum 1 pA. The signal conditioning block has in total 12 outputs correspondent to the memristive nanowires.

The Mux & ADC block takes inputs from the signal conditioning block. For the Mux ADG428BRZ is used while for the ADC, the 20-bit AD7785BRUZ chip is

used. The Mux selects sequentially each signal conditioning output, then the signal is converted inside ADC and is then read by the micro-controller in the central control block.

The DAC & Amp block is composed of AD5686RBRUZ and AD8641 chips. it is possible to generate very accurate stimulation signal thanks to the 16-bit DAC.

D) Serialport & Storage. This block is dedicated to the serial port communication and local data logging in the μ SD Card. The serial port is composed of FT232 Module that converts UART to USB, while the μ SD Card holder supports the microSDXC card (64 GB, SDCA3, speed class 10) for storing local data.

E) Post processing. The post processing block is composed of two sub-blocks: data processing and visualization. For the data processing and visualization, the high-performance Raspberry Pi (RPi) 3 is used. It communicates with the STM32F446RE micro-controller through the serial port block. The RPi has integrated WiFi chip and it supports IoT applications.

Software Components Design

This section describes in details the design of the software blocks that run inside the STM32F446RE Micro-controller and RPi 3.

A) GUI. The GUI is designed in order to make the system easy to use and flexible. It is developed in Qt Creator 5.3 using C++ and it runs inside the RPi 3. It is shown in Figure 5.9.

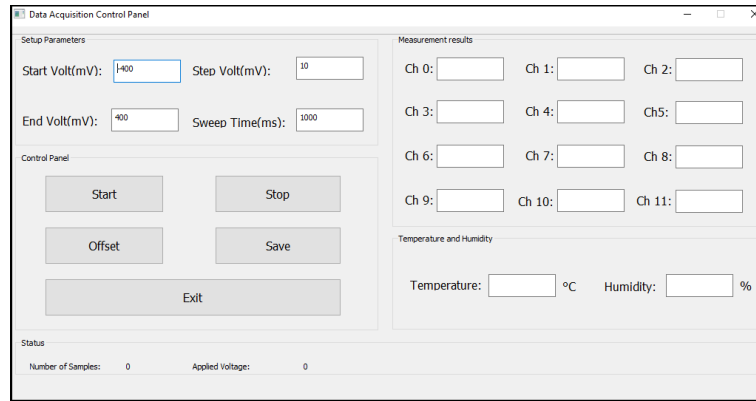


Figure 5.9: GUI for controlling the measurement

It contains parameters related to the test such as: start voltage, stop voltage, step voltage and sweep time or step width. After the parameters are set, they are

sent to the STM32 micro-controller via serial port and then the micro-controller can configure the internal hardwares such as the timer, ADC and DAC for the test.

B) Central Control. This block initializes all the hardware and software inside the micro-controller and the work flow of the central control is shown in Figure 5.10.

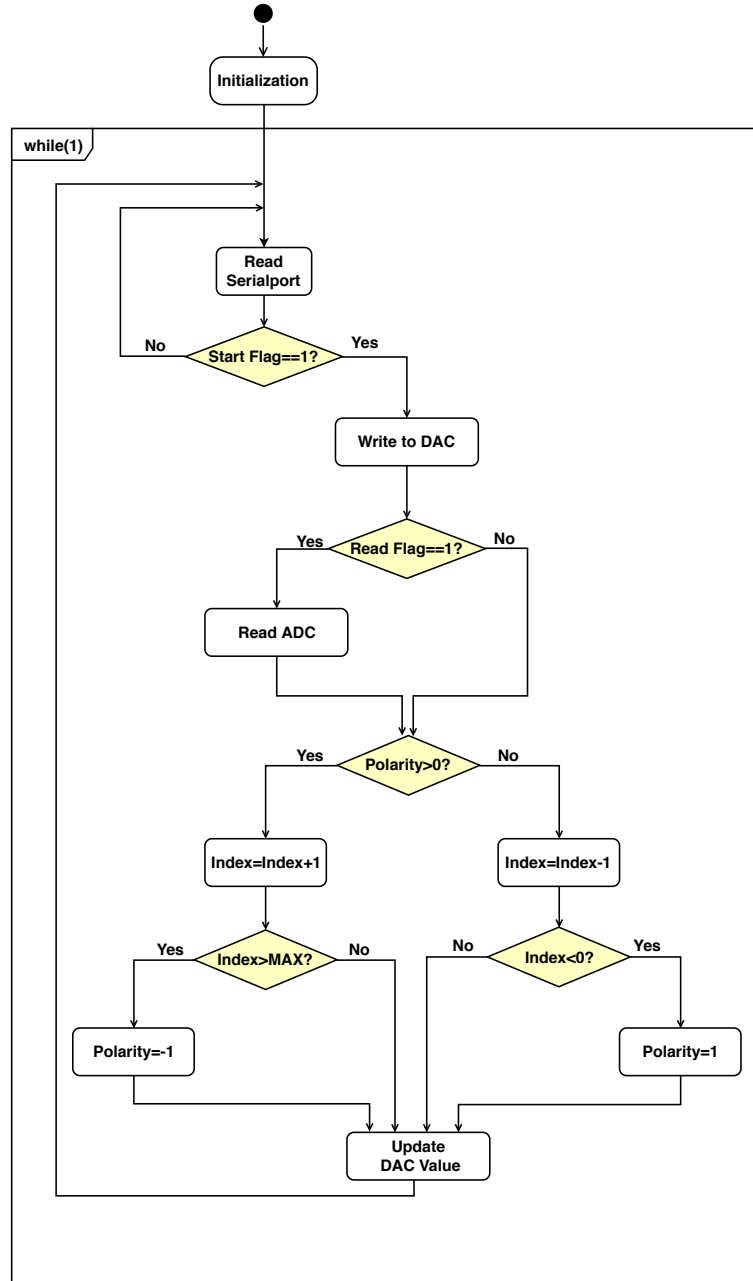


Figure 5.10: Work flow of the central control block

From the Figure 5.10 it can be seen that, after the initialization of hardware and software components, the central control block enters a continuous while loop. First, it reads the serial port to see if there is any data packet arrived from the external GUI. If yes, then it parses the data packet, extracts the commands and test parameters. If it is the start command, then the Start Flag is set to 1 and measurement on biosensors starts. If it is the stop command, current ongoing measurement will stop. After the start command is received, the central control block writes to the DAC block to generate the stimulation voltage. Then it checks the Read Flag. If the flag is set, then the digital value from ADC block is read and sent to serial port. After that, according to the polarity flag, the index that decides the digital value of DAC will increase or decrease and a new DAC value is calculated for writing to the DAC chip. Then the loop repeats until the stop command is received from serial port. Here the timer library controls the read and polarity flag.

C) DAC. This software library controls the generation of stimulation voltage via write to the DAC chip. The stimulation voltage range is from 0 to 2.5 V, then after the amplification circuit with a gain of 2, the final output voltage has a range of 0 to 5 V. Besides that, outputs of the biosensor chip are referenced at 2.5 V. Therefore, it is possible to apply a voltage sweep in the range of ± 2.5 V between common source and individual drain on the biosensor chip shown in Figure 5.7. The relationship between the digital value and actually generated voltage at the output of the DAC chip is following:

$$V_{out} = \frac{D}{65535} \times 2.5(V). \quad (5.3)$$

The maximum value 65535 corresponds to the 2.5 V and after amplification, it is 5 V. So, the actual applied voltage difference between the source and drain terminal of the biosensor is:

$$V_{out} = \left(\frac{2D}{65535} - 1 \right) \times 2.5(V). \quad (5.4)$$

The writing value and its duration can be precisely controlled through the timer library during the voltage sweep and the applied voltage to the biosensors has the following profile shown in Figure 5.11.

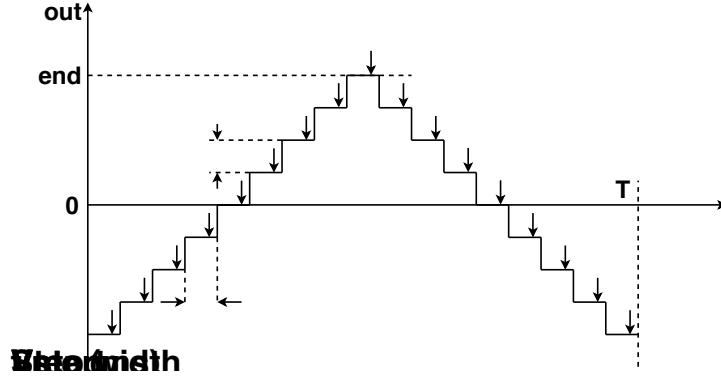


Figure 5.11: Voltage sweep during measurement

D) Mux & ADC. The multiplexer is controlled by writing to the corresponding gpio pins of the micro-controller so that desired signal conditioning channel can be selected for signal sampling. The ADC is configured as bipolar with Gain equal to 1 and external 5 V reference voltage. The ADC is controlled through the timer library and it samples when the timer triggers it. The output results are 24-bit and the upper 4 bits are neglected. The output coding is calculated through the following equation:

$$Code = 2^{N-1} \times [(Vin \times \frac{GAIN}{V_{REF}}) + 1]. \quad (5.5)$$

In our case, the N is equal to 20, the V_{REF} is 5 V, and Gain is set to 1. So, from the output result, it is possible to calculate the input voltage:

$$Vin = (\frac{D}{524288} - 1) \times 5(V). \quad (5.6)$$

E) Data Processing. The data processing block is dedicated to the inverse calculation of the generated current on each biosensor from applied voltage and then to find out the voltage gaps described in previous sections. This block is part of the GUI application inside RPi 3. The applied voltage is calculated from 5.4 and measured voltage is calculated from 5.6. The generated current is calculated according to the input output relationship of the signal conditioning hardware block:

$$sensor_current = -(\frac{470 \times 234.5}{471 \times 233.5 \times 2.5} - \frac{measured_voltage}{233.5}) \times 5 \times 10^4(pA). \quad (5.7)$$

After the sensor current is calculated, then the logarithmic value of its module is calculated:

$$Log_I = \log_{10}(Abs(sensor_current)). \quad (5.8)$$

Then the Applied_voltage vs. Log_I graph is plotted and the voltage gap is obtained at the two minimum Log_I values. This will be shown in the experimental results section.

5.2.5 System Integration

The next step is to integrate the whole system and carry out tests and debugging. The first prototype of the biosensing control system is shown in figure 5.12.

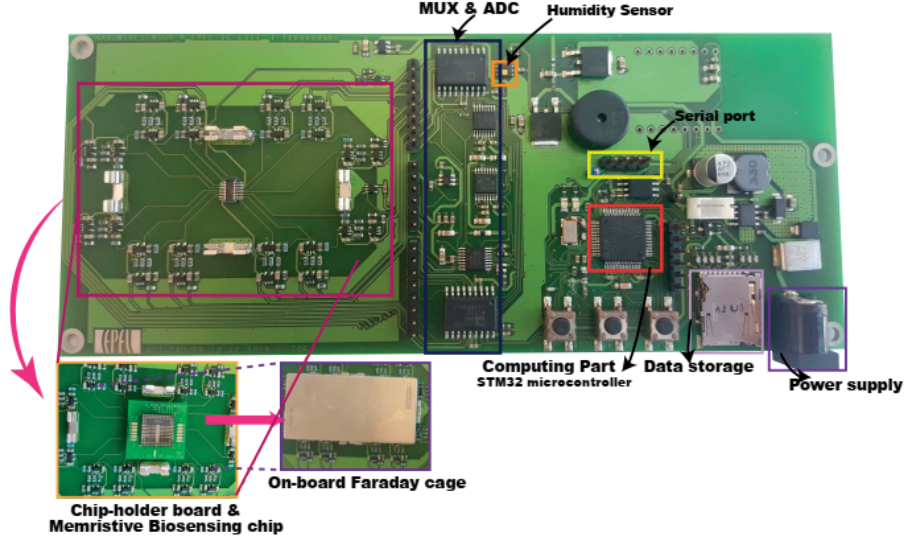


Figure 5.12: The first prototype of biosensing control system

The post processing block is composed of a RPi and a uart to serial converter. So, the final system is shown in Figure 5.13.

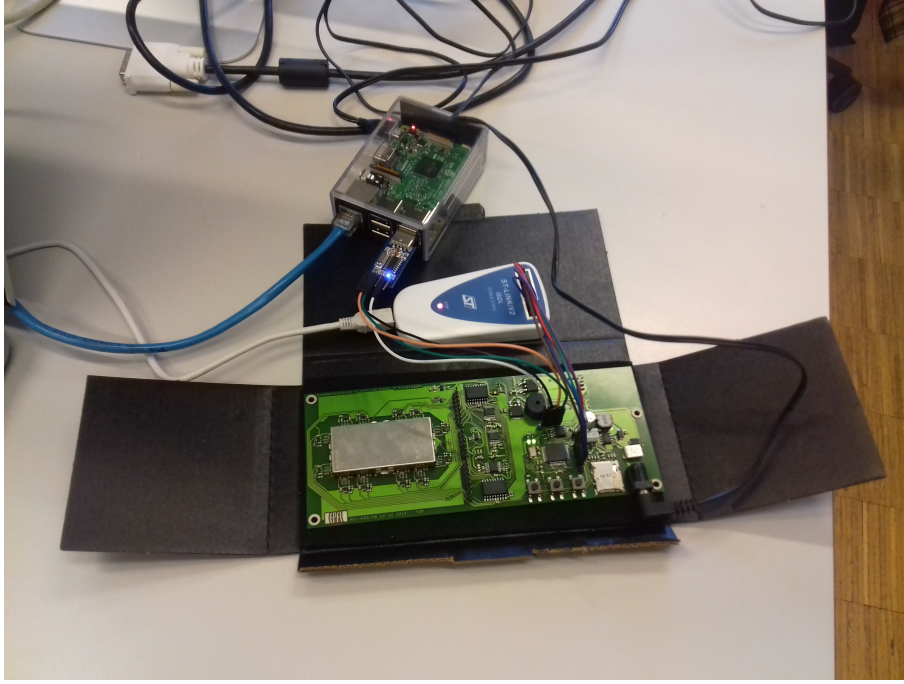


Figure 5.13: The complete memristive biosensing platform

The RPi can be accessed through NX Server via ethernet connector from PC, so there is no need for additional monitor, keyboard and mouse. The next sections present the test results and validate the design.

5.3 Experimental Results

After the complete system is ready, the next step is to carry out experiments on the fabricated memristive biosensor chips. Initial test is carried out on bare memristive nanowires that are newly fabricated. Then there is the antibody printing step followed by the antigen detection step.

5.3.1 Test on Silicon Nanowires

In this test, the silicon nanowires do not yet have any antibodies on top of them and the test is simply the current to voltage response. It demonstrates the memristive hysteresis properties shown in Figure [5.14](#).

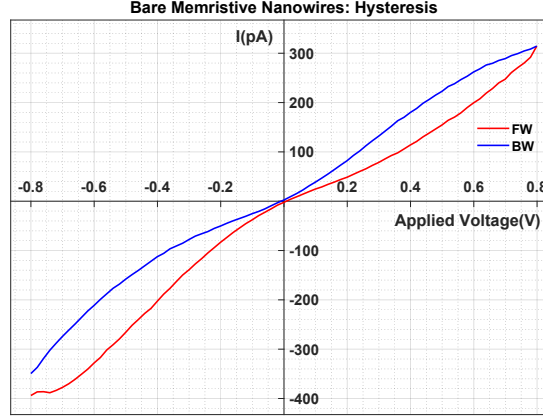


Figure 5.14: Hysteresis curve of the bare memristive nanowire chip

In this test, the start voltage is -0.8 V, the end voltage is 0.8 V, the step voltage is 0.2 V and the step width is 1 second. Besides the hysteresis curve, we also have the curve of the applied voltage and logarithmic current module shown in Figure 5.15.

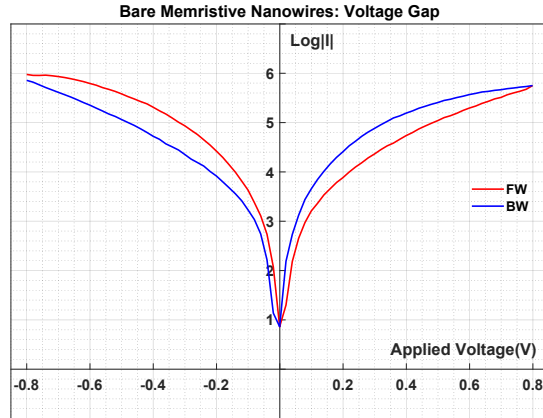


Figure 5.15: Voltage gap of the bare memristive nanowire chip

In the voltage gap curve, it is obvious that for the memristive nanowires before bio-functionalization, the voltage gap is almost zero. The hysteresis curve is also not very flat near the origin.

5.3.2 Test on Antibody-based Memristive Biosensors

In this test, the memristive nanowires go through the antibody printing. This process will change the electrical response of the silicon nanowires and we observe different hysteresis curve shown in Figure 5.16.

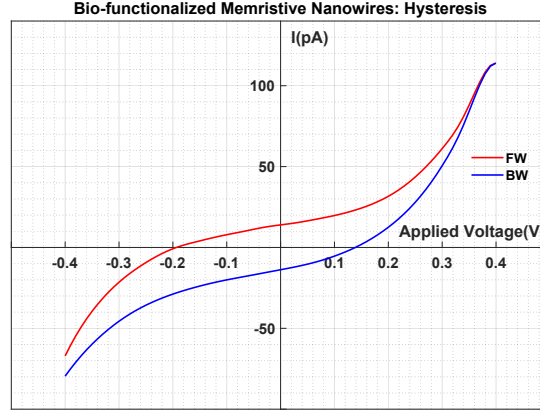


Figure 5.16: Hysteresis curve of the bio-functionalized memristive biosensor chip

Besides that, the voltage gap curve is also different shown in Figure 5.17 and the voltage gap is close to 0.34 V. So, the antibody has changed the hysteresis property of the silicon nanowires on the chip holder and this is related to the change of Debye Length on the surface charges on the nanowires.

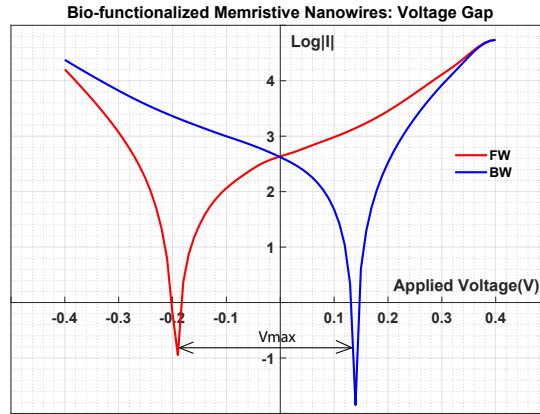


Figure 5.17: Voltage gap of the bio-functionalized memristive biosensor chip

5.3.3 Test on Prostate Specific Antigen (PSA)

In this test, the Prostate Specific Antigen (PSA) is used as a cancer marker of Prostate Cancer and two different concentrations 3.3 fM and 330 fM are tested. The voltage gap in the logarithmic curve of the current changes with the concentration of the antigen and by using the calibration curve that relates the voltage gap and concentration of the PSA or other antigens, it is possible to obtain the concentration from voltage gap values. In this test, first a PSA concentration of 3.3 fM is tested, then 330 fM is tested. The comparison of the hysteresis is shown in Figure 5.18.

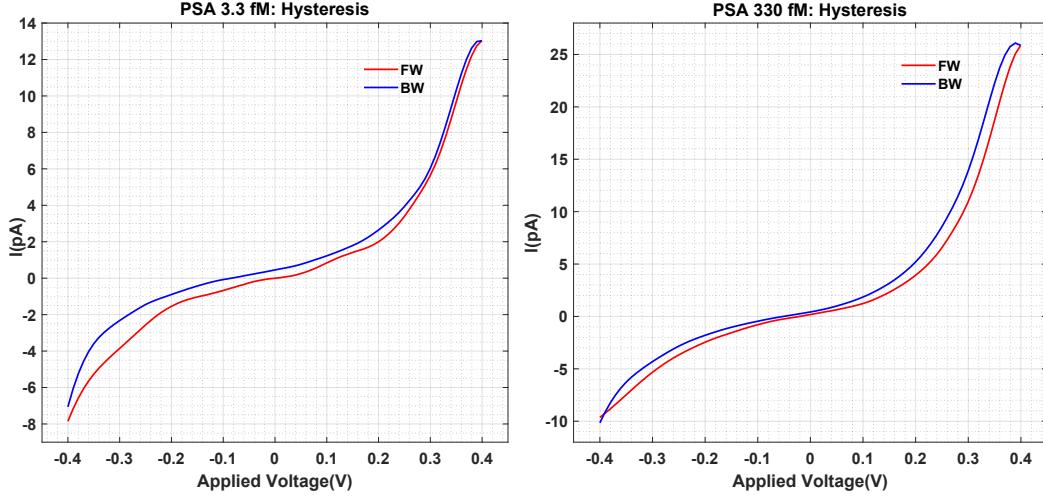


Figure 5.18: Comparison of hysteresis for 3.3 and 330 fM PSA

In Figure 5.19, the two voltage gaps are compared with each other and it is expected to have a decrease in the voltage gap with respect to the increase in concentration and the assumption is validated in the test.

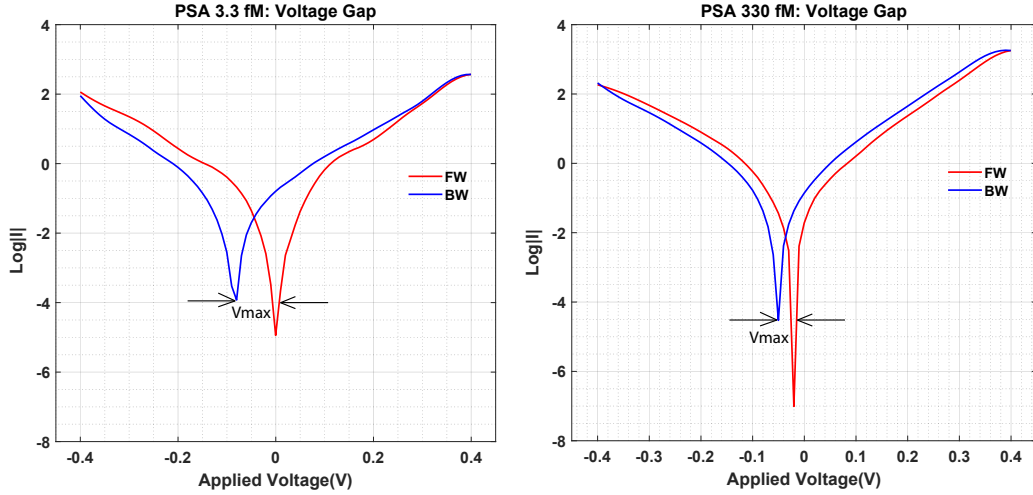


Figure 5.19: Comparison of voltage gaps for 3.3 and 330 fM PSA [78]

5.4 Discussion and Conclusion

Here we discuss the results and conclude. In this chapter, a novel memristive biosensing platform is presented. The design of the system has followed hardware/software concurrent design methodology and the overall design time was optimized thanks to this approach. The system was designed in order to optimize

the measurement process. Previously, the Cascade Microtech Probe Station and a Hewlett-Packard 4165A Precision Semiconductor Parameter Analyzer were used for sensing and actuating the memristive biosensors during the measurement and the measurement time was around 40 minutes for 16 memristive nanowires, approximately 3 minutes for each of them and the test was done manually [76][78]. Now, the whole test for 12 memristive biosensors takes around 3 minutes. Furthermore, the test is controlled flexibly and the data processing is done automatically in the GUI in a smart way. The calculation of voltage gaps is also done within the software and at the end of the test, the voltage gaps are available as final results. It is also possible to see how the memristive biosensors respond to the stimulation and their electrical behavior can be monitored in real-time during the test [76]. Besides that, the designed embedded system is portable, consumes low power, can be powered by a battery and costs around 200\$ which is much cheaper compared to the prices of the commercial probe station and parameter analyzer used in the previous research. So, this is a very novel biosensing platform that can be very useful for the early stage cancer detection thanks to the ultra-high sensitivity of the memristive biosensors [14] and also thanks to the automatic and easy-to-use embedded biosensing platform.

Chapter 6

General Purpose Biosensing Platform Design

6.1 Introduction

In health care research and promotion and delivery, the main aim is to assess disease progression, health status and monitor the outcome of a treatment by using a non-invasive method. It requires three preconditions in order to achieve this goal: specific biomarkers that can indicate healthy or diseased states; a possible non-invasive approach for detection and monitoring the biomarkers; and finally the technology for discriminating biomarkers [79].

6.1.1 Biosensors in Health Care

Biosensors are being widely used in medical diagnostics and scientists are carrying out extensive research in developing innovative technologies and newer tools. Since the biosensors have immense potentiality in medical diagnostics, as they are simple in operation, they have high sensitivity, they could perform multiplex analysis, and they are capable of being integrated into the same chip with different functionality [80].

Biosensors can be categorized into different groups based on their transduction element or biological element. The biological elements can be antibodies, enzymes, biological tissue, organelles and micro-organisms. Depending on their transducer elements, the biosensors can be piezoelectric, optical and electrochemical types [81].

6.1.2 Definition and Characteristics of a Biosensor

A biosensor is described as an analytical device that is used for detecting chemical substances and converts a biological signal to a processable and quantifiable signal.

Generally, every biosensor is composed of a biological component that senses the substances of interest and an electronic component that captures and transmits the biological signal [82].

A biosensor can be composed of the following parts, as shown in Figure 6.1 [83]:

- **Analyte:** A substance that needs to be detected. For example, in a glucose biosensor, the 'analyte' is the glucose.
- **Bioreceptor:** A molecule that recognizes only a specific type of analyte.
- **Transducer:** It is an element that is dedicated to converting an energy from one type to another. The role of it in biosensor is to convert the biological signal into a measurable signal. The signals can be electrical or optical depending on the type of transducers.
- **Electronics:** It is the part that is used to process the signal coming from the transducer and to prepare it for post-processing or display. It is composed of electronic circuitry that carries out signal conditioning and conversion.
- **Display:** This part is used for quantifying the processed signals coming from electronics. The display can be graphic, numeric, an image or tabular, depending on the actual output requirements of an application.

The typical characteristics of a biosensor [83] are:

- **Selectivity:** The selectivity is defined as the ability of a biosensor in detecting a specific analyte in samples that contain other contaminants and admixtures. A good example can be the interaction of an antigen with an antibody. The antibodies are bioreceptors immobilized on the surface of the transducer. When the antibody is introduced into a solution that contains the antigen, then it interacts only with the antigen. So, during the construction of a biosensor, the main consideration in choosing the bioreceptors is the selectivity.
- **Reproducibility:** This the ability of a biosensor to show identical responses for a duplicated experimental set-up. In a biosensor, reproducibility is characterized by the accuracy and precision of the transducer plus electronics. Reproducibility plays an important role in providing robustness and high reliability in understanding the response of a biosensor.

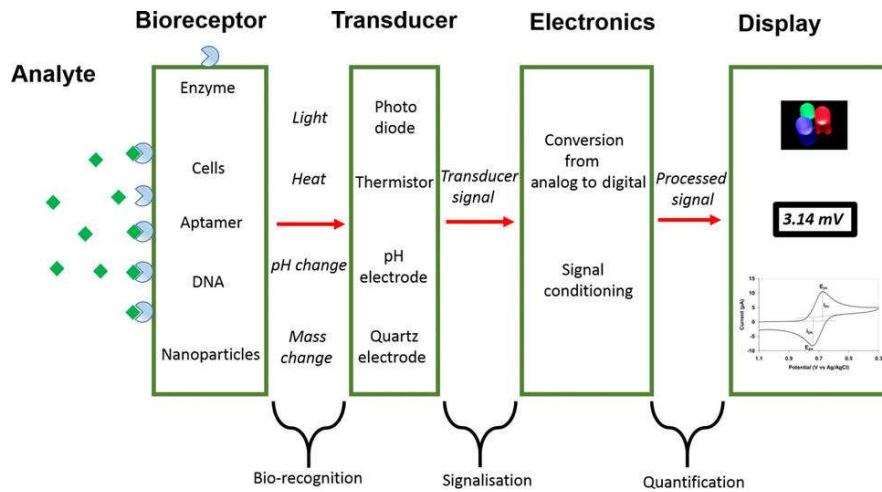


Figure 6.1: Internal blocks of a biosensor [83]

- **Stability:** It is defined as the degree of susceptibility of the biosensor to the ambient disturbances. The output signals of a biosensor could be subject to a drift due to these disturbances, which results in erroneous measurement in concentration and will affect the accuracy and precision of the biosensor. It is very crucial for a biosensor to be stable in continuous monitoring or in situations where the biosensor would long incubation steps.
- **Sensitivity:** It is also called the limit of detection (LOD) and it is defined as the minimum amount of analyte a biosensor could detect. In many environmental and medical applications, the biosensor is required to have a very high sensitivity in order to confirm if a sample contains possible analytes. For example, in the early stage prostate cancer detection, the doctors will suggest biopsy tests for a prostate-specific antigen (PSA) concentration of 4ng/ml in blood.
- **Linearity:** It is an attribute linked to the range of analyte concentrations and resolution of biosensor under test. The resolution of a biosensor can be understood as how much change in the analyte concentration could cause a change in biosensor response. The linearity of a biosensor is required in order to guarantee that the biosensor works in a wide range during the measurement of analyte concentration.

6.1.3 Electronics for Biosensors

In a biosensing platform, the transducer or biotransducer converts the biological or electrochemical changes into a detectable electrical signal. Depending on the

type of biotransducer, the electrical output signal can be different. In electrochemical sensors, the electrochemical changes that are taking place on the surface of the electrodes that are interacting with the analyte. These changes can be amperometric, potentiometric or conductometric. So, the output signals are current, voltage or conductance. In optical sensors, the electrical signal that changes is the properties of light, which can be correlated with the changes in concentration, mass or molecule number in the cells. In piezoelectric sensors, the output of the transducer is the resonant frequency of the crystal which results in an oscillating voltage that can be tracked by an acoustic wave sensor. In thermal or calorimetric sensors, the output signal is the temperature and by measuring it, the concentration of analytes can be determined.

In order to carry out the measurements on the current, voltage, conductance, temperature or other electrical signals, an electronic system would be necessary and it would perform different operations such as amplification, filtering, level shifting, attenuation, conversion, linearization, electrical isolation, excitation, etc.

In different biomedical applications, one might find different electronic systems that are specific to the selected biosensors. For example, let us consider three biosensing platforms based on different biosensors: 1) a point-of-care memristive biosensing platform is developed for the early stage cancer detection [78] 2) an electrochemical sensor based biosensing platform is presented for on-line monitoring of anesthesia in [44] 3) A flexible biosensing platform for wearable electrochemical sensing [84].

In all the three applications, there are different biosensors or sensors, such as memristive biosensor, electrochemical sensor and ion-sensitive biosensor. The custom electronic system developed for each sensor cannot be shared with each other and no standard interface which allows the interconnection between the sensor and electronic platform is available. Therefore, if there is a need to develop a biosensing platform for another type of sensor or biosensor, the electronics that conditions the signal, processes it and processes and displays the data will be different and has to be designed from scratch and none of the three electronic parts of the three examples could be used due to the lack of the compatibility between each other.

6.1.4 Hewlett Packard Interface Bus (HP-IB)

In 1960s, the Hewlett-Packard (HP) had the similar problem of interconnection between its wide range of products, as when different products needed to be connected to each other, they suffered problems related to the electrical, mechanical functional and hardware compatibility [85]. So, the HP developed a Generic Purpose Interface Bus (GPIB), also called HP-IB in order to facilitate the interconnection between various controllers and instruments Later it was defined as a standard digital interface, named IEEE-488 [86]. The communication protocol between devices connected with GPIB is defined by the IEEE-488 and the GPIB connector contains 24 pins that contain address, data, command, clock and power

lines. Different devices can be connected to a same host controller through this bus which acts as a simple and standard hardware interface.

6.1.5 Research Objective

Similar approaches can be adopted in order to make the interconnection possible between different types biosensors and a same signal processing hardware platform. So, there is a need to develop an electronic platform that provides a standard interface bus and supports any kinds of sensors or biosensors. In order to design such general purpose electronic platform, it is important to find out first the general characteristics of biosensing platforms. As previously mentioned, in a biosensor, the the bioreceptor is specific to a given type of analyte. The transducer converts the biological signals coming from bioreceptors into electrical signals. The output of the transducer can be electrical or optical depending on the transducer. The electronics processes the electrical or optical signal and provides relevant information on the measurement.

Among these different components, it is hard to generalize bioreceptor due to its selectivity. The transducer can also be hard to generalize as it is difficult to design a general purpose transducer that can convert any types of biological signals into a given type of electrical signal. However, the electronics that is responsible for signal conditioning and processing can be generalized, because the output signals of the transducer can be converted into a single type of electrical signal such as a voltage signal through specific electronic circuitry. For example, a current signal can be converted into a voltage signal through a current to voltage conversion. A frequency signal can can be converted into a voltage signal through a frequency to voltage conversion. An impedance signal can be converted to a voltage signal through a voltage division. A temperature signal can be converted to voltage signal through a temperature to voltage converter, etc.

In all these cases, the output signals are converted into a voltage signal, because the voltage signal can be processed easily and can be given to analog to digital converters or other signal processing circuitry for the post processing. So, the final aim of the research in this project is to develop a novel general biosensor interface bus that we named GBIB (Generic Bio-Interface Bus) with a standard interface that supports as many types of biosensors as possible. Such platform can be very useful, as during the design of a biosensor, the designers will only need to develop the biosensor specific parts such as bioreceptor, transducer and a circuit that converts the output signal into a voltage signal. Then the GBIB platform can be used for the rest of the stages.

6.2 Project Analysis

Depending on the types of biosensors, there can be different requirements on the system in terms of performance, signal processing channels, processing time, etc. So, the GBIB system should be flexible, programmable and easy to use. Besides the development of the general purpose platform, it is also necessary to validate it by interfacing with biosensors that may contain bioreceptors, transducers and signal conversion circuitry. The development involves in hardware, firmware and software. The hardware design includes designing the GBIB and biosensor specific hardware. So, the design follows hardware/software design methodology in order to optimize the coordination between different designs. With this design approach, different designs can go in parallel and overall design time can be reduced.

6.3 Model Implementation

In this model the hardware design and software design are implemented in parallel and this section includes all the design steps that are carried out during the development.

6.3.1 Requirements

The requirements are the first step in the design steps and they include both functional and non-functional requirements.

The functional requirements are following:

- The GBIB system should contain a connection interface for biosensor specific circuitry.
- The GBIB system should contain a graphical user interface for controlling a test or for visualizing measurement results.
- The GBIB system should contain signal processing blocks.
- The GBIB system should contain data processing blocks.
- The GBIB system should also support applications that need digital signals.
- The GBIB system should contain at least 4 voltage signal generation blocks.
- The GBIB system should contain at least 4 current signal generation blocks.
- The GBIB system should support at least 16 biosensor measurement channels.
- The GBIB system should contain a connector that is used for interconnection.

- The GBIB system should contain a programming interface for updating internal firmware.
- An electrochemical sensor specific system would be required to test the inter-connectivity with the GBIB system.
- The electrochemical sensor specific system should contain 3 measurement channels.
- An ion-sensitive biosensor specific system would be required to test the inter-connectivity with the GBIB system.
- The ion-sensitive biosensor specific system should contain 10 measurement channels for ion detection and one channel for temperature measurement.
- A memristive biosensor specific system would be required to test the inter-connectivity with the GBIB system.
- The memristive biosensor specific system should support at least 12 memristive biosensor connection.

The non-functional requirements are following:

- The GBIB system should have high performance to support possible real-time applications.
- The GBIB system should consume low power.
- The GBIB system should be portable, should have moderate dimensions and weight.
- The GBIB system should help the designer to lower the design costs.

6.3.2 Specification

The specification is the bridge between the requirements and architecture. It describes what the system should do. In this project the specifications are described as following: the GBIB system shall communicate with other biosensor specific systems through its connection interface. The connection interface will power up the biosensor specific systems, provide biosensor specific systems with required voltage or current stimulation signals or other types of digital signals. This connection interface will accept the incoming voltage signals from these biosensor specific systems. The connection interface will read some information from these biosensor specific systems when needed. The GBIB system will process the incoming voltage signal and convert it to digital signal. Then the system will process the digital signal and visualize it or transmit it to external servers wirelessly.

The biosensor specific systems will connect to GBIB system for accepting the stimulation or excitation signals through the general connection interface. These systems shall convert the output signals from bioreceptors into the voltage signals and provide the signals to the GBIB system for a signal measurement. In order to guarantee the compatibility with the general connection interface on the GBIB system, the biosensor specific systems should contain a specific interface driver for the connection.

6.3.3 Architecture

The architecture design contains two parts: hardware and software. The hardware includes the hardware functional blocks, while the software corresponds to the software functional blocks. The architecture design describes how the system implements the requirements and specifications described earlier. In order to do that, the system would need both hardware and software blocks.

Hardware Architecture

In the hardware of the GBIB system, possible hardware blocks are: GBIB control and data processing blocks. The GBIB control block contains the blocks related to the measurement and generation of signals, general connection interface to biosensor specific systems, data processing blocks, and data logging or transmission blocks. Besides that, there is also the interface driver that connects the biosensor specific systems to the GBIB system. A simplified hardware architecture that includes both GBIB system and biosensor specific systems is presented in Figure 6.2. As it can be seen from the Figure 6.2, the simplified architecture contains the GBIB interface that connects the biosensor specific systems, called electronic biosensor to the GBIB system. The central control block processes the data and commands, controls the other hardware and communicates with the post processing block. The sensing and actuation block generates voltage and current signals and it also measures the incoming voltage signals. In the post processing block, the cloud IoT interface can be useful for Internet of Things (IoT) applications, while the smart data analysis processes and visualizes the data coming from the serialport communication in the GBIB Control block.

In the electronic biosensor block, the interface driver is dedicated to the connection with GBIB System. The sensor front end transduces the biological or electrochemical signals coming from the biosensor block into voltage signals.

A more detailed hardware architecture is shown in Figure 6.3. In the central control block, besides the micro-controller that processes the data and commands, there is the voltage regulator block that supplies the whole system with a stable operating voltage. There is also the humidity and temperature sensor module that is used to measure the humidity and temperature of the experimental environment.

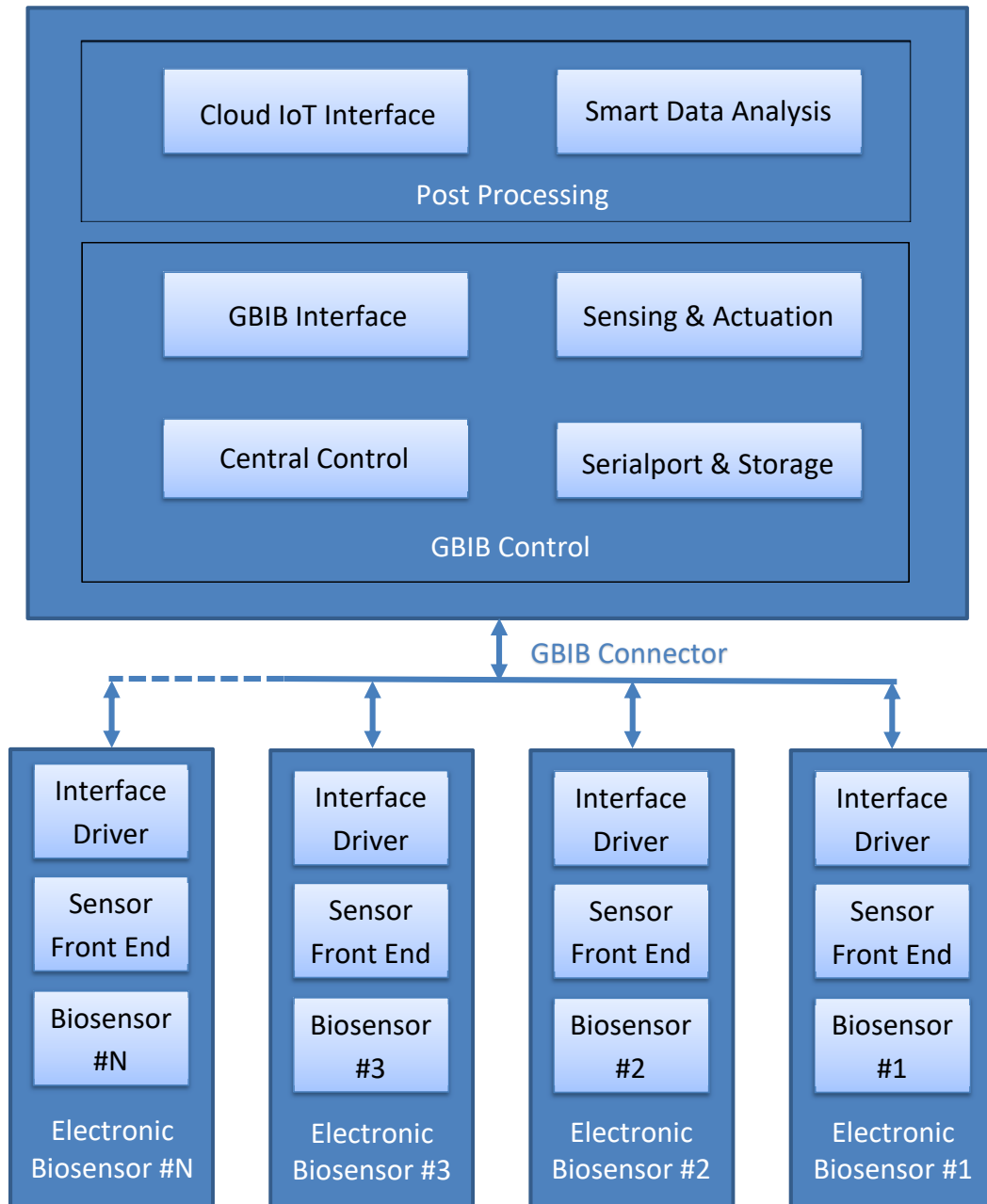


Figure 6.2: Simplified hardware architecture of the overall system

In the sensing and actuation block, the voltage signals are generated from Digital to Analog Converter (DAC) block, while the current signals are generated from the current generator block. The measurement of the signal is done by the Analog to Digital Converter (ADC) block.

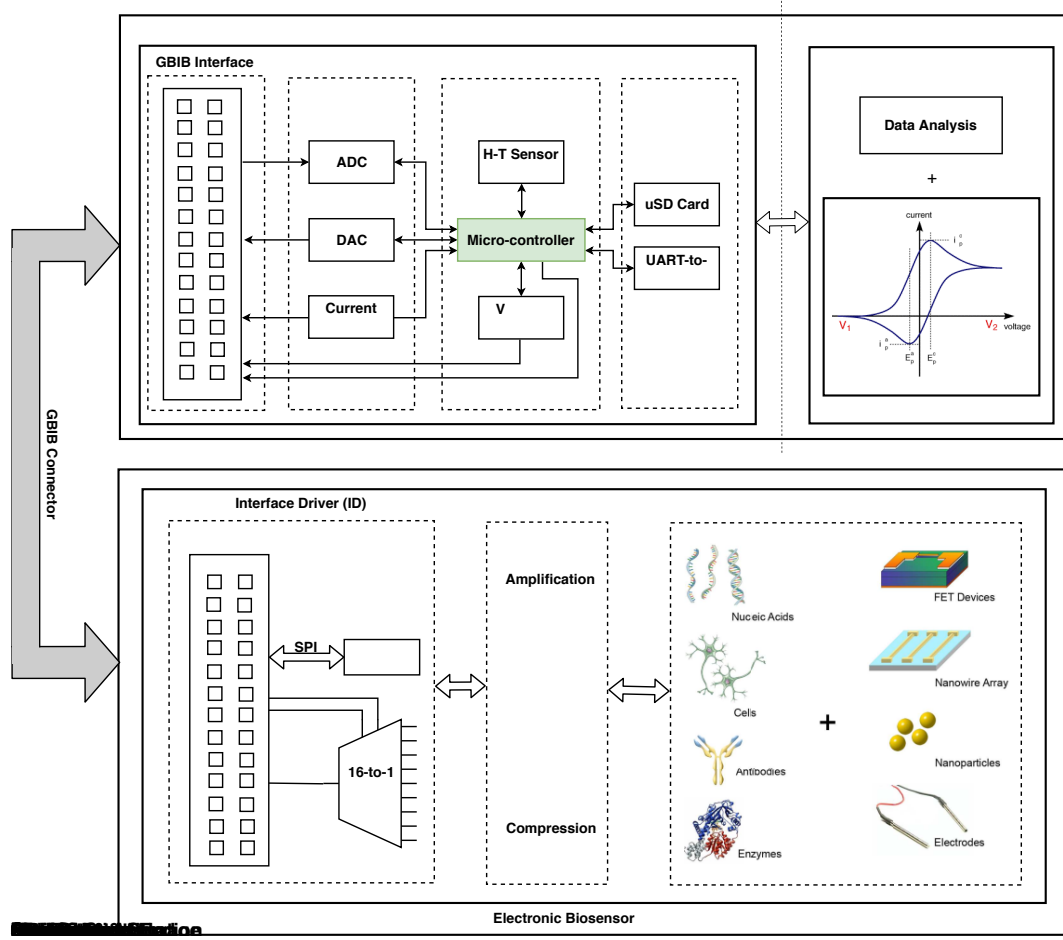


Figure 6.3: Detailed hardware architecture of the GBIB Platform

The GBIB interface block is dedicated to the interconnection with electronic biosensors and it contains a header with 26 pins.

The serialport and storage block enables the possibility of storing measurement data on local μ SD Card or transfers the data to post processing block through a serial port.

In the interface driver block, the 26 pin header block is dedicated to the interconnection with GBIB board. The SPI Flash memory block is used for storing the test parameters of the electronic biosensor. The multiplexer block enables the possibility of selecting between 16 different voltage signals coming from the sensor front end block.

The sensor front end block conditions the signals from the transducers, converts to voltage signals and forwards them to the multiplexer input.

Software Architecture

In the software architecture, the software blocks carry out different operations required by the system. According to the previously mentioned requirements and specifications, a possible software architecture can be following as shown in 6.4.

In this architecture, the Graphical User Interface provides the user the possibil-

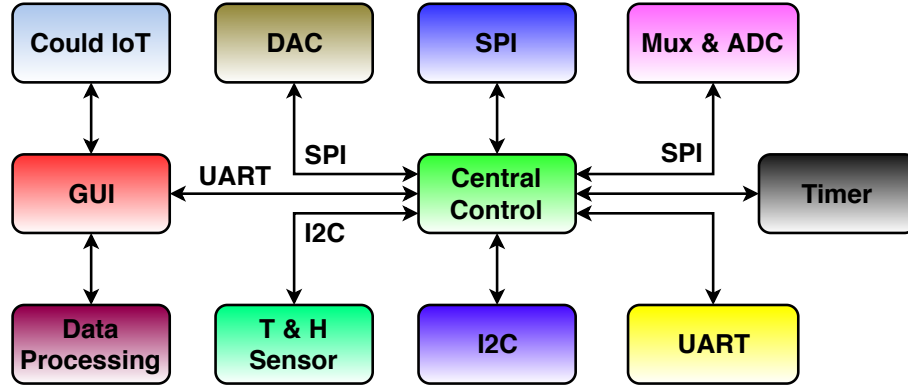


Figure 6.4: Software architecture of the GBIB system

ity of controlling the whole system, graphically analyzing or visualizing the data. The central control block executes the commands coming from the GUI and also other operations needed to guarantee a safe software working environment. It controls the Mux and ADC block and retrieves measurement results from the ADC. The central control block also controls the DAC block via SPI interface and generates excitation signals by writing digital samples into the DAC. It can also read the environmental temperature and humidity from the H&T sensor module. The timer block is responsible for generating interrupt signals and carrying out periodic operations. It is also controlled by the central control block.

6.3.4 Components Design

In this section, the previously mentioned hardware and software architectures are implemented in actual hardware and required components are selected in this step. In this section, each of the hardware and software block is analyzed and a corresponding hardware component or setup is designed or selected.

Hardware Components Design

A) GBIB Interface. The GBIB interface is composed of a 26-pin female header and it is used for communicating with the Interface Driver (ID) in the electronic biosensor. In the Figure 6.5, the detailed information on each pin is shown: The GBIB Interface contains voltage supply lines of ± 3.3 V, ± 5 V, and a ground

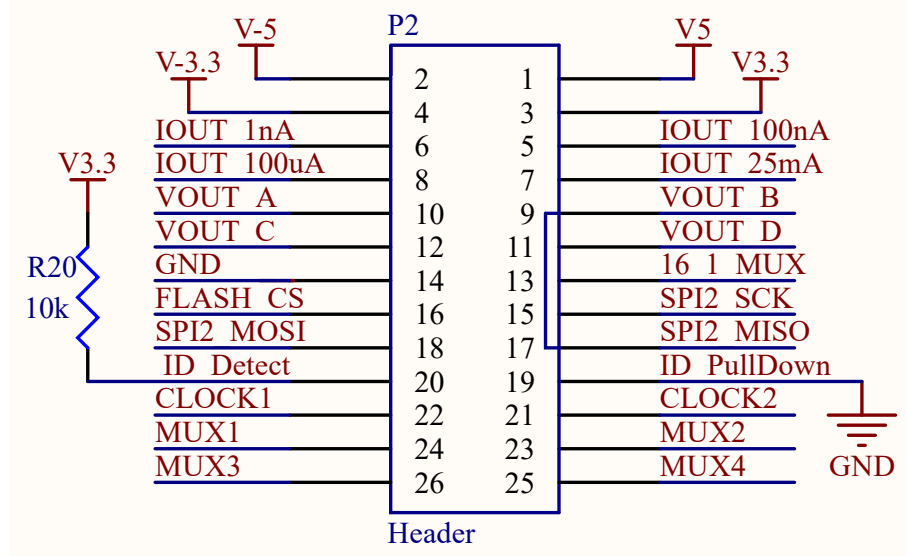


Figure 6.5: GBIB Interface pinout

line. These voltage levels are commonly seen in biosensing applications. There are also 4 SPI connection lines for communicating with the flash memory inside the electronic biosensor. For some biosensing applications, clock signals would be required, so two clock lines are included. The ADC block inside the sensing and actuation block has a single ADC input. So, one line is dedicated for connecting external voltage signal to the input of the ADC. There are 4 voltage signal lines and 4 current signal lines for applications that need excitation or stimulation signals. Other two wires are used for dynamically detecting external electronic biosensors when they are connected to the GBIB interface.

B) Central Control. For processing the data and commands, the central control block uses the high performance STM32F769BGT6 micro-controller (μC). The STM32F769BGT6 μC has a 216 MHz clock frequency, contains plenty of internal hardware resources, and supports low power applications. For applications that require the humidity and temperature of the surrounding environment, the Adafruit SHT31-D module is selected. this module has $\pm 0.3^\circ C$ accuracy and $\pm 2\%$ relative humidity.

C) Sensing and Actuation. An internal structure of the sensing and actuation block is shown in Figure 6.6. The ADC block contains the 24-bit LTC2380-24 ADC and this ADC chip has a very high accuracy. It has a single input channel and it can support upto 1.5Msps/2Msps sampling frequency. It also consumes very low power. The DAC block is based on a 16-bit AD5686R and this DAC has 4 output channels. The current generator block can generate 4 different ranges of

current signals: 0 to 1 nA, 0 to 100 nA, 0 to 100 μ A and 0 to 25 mA. This block contains a AD5686R chip and several voltage to current conversion circuits.

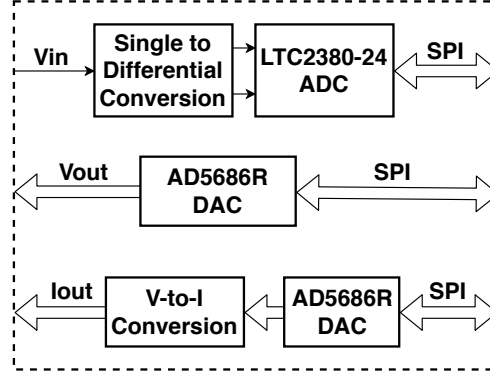


Figure 6.6: Sensing and Actuation.

In the current generator block, there are the DAC that generates voltage signals and a voltage to current conversion block. The schematics of the voltage to current conversion block is shown in Figure 6.7.

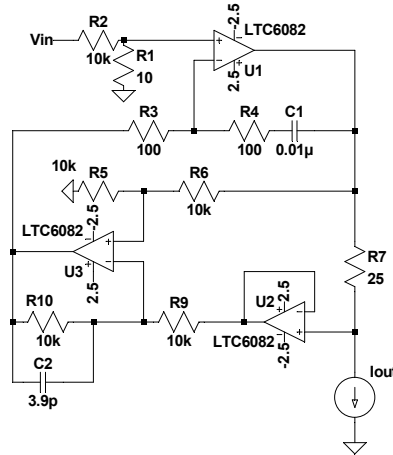


Figure 6.7: Schematics of the bipolar voltage to current converter

In this circuit, the 60812fd chip is used and it contains 4 operational amplifiers. Here the relationship between the output current and input voltage is following:

$$I_{out} = \frac{V_{in}}{1000 \times R_7}. \quad (6.1)$$

So, if the input voltage is in the range of ± 2.5 V and R_7 is 25 Ω , then the output current is in the range of ± 100 μ A. By changing the value of R_7 , it is possible to obtain the different current ranges mentioned earlier.

D) Serialport and Storage. After the measurement results are processed by the STM32F769BGT6 μ C, it is needed to transfer the data to post processing blocks. So, a uart-to-serial conversion block is needed in the GBIB control block for the serial port communication. This conversion block is based on FT232RL chip. Besides sending the measurement results to other blocks, some applications may require data logging into a μ SD Card. In this case, it is necessary to have a μ SD Card slot in the system.

E) Post Processing Block. This block is responsible for the post processing of data and analyzing the results. Some applications require high performance processors for real-time processing. So, the Raspberry Pi (RPi) 3 Model B embedded computer is selected for this purpose. It has a high frequency Quad-core GPUs for carrying out complex tasks and calculations during the data analysis. The RPi also contains an integrated WiFi module, so it supports IoT and Cloud based applications. Besides that, it has the Raspbian Operating System (OS) running inside and it supports the development of software applications.

F) Interface Driver. The interface driver bridges the electronic biosensor with the GBIB board through the GBIB connector. During the design of the interface driver, the W25Q80JVSNIQ SPI-Flash memory is used for storing test parameters and information related to the biosensor. The CD74HC4067SM96 chip is selected due to its very low switching time and on-state resistance.

Software Components Design

In this section, the implementation of the software blocks run inside the STM32F769BGT6 Micro-controller and RPi are described.

A) GUI. Inside the Raspbian OS of the RPi, it is possible to develop software applications using the Qt Creator programming environment. So, a GUI is developed in C++ for controlling the GBIB system and also for the post processing and visualization of the data coming from GBIB system as depicted in Figure 6.8. In the GUI, there are three types of measurement options: Electrochemistry for the test with Electrochemical Electronic Biosensors, Voltage Sweep for Memristive Electronic Biosensors and Open Circuit Potential for ion-sensitive Electronic Biosensors.

The Electrochemistry option allows electrochemical techniques such as CA, CV and DPV along with the test parameters. The Voltage Sweep panel provides options for setting up test parameters for the Memristive biosensors. The OCP panel provides the options for selecting the input channels and carrying out the sampling of the signals.

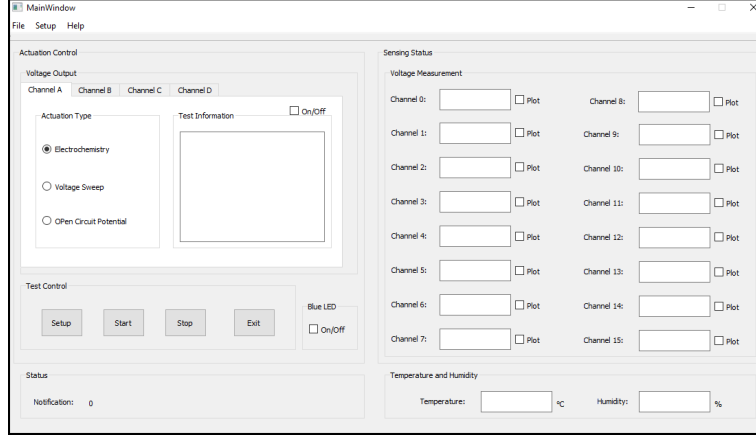


Figure 6.8: GUI for controlling the whole system

B) Central Control. All the hardware and software inside the micro-controller are initialized by the central control block. Then after the initialization, the central control enters the continuous while loop and checks the serialport to see if there is any command arrived from the GUI. When on the GUI side the experiment type, its relevant parameters are selected and sent to the central control over the serialport, then the central control will extract all the information, setup the timer and DAC blocks and then carries out the measurements. Here the timer library controls all the measurement flags and also when to write to the DAC block.

C) DAC. The DAC library is used to write to the DAC and generate a voltage signal. The generated voltage ranges from 0 to 2.5 V, then after the doubling circuit, the final output voltage will be in the range of 0 to 5 V. The relationship between the digital value and actually generated voltage at the output of the DAC chip is following:

$$V_{out} = \frac{D}{65535} \times 2.5(V). \quad (6.2)$$

Thanks to the timer library, it is possible to control the digital value very precisely and the desired output voltage shape can be generated at the output of the actual DAC chip.

D) Mux & ADC. By writing to the GPIO pins of the micro-controller, it is possible to control the multiplexer located inside the interface driver of the electronic biosensor and the desired voltage channel can be selected for the sampling. Once the multiplexer selects which channel to read, the ADC block will carry out sampling of the voltage signal and the output results will be read by the central block through the SPI port. The output results have 24 bits and the input voltage

can be calculated through the following equation:

$$V_{in} = \left(\frac{Output_code}{2^N} \right) \times V_{REF}. \quad (6.3)$$

In our case, the N is equal to 24, the V_{REF} is 5 V.

E) Data Processing. In this block, the data processing and visualization takes place. it is implemented as a part of the GUI application. The data processing is different according to the type of measurements, as in some cases, the input electrical signal at the sensor front end is a current signal and in other cases it can be a voltage signal or other types of electrical signals. This is dependent on the actual application.

6.3.5 System Integration

After the hardware and software components are complete, the next step is to integrate them and carry out relevant tests. Figure 6.9 shows the first prototype of the GBIB Platform plus 3 electronic biosensors. The electronic biosensors can be

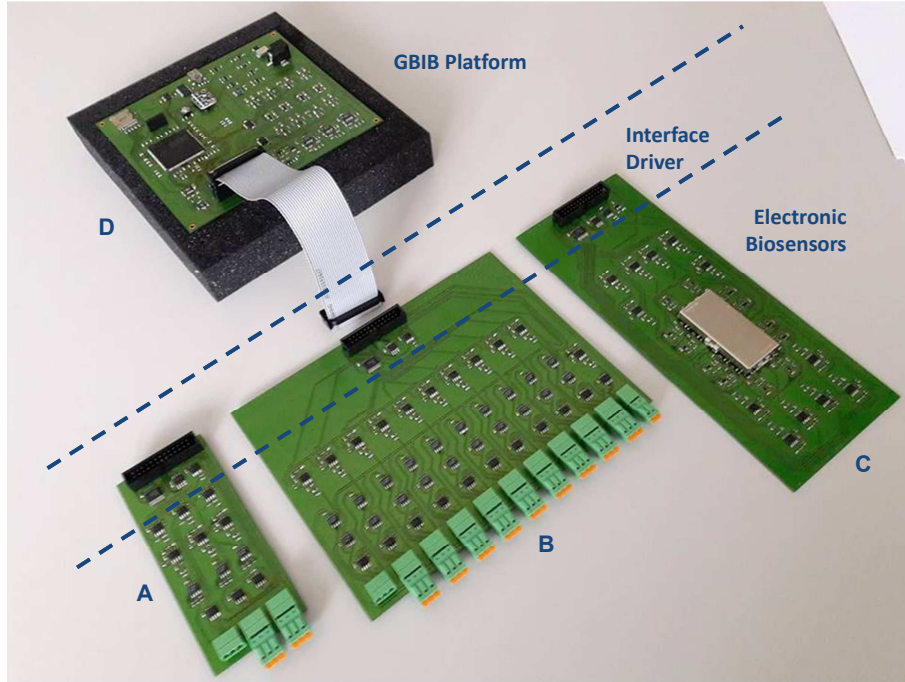


Figure 6.9: First prototype of the system. A) amperometric biosensors B) Ion-Sensitive biosensors C) Memristive biosensors D) GBIB Platform

connected to the GBIB platform through the 26-pin flat cable and relevant tests can be performed by configuring the GBIB platform through the GUI inside the RPi.

The next step is to carry out experiments with the GBIB platform and electronic biosensors.

6.4 Experimental Results

6.4.1 Electrochemical Sensor Experiment

To verify the performance of the GBIB with the amperometric electrochemical sensing platform (intended as sensor connected to frontend and interface driver), we have carried out a 6-point CV calibration of Paracetamol (APAP) drug in Phosphate Buffered Saline (PBS) as background electrolyte. A staircase voltage between -0.1 V and 1.1 V have been applied on the electrochemical cell by the GBIB system and a current, proportional to APAP concentration in solution, have been measured back by the system. The calibration line obtained by the six increasing APAP concentrations measurements was compared with the calibration line obtained by a commercial instrument, a Metrohm Autolab system (PGSTAT 302N), in the same conditions. As shown in Figure 6.10, the two calibration lines are highly comparable, and the GBIB system results to have an higher sensitivity respect to the commercial Autolab ($1 \times 10^{-7} A/\mu M$ vs. $5 \times 10^{-8} A/\mu M$). Therefore, we confirmed the efficacy of GBIB with the Electrochemical Biosensor Board.

6.4.2 Ion-Sensitive Biosensor Experiment

Potentiometric experiments were carried out to prove the efficacy of our GBIB board in combination with the Ion-sensitive Biosensor Board (Figure 6.9.B). Previously developed [87] all-solid state ion-selective sensors based on nanostructured platinum contacts were used for this purpose. The results are reported in Figure 6.11 in comparison with a commercial Autolab potentiostat (Metrohm, Switzerland). It is possible to observe that in both cases very smooth and stable responses are obtained with quasi-nernstian slope. From the small insets showing the time trace during successive solute additions, it is evident that the proposed electronic device offers sharper steps, with lower potential drift especially at high concentrations. In addition, a slightly lower Limit of Detection (LOD) is achieved with the GBIB system with respect to the commercial one ($8.5 \times 10^{-6} M$ vs. $1.3 \times 10^{-5} M$).

6.4.3 Memristive Biosensor Experiment

One of the most important features in the electrical response of the memristive devices is the characteristic hysteresis loop. The memory effect can be attributed to the rearrangement of the charge carriers at the nanoscale due to external perturbation like the applied voltage bias. For most of the bare nanowire devices this hysteresis appears fully pinched at zero voltage or almost pinched at very close

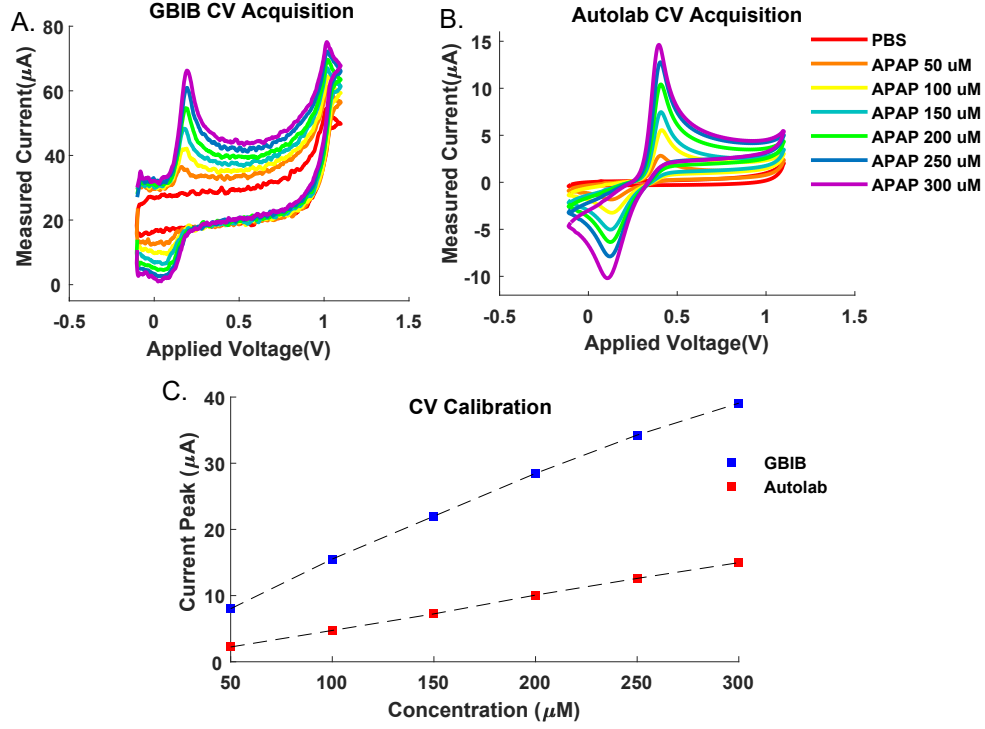


Figure 6.10: A) CV acquisition from GBIB system B) CV acquisition from Autolab C) Comparison of calibration lines obtained for CV measurements of six increasing concentrations of APAP (50;100;150;200;250;300) μM

to zero voltage values due to the impact of environmental conditions, such as the ambient humidity. While, usually, the fully-pinned hysteresis is then lost during bio-detection. Figure 6.12 shows acquisitions done with our boards as compared with previously designed Memristive Biosensing System [78].

As it can be seen from Figure 6.12.B, the measurement is carried out successfully by using the Memristive Electronic Biosensor Board (Figure 6.9.C) together with the GBIB Platform. However, the fully-pinned hysteresis is not present unlike the one in Figure 6.12.A. The Memristive Electronic Biosensor board is designed as a two-layer PCB and since the measured current is in the picoAmpere range, the noise contribution is too much. But this can be addressed by designing the board with a 4 or more layer with proper PCB layout and most importantly, the interfacing between the Memristive Electronic Biosensor Board and GBIB Platform is successful and all the blocks in the GBIB Platform and the interface driver have operational as expected.

Therefore, from the experimental results, we can confirm that the demonstrator can successfully interface with the three different electronic biosensors.

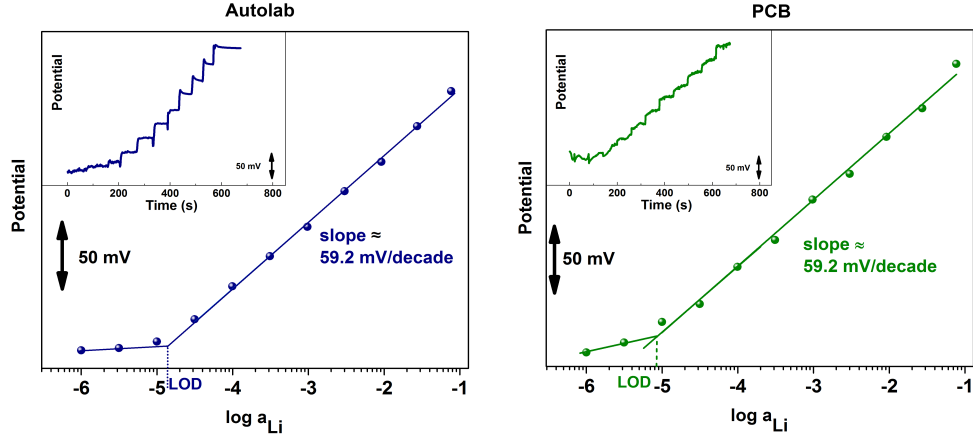


Figure 6.11: Comparison of lithium ion detection with a commercial Autolab potentiostat (A) and with our GBIB system (B). The small insets show the time trace during successive solute additions, while the main graphs display the corresponding calibration curves.

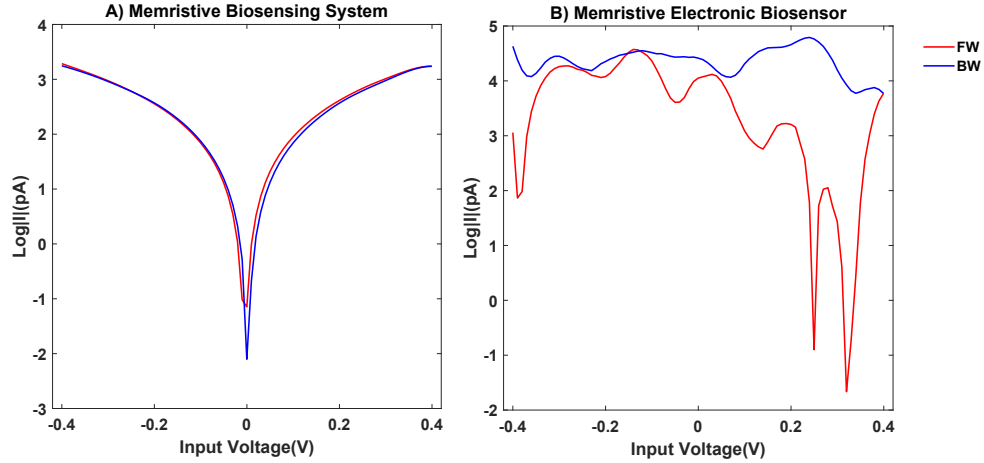


Figure 6.12: Comparison of voltage gaps on bare memristive nanowires between A) Memristive Biosensing System [78] and B) Memristive Electronic Biosensor (Figure 6.9.C).

6.5 Conclusion

From the experimental results, we can conclude that the GBIB Approach works for solving the problem of interconnection between different biosensing platforms and biosensors. It was validated the general purpose of the GBIB system by interfacing it with three different electronic biosensors and proving its efficacy in performing high-performance measurements. The main advantages and performances

of this GBIB Platform are:

- 1) having a unique protocol to interface all kind of electronic biosensors;
- 2) providing a standard for biosensors future developments;
- 3) assuring a strict co-design for advanced bio/CMOS interface in molecular detection.

The design of the whole system has strictly followed the hardware/software design methodology and the different design sections are implemented in parallel. The functionality of the system is also verified through the experimental step and this is the very first general purpose embedded system for electronic biosensors. Furthermore, the system is smart in a way that it can detect automatically the connected electronic biosensor board, extract the board information and provide initial test parameters relevant to the board from GUI control panel.

In future works, a further validation with memristive electronic biosensor board (Figure 6.9.C) will be carried out after the optimization phase of the board. The implementation of artificial intelligence algorithms, e.g., by exploiting Deep Learning architectures, will be further implemented in the RPi in order to further improve the performances as well as the self-autonomy of the general sensing system as a global and autonomous acquiring system. Besides that, the GBIB Platform will be designed as a multilayer PCB with proper shielding in order to reduce the noise and electromagnetic interference.

Chapter 7

Conclusion and Future Work

The overall objective of the thesis was to apply the embedded system design methodologies in real-world biomedical applications. Design methodologies were applied in five different complex projects in order to validate the design approach and to provide a guideline on how to design an embedded system for a given application. This is very important, because the applications can be very different, but the idea behind how to proceed with the design of an embedded is generally the same. The importance and advantages of the design methodologies are confirmed through different embedded system design use cases mentioned in previous chapters (Chapter Two to Chapter Six).

Main achievements

The major achievement in this thesis is to demonstrate how to choose a proper design methodology, implement it and come out with a successful design of an embedded. The selection of the design methodology is very important for numerous reasons mentioned in the Chapter One. The thesis analyzes the possible reasons and situations for selecting a design methodology and this can be greatly useful for designers during the design of an embedded system.

During the development of the electrical and mechanical stimulation and monitoring system for cell differentiation in Chapter Two and the wearable sEMG system in Chapter Three, the successive refinement method is used for the following reasons:

- In both applications, there is not enough information regarding the biological impacts and the output behaviour of the embedded system, so the designed system might not work as expected in a first round. Therefore, the design concepts and technology have to be tested through the first prototype of the system and then are gradually refined and improved.

- Additional requirements and features need to be added after the first prototype.
- The target application requires continuous improvement and updates on the embedded system.
- Multiple design cycles are supported by the target application in terms of cost and design time.

In these two projects, some of the ready-to-use components are selected in order to reduce the design efforts. For example, the embedded system for the cell stimulation is based on Raspberry Pi 3. The central node of the sEMG system is based on nRF52 development board, while the measurement nodes are custom designed. During the development of the drug monitoring system in Chapter Three, the memristive biosensing platform in Chapter Four and the general purpose interface bus system in Chapter Five, the hardware/software design method is used. The reasons are following:

- These systems are complex and they can be split into sub-blocks for parallel design.
- There is a strict constraint on the design time of the system.
- There is relatively enough information regarding the expected functionality and behaviour system.
- Design techniques and hardware architectures are relatively mature and no additional design cycles are required.
- There are enough design teams available.

In contrast, a designer can consider using the waterfall model in the following cases:

- The requirements and specifications of the system are clear, well documented and fixed.
- Technology is well understood and is not dynamic.
- Product definition is stable.
- No ambiguous requirements are present.
- Enough resources and design expertise are available to support the product.
- The project is relatively short.

While the spiral model can be considered in following situations:

- When the project is very large and is a medium to high-risk project.
- When the target application allows to create a prototype.
- When the risk and cost evaluation is important.
- When the requirements and specifications are complex and unclear.
- When changes may be required at any time.
- When there is a need to frequently release a product.
- When long-term commitment of the project is not feasible and continuous evaluation of the project is required.

After the selection of a design methodology, it is preferable to choose ready-to-use components or modules whenever they are available and meet the requirements of the target project. This is important because it can help reduce the design efforts, cost and time. If no ready-to-use components or modules are available, then one can design his custom component or module. In this case, it would be preferable to design a reusable module, so that the same custom platform or module can be adopted for other applications as a ready-to-use block.

Further achievements

Further achievements in this thesis are the successful development and validation of novel embedded systems for five different biomedical applications and the scientific impacts and innovative contributions of these systems are summarized below.

- **High performance electrical and mechanical cell stimulation and monitoring system.** The aim of this design is to develop a robust, easy to use bio-reactor system that is capable of generating electrical and mechanical stimulation signals and monitoring in real-time the effects of the stimulation process. The system is intended to be used for stem cell differentiation in tissue engineering. The system is described in details in Chapter Two.

The hardware of the system is flexible and most of the components are connected in plug-and-play manner in the system so that individual parts can be easily replaced for upgrades. It has independent signal generation units that can generate electrical or mechanical stimulation signals with high accuracy and it is confirmed by observing the electrical outputs of the stimulation units through an oscilloscope.

Development of such system is extremely important, as it can provide an ideal platform that can provide proper physiological conditions to the stem cells and differentiate them into the proper organs or tissues that are required. After the bioreactor system is complete, it is used for tendon regeneration

experiment. The cell cultures are mechanically stimulated in a bioreactor showing the positive role of the tested dynamic culture condition on cell alignment and tenogenic differentiation. The synergistic effect of mechanical stimulation results in an enhancement of cell adhesion, proliferation, alignment, and differentiation, illustrating the potential of the bioreactor system for tendon tissue engineering. These results provide insight on selection of proper culture conditions for engineering highly organized and biomimetic tendon tissues. In addition, the proposed multi-layered constructs in which each compartment can be independently tailored paves the way for engineering tissue-like constructs with suitable mechanical properties at both tissue and cell levels [23].

- **Ultra low-power wearable wireless surface EMG system.** In rehabilitation therapy, it is often necessary to carry out long-term continuous monitoring of the muscle activities of the patients. Therefore, the clinicians would need a system that could carry out long-term monitoring. But the commercially available devices could not support the long term monitoring due to their battery life, so a low-power wearable long term monitoring system is designed and testes for this application. The system is described in details in Chapter Three.

The experiments indicate that the designed system can operate in wireless transmission mode where the acquired data are transmitted in real-time via custom wireless communication as well as in offline mode where the data are stored into a local μ SD Card. Dynamic configuration of the wireless radio protocol ensures safety of the data packets, reliability and robustness in the communication. In each working mode, three acquisition techniques are supported, such as raw surface EMG data acquisition, envelope data acquisition and Adaptive Threshold Crossing. Most importantly, the optimized hardware and software design enables the system to consume very low power and a long-term monitoring of 32 to 61 hours is possible under a 450 mAh coin battery.

The 10 μ s synchronization accuracy is achieved among multiple measurement nodes and up to 100 nodes are supported by the system thanks to the dynamic frequency hopping technique integrated into the system. Optimized area and reduced cost give the system more advantages in going to the market.

Future work in this application can be to investigate the possibility of automatic muscle synergy extraction and real-time display. This can be very useful as it will provide a direct information on the muscle under the measurement. The area of the system could be optimized by applying multi-stack architecture and the quality of the signals can be improved by multi-layer PCB design and by proper shielding.

- **Multi-channel electrochemical biosensing platform.** In drug delivery,

there are many potential risks and challenges regarding the effects of a drug in a patient as its effect changes with the physical status of the patient, his living environment and health status. Therefore, it is very critical to ensure a correct delivery of a drug to the patient. The designed three-channel electrochemical biosensing platform is dedicated to continuous monitoring and delivery of anesthesia in surgeries or Intensive Care Units. Such platform is very important in tracking the amount of anesthesia in patient blood and delivering the right amount of dosage to the patient. The system is described in details in Chapter Four.

Experimental results confirm that the designed biosensing platform is capable of monitoring the anesthesia compounds, such as Paracetamol and Propofol. Through the experiments, it is also confirmed that each measurement channel is able to carry out electrochemical techniques such as ChronoAmperometry (CA), Cyclic Voltammetry (CV) and Differential Pulse Voltammetry (DPV) for the detection of paracetamol and propofol.

The test results also confirm that the system has better performances and several advantages compared to the commercial Autolab potentiostat produced by Metrohm PGSTAT302N. The designed system has very low cost, simultaneous detecting capability of several drugs and temperature and pH, high portability and small dimension ($27 \times 21 \times 13$ cm). Integrated WiFi module in the system has made it possible to remotely access the system for monitoring the status of the patients, for keeping control over the monitored parameters and controlling the drug delivery remotely.

Further tests are carried out in the undiluted human serum medium and the system is able to detect paracetamol and propofol in such medium. This is the first ever successful simultaneous detection of these compounds in human serum that has lasted over 24 minutes [44]. Besides that, the multiple measurement channels in the system make it possible to be used for multiplexed drug monitoring applications.

- **Portable point-of-care memristive biosensing platform.** Cancer is one of the main causes for many deaths every year and researchers are studying cancer extensively in order to diagnose it in early stage and apply some cures to the patient. The early stage cancer diagnostics is very crucial and important, because if the cancer is detected in its early stage, then there would be the possibility to stop or at slow down its evolution.

The memristive biosensors proved to be excellent candidates in detection of cancer and other molecules thanks to their ultrahigh sensitivity. However, the memristive biosensors need to be integrated with electronics and for that reason, a portable, low cost and low power embedded biosensing platform is developed. The system is described in details in Chapter Five. Experimental results confirm the advantages of the biosensing platform compared to

the previously used commercial probe stations and parameter analyzers for memristive biosensors. The results confirm that the system is able to carry out measurements in a relatively short time, such as couple of seconds with respect to 40 minutes in the case of commercial probe stations and parameter analyzers. The small area, low cost, low power consumption, portability and programmability makes the system more preferable compared to industrial instruments in cancer detection related research. The disposable memristive biosensing chips enable the system to perform various independent clinical tests on different patients. In the next steps, multi-panel detection property will be investigated by automatic antibody spotting machine. This enables the printing of multiple types (up to 12 types) of antibodies on a single memristive biosensing chip and this paves the way for a simultaneous detection of several diseases through a single measurement.

With the designed system we have achieved the first ever detection of immune attacks at an ultra-high sensitivity as few as six cancer marker molecules in a five micrometers section of breast tumor tissue. This is a technological breakthrough in the momentum of breast cancer immunotherapy and it has tremendous potential for guiding precision oncology. The relevant results are submitted to the Science Advances Journal.

- **General purpose biosensing interface bus system for biosensors.** Biosensors have the property of selectivity and the electronic systems that are designed so far are biosensor specific. This means that one electronic system for one type of biosensor could not be used for another type of biosensor as they are customized for the biosensor of interest. In this application, a novel, general purpose embedded system is developed in order to provide a standard connection interface that can be supported by any types of biosensors with proper interface driver and signal conversion units. The system is described in details in Chapter Six.

Designing such system is very important as it addresses the incompatibility between electronic platforms and biosensors. It also provides a ready-to-use electronic system that can be used to interface with the biosensor and to reduce the overall design time and cost in the development of a complete biosensing platform. The system is capable of producing highly precise voltage and current signals and can carry out high-speed data processing.

Experimental results on electrochemical biosensors show that the general purpose platform can be interfaced with electrochemical electronic biosensors and carry out electrochemical tests, such as Cyclic Voltammetry in this case. The results on ion-sensitive biosensors show that the general platform is also able to be used with electronic biosensors that are dedicated to open circuit potential measurement. The different experiments are selected and configured on the graphical user interface inside the system. The successful results indicate

the robustness, flexibility of the graphical user interface.

More importantly, these test results on different biosensors using same general platform paves the way to present a new design approach for advanced bio/CMOS interfaces and a new concept in the definition of a biosensor.

The design of these embedded systems are the first stage of possible future integrations and they are designed in direct cooperation with hospitals and specific research institutes. This helps us collect useful information for passing to a second stage to design integrated solutions with FPGAs or Integrated Circuits that are ready to become medical devices.

Future Research Directions

Artificial Intelligence (AI) is gaining more attention in many areas, as well as in bio-medical applications. By integrating the AI, an embedded system can become 'intelligent', in the sense that it can perform analysis of data, images just like clinicians or doctors.

In the stem cell stimulation and monitoring system, the neural network algorithms should be exploited to process real-time monitoring images and track the status of the stimulation. The possible of generating ambient specific stimulation signals should also be taken into account.

In the surface EMG system, a trained neural network may give the possibility of real-time extraction of muscle synergies from surface EMG data.

In the memristive biosensing platform, AI algorithms can be incorporated into the system in order to obtain directly the actual status and relevant information of the cancer or other diseases.

In the electrochemical biosensing platform for the anesthesia, the AI algorithms may give the possibility of extracting some key values such as current peaks and positions of the currents and this would reduce greatly the transmitted amount of data during the measurement.

In the general purpose platform, an AI algorithm may give the possibility to automatically setup can carry out the experiment based on the connected electronic biosensors and analyze the results in a smart way.

From the examples above, using AI in biomedical applications can have many advantages as listed in the examples above. Especially when there is a huge amount of data to be processed or transmitted, an AI algorithm could be helpful in extracting the useful results.

So, the future trend of my research would be to design AI based embedded systems for biomedical applications using previously described design methodologies.

As a final conclusion, this thesis demonstrates how to apply embedded system design methodologies in various types of biomedical applications and validates the design approach with experimental results.

References

- [1] A. Suliman and N. Nazri. “A new hybrid model of software engineering and systems engineering for embedded system development methodology”. In: *ICIMU,2014 IEEE*. IEEE. 2014, pp. 346–350.
- [2] Steve Heath. *Embedded Systems Design*. Butterworth-Heinemann, 1997.
- [3] Arnold Berger. *Embedded Systems Design—An Introduction to Processes, Tools, and Techniques*. CMP Books, 2002.
- [4] Wayne Wolf. *Computers as Components - Principles of Embedded Computing System Design*. Morgan Kaufmann, 2008.
- [5] Iuliana Chiuchisan and Oana Geman. “Trends in Embedded Systems for e-Health and Biomedical Applications”. In: *EPE,2016 IEEE*. IEEE. 2016, pp. 1–5.
- [6] Ascensia. *CONTOUR-XT*. 2019. URL: <https://www.diabetes.ascensia.it/prodotti/contour-xt>.
- [7] OMRON. *M3 Comfort*. 2017. URL: https://www.omron-healthcare.it/it/misuratori-di-pressione/M3_Comfort.html.
- [8] Joseph A. Potkay. “Long term, implantable blood pressure monitoring systems”. In: *Biomedical Microdevices* 10.3 (2008), pp. 379–392.
- [9] Zita M. Jessop¹ et al. In: *BMC Medicine* 115 ().
- [10] A. Pavesi et al. “Electrical Conditioning of Adipose-Derived Stem Cells in a Multi-Chamber Culture Platform”. In: *Biotechnol. Bioeng* 111 (2014), pp. 1452–1463.
- [11] Mantero S. et al. “A new electro-mechanical bioreactor for soft tissue engineering”. In: *Journal of Applied Biomaterials & Biomechanics* 5.2 (2007), pp. 107–116.
- [12] IATDMCT Executive Committee. *Definition of TDM*. 2004.
- [13] Marshall WJ and Bangert SK. *Clinical Chemistry, 6th Edition*. Mosby Elsevier, 2008.
- [14] Ioulia Tzouvadaki et al. “Label-Free Ultrasensitive Memristive Aptasensor”. In: *Nano Letters* 16.7 (2016), pp. 4472–4476.

- [15] HOUSE OF LORDS. *Regenerative medicine*. 2013.
- [16] V. Ramakrishna¹, P. B. Janardhan, and L. Sudarsanareddy. “Stem Cells and Regenerative Medicine – A Review”. In: *Annual Review & Research in Biology* 1.4 (2011), pp. 79–110.
- [17] Gareth Turnbull et al. “3D bioactive composite scaffolds for bone tissue engineering”. In: *Bioactive Materials* 3 (2018), pp. 278–314.
- [18] Adrian Chlanda et al. “Structure and physico-mechanical properties of low temperature plasma treated electrospun nanofibrous scaffolds examined with atomic force microscopy”. In: *Micron* 107 (2018), pp. 79–84.
- [19] DROR SELIKTAR. “Extracellular Stimulation in Tissue Engineering”. In: *Annals of the New York Academy of Sciences* 1047 (2005), pp. 386–394.
- [20] Chiara Rinoldi et al. “Nanobead-on-string composites for tendon tissue engineering”. In: *J. Mater. Chem. B* 6 (2018), pp. 3116–3127.
- [21] Raspberry Pi Organization. *Raspberry Pi 3*. 2012. URL: <https://www.raspberrypi.org/products/raspberry-pi-3-model-b/>.
- [22] David Alejandro Fernandez Guzman. “Electromechanical Stimulation and Monitoring System for the Development of Cardiac Cell Cultures”. MA thesis. POLITECNICO DI TORINO, 2016.
- [23] Rinoldi Chiara et al. “Mechanical and Biochemical Stimulation of 3D Multilayered Scaffolds for Tendon Tissue Engineering”. In: *ACS Biomater. Sci. Eng.* (2019).
- [24] S. Center and KPKinteractive. *Understanding Spinal Cord Injury*.
- [25] J. Gordon Betts et al. *Anatomy and Physiology*. OpenStax, 2013.
- [26] Cindy L Stanfeld. *Principles of Human Physiology*. Pearson Education UK, 2013.
- [27] M.B.I. Raez, M.S. Hussain, and F. Mohd-Yasin. “Techniques of EMG signal analysis: detection, processing, classification and applications”. In: *Biological Procedures Online* 8 (2006), pp. 11–35.
- [28] Matthew C. Tresch, Vincent C. K. Cheung, and Andrea d’Avella. “Matrix Factorization Algorithms for the Identification of Muscle Synergies: Evaluation on Simulated and Experimental Data Sets”. In: *Journal of Neurophysiology* 95 (2006), pp. 2199–2212.
- [29] Adrian Burden. *Surface electromyography. Biomechanical evaluation of movement in sport and exercise*. Routledge, 2008.
- [30] M.A. Cavalcanti Garcia and T.M. M. Vieira. “Surface electromyography: Why, when and how to use it”. In: *Revista Andaluza de Medicina del Deporte* 4 (2011), pp. 17–28.

-
- [31] Spinelli E. M., Pallas-Areny R., and Mayosky M. A. “AC-Coupled Front-End for Biopotential Measurements”. In: *IEEE Transaction on Biomedical Engineering* 50 (2003), pp. 391–395.
 - [32] Texas Instruments. *INA321 Micropower single-supply CMOS Instrumentation Amplifier, Rev. D*. 2006. URL: <http://www.ti.com/product/INA321>.
 - [33] Nordic Semiconductor. *nRF52832 Product Specification v1.4*. 2017. URL: <https://www.nordicsemi.com/Products/Low-power-short-range-wireless/nRF52832>.
 - [34] Vogenberg FR, Isaacson Barash C, and Pursel M. “Personalized Medicine Part 1: Evolution and Development into Theranostics”. In: *P&T* 35 (2010), pp. 560–576.
 - [35] Mathur S and Sutton J. “Personalized medicine could transform healthcare (Review)”. In: *BIOMEDICAL REPORTS* 7 (2017), pp. 3–5.
 - [36] J. Cranshaw, K. J. Gupta, and T. M. Cook. “Litigation related to drug errors in anaesthesia: an analysis of claims against the NHS in England 1995–2007”. In: *Anaesthesia* 64 (2009), pp. 1317–1323.
 - [37] Alevtina Dubovitskaya et al. “TUCUXI: An Intelligent System for Personalized Medicine from Individualization of Treatments to Research Databases and Back”. In: *Proceedings of the 8th ACM International Conference on Bioinformatics, Computational Biology, and Health Informatics*. ACM-BCB 2017. 2017, pp. 223–232.
 - [38] Joseph Wang. “Electrochemical biosensors: Towards point-of-care cancer diagnostics”. In: *Biosensors and Bioelectronics* 21 (2006), pp. 1887–1892.
 - [39] Allen J. Bard and Larry R. Faulkner. *ELECTROCHEMICAL METHODS Fundamentals and Applications*. JOHN WILEY & SONS, INC, 2001.
 - [40] Sandro Carrara. *Bio/CMOS Interfaces and Co-Design*. Springer, 2013.
 - [41] Francesca Stradolini. “IoT Bio-Electronic Multi-Panel Device for On-line Monitoring of Anaesthesia Delivery”. PhD thesis. Ecole polytechnique fédérale de Lausanne (EPFL), 2018.
 - [42] Microchip. *XMEGA E5 Data Sheet*. 2018. URL: <https://www.microchip.com/wwwproducts/en/ATxmega32E5>.
 - [43] Inc Braintree Scientific. *TMNE-1000 Programmable Single Syringe Pump*. 2014. URL: <https://syringepumppro.com/braintree-scientific/>.
 - [44] F. Stradolini et al. “An IoT Solution for Online Monitoring of Anesthetics in Human Serum Based on an Integrated Fluidic Bioelectronic System”. In: *IEEE Transactions on Biomedical Circuits and Systems* 12 (2018), pp. 1056–1064.

- [45] F. Stradolini et al. "IoT for Telemedicine Practices enabled by an Android Application with Cloud System Integration". In: *ISCAS,2018 IEEE*. IEEE. 2018, pp. 1–5.
- [46] P. Matlani and N. D. Londhe. "A cloud computing based telemedicine service". In: *PHT,2013 IEEE*. IEEE. 2013, pp. 326–330.
- [47] Francesca Stradolini et al. "Raspberry-Pi based system for propofol monitoring". In: *Integration* 63 (2018), pp. 213–219.
- [48] F. Stradolini et al. "Raspberry Pi Based System for Portable and Simultaneous Monitoring of Anesthetics and Therapeutic Compounds". In: *NG-CAS,2017 IEEE*. 2017, pp. 101–104.
- [49] N. Ding et al. "Determination of the diffusion coefficient of lithium ions in nano-Si". In: *Solid State Ionics* 180 (2009), pp. 222–225.
- [50] Ozcan L, Sahin M, and Sahin Y. "Electrochemical Preparation of a Molecularly Imprinted Polypyrrole-modified Pencil Graphite Electrode for Determination of Ascorbic Acid". In: *Sensors* 8 (2008), pp. 5792–5805.
- [51] S. Carrara, F. Stradolini, and T. Kilic. *Fouling-resistant pencil graphite electrode*. 2017.
- [52] B. Donato et al. "Raspberry Pi driven flow-injection system for electrochemical continuous monitoring platforms". In: *BioCAS,2017 IEEE*. IEEE. 2017, pp. 1–4.
- [53] Carioli G et al. "Global trends in nasopharyngeal cancer mortality since 1970 and predictions for 2020: Focus on low-risk areas". In: *International Journal of Cancer* 140 (2017), pp. 2256–2264.
- [54] Baj-Rossi C, De Micheli G, and Carrara S. "Electrochemical detection of anti-breast-cancer agents in human serum by cytochrome P450-coated carbon nanotubes". In: *Sensors* 12 (2012), pp. 6520–6537.
- [55] Hande et al. "Pharmacokinetics of High-Dose Etoposide (VP-16-213) Administered to Cancer Patients". In: *Cancer Research* 44.1 (1984), pp. 379–382.
- [56] Arbuck et al. "Etoposide pharmacokinetics in patients with normal and abnormal organ function." In: *Journal of Clinical Oncology* 4.11 (1986), pp. 1690–1695.
- [57] Erik De Clercq. "Anti-hiv drugs: 25 compounds approved within 25 years after the discovery of hiv". In: *International Journal of Antimicrobial Agent* 33 (2009), pp. 307–320.
- [58] Hamed Laroui et al. "Nanotechnology in diagnostics and therapeutics for gastrointestinal disorders". In: *Digestive and Liver Disease : official journal of the Italian Society of Gastroenterology and the Italian Association for the Study of the Liver* 45 (2013), pp. 995–1002.

- [59] Kewal K. Jain. “Nanotechnology in clinical laboratory diagnostics”. In: *Clinica Chimica Acta* 358 (2005), pp. 37–54.
- [60] Mainak Chakraborty, Surangna Jain, and Vibha Rani. “Nanotechnology: Emerging tool for diagnostics and therapeutics”. In: *Applied Biochemistry and Biotechnology* 165 (2011), pp. 1178–1187.
- [61] Leila Syedmoradi et al. “Point of care testing: The impact of nanotechnology”. In: *Biosensors and Bioelectronics* 87 (2017), pp. 373–387.
- [62] L. Chua. “Memristor-the missing circuit element”. In: *IEEE Transactions on Circuit Theory* (1971).
- [63] Dmitri B. Strukov et al. “The missing memristor found”. In: *Nature* 453 (2008), pp. 80–83.
- [64] G. S. Rose et al. “Leveraging Memristive Systems in the Construction of Digital Logic Circuits”. In: *Proceedings of the IEEE* 100 (2012), pp. 2033–2049.
- [65] Rainer Waser and Masakazu Aono. “Nanoionics-based resistive switching memories”. In: *Nature Materials* 6 (2007), pp. 833–840.
- [66] Yuriy V. Pershin and Massimiliano Di Ventra. “Experimental Demonstration of Associative Memory with Memristive Neural Networks”. In: *Neural Netw.* 23.7 (2010), pp. 881–886.
- [67] Giacomo Indiveri et al. “Integration of nanoscale memristor synapses in neuromorphic computing architectures”. In: *Nanotechnology* 24.38 (2013), p. 384010.
- [68] Sung Hyun Jo et al. “Nanoscale Memristor Device as Synapse in Neuromorphic Systems”. In: *Nano Letters* 10.4 (2010), pp. 1297–1301.
- [69] D. Sacchetto et al. “Applications of Multi-Terminal Memristive Devices: A Review”. In: *IEEE Circuits and Systems Magazine* 13.2 (2013), pp. 23–41.
- [70] Shinhyun Choi, Patrick Sheridan, and Wei D. Lu. “Data Clustering using Memristor Networks”. In: *Scientific Reports* 5 (2015).
- [71] Sandro Carrara. *Nano-bio-sensing*. New York: Springer, 2010.
- [72] Gengfeng Zheng et al. “Multiplexed electrical detection of cancer markers with nanowire sensor arrays”. In: *Nature Biotechnology* 23 (2005), pp. 1294–1301.
- [73] a.M.D.V. Yuriy and V. Pershin. “Memory effects in complex materials and nanoscale systems”. In: *Advances in Physics* 60 (2011), pp. 145–227.
- [74] Xiangfeng Duan, Yu Huang, and Charles M. Lieber. “Nonvolatile Memory and Programmable Logic from Molecule-Gated Nanowires”. In: *Nano Letters* 2.5 (2002), pp. 487–490.

- [75] Davide Sacchetto et al. “New Insight on Bio-sensing by Nano-fabricated Memristors”. In: *BioNanoScience* 1.1 (2011), pp. 1–3.
- [76] I. Tzouvadaki et al. “Bio-functionalization study of Memristive-Biosensors for early detection of prostate cancer”. In: *2015 11th Conference on Ph.D. Research in Microelectronics and Electronics (PRIME)*. 2015, pp. 17–20.
- [77] Sandro Carrara et al. “Memristive-biosensors: A new detection method by using nanofabricated memristors”. In: *Sensors and Actuators B: Chemical* 171-172 (2012), pp. 449–457.
- [78] I. Tzouvadaki et al. “Portable Memristive Biosensing System as Effective Point-of-Care Device for Cancer Diagnostics”. In: *2018 IEEE International Symposium on Circuits and Systems (ISCAS)*. 2018, pp. 1–5.
- [79] Cibele Gouvea. “Biosensors for health applications”. In: *Biosensors for Health, Environment and Biosecurity*. Ed. by Pier Andrea Serra. Rijeka: IntechOpen, 2011. Chap. 3.
- [80] Suprava Patel et al. “Biosensors in Health Care: The Milestones Achieved in Their Development towards Lab-on-Chip-Analysis”. In: *Biochemistry Research International* 2016 (2016).
- [81] Shagun Malhotra et al. “BIOSENSORS: PRINCIPLE, TYPES AND APPLICATIONS”. In: *IJARIIIE* 3 (2017).
- [82] Christopher R. Lowe. “Biosensors”. In: *Trends in Biotechnology* 2 (1984), pp. 59–65.
- [83] Bhalla N et al. “Introduction to biosensors”. In: *Essays in Biochemistry* 60 (2016), pp. 1–8.
- [84] I. N. Hanitra et al. “A Flexible Front-End for Wearable Electrochemical Sensing”. In: *2018 IEEE International Symposium on Medical Measurements and Applications (MeMeA)*. 2018, pp. 1–6.
- [85] Hewlett-Packard. “Tutorial Description of the Hewlett-Packard Interface Bus”. In: *Hewlett-Packard*. Hewlett Packard, 1980.
- [86] IEEE. “IEEE Standard Digital Interface for Programmable Instrumentation”. In: *IEEE Std.* IEEE, 1987.
- [87] F. Criscuolo et al. “Highly-stable Li⁺ ion-selective electrodes based on noble metal nanostructured layers as solid-contacts”. In: *Analytica Chimica Acta* 1027 (2018), pp. 22–32.
- [88] Ioulia Tzouvadaki. “Nanoscale Sensors for Ultrasensitive Label-free Detection of Cancer Biomarkers and Monitoring of Therapeutic Compounds”. PhD thesis. Ecole polytechnique fédérale de Lausanne (EPFL), 2017.

This Ph.D. thesis has been typeset by means of the \TeX -system facilities. The typesetting engine was pdf \LaTeX . The document class was `toptesi`, by Claudio Beccari, with option `tipotesi=scudo`. This class is available in every up-to-date and complete \TeX -system installation.